Studies on the utilization of red mud for environmental application

Manoj Kumar Sahu

Department of Chemistry
National Institute of Technology Rourkela

Studies on the utilization of red mud for environmental application

Dissertation submitted in partial fulfillment

of the requirements of the degree of

Doctor of Philosophy

in

Chemistry

by

Manoj Kumar Sahu

(Roll Number: 511CY605)

based on research carried out

under the supervision of

Prof. Raj Kishore Patel

January, 2017

Department of Chemistry

National Institute of Technology Rourkela

Department of Chemistry
National Institute of Technology Rourkela

January 16, 2017

Certificate of Examination

Roll Number: *511CY605*
Name: *Manoj Kumar Sahu*
Title of Dissertation: *Studies on the utilization of red mud for environmental application*

We the below signed, after checking the dissertation mentioned above and the official record book (s) of the student, hereby state our approval of the dissertation submitted in partial fulfillment of the requirements of the degree of *Doctor of Philosophy* in *Chemistry* at *National Institute of Technology Rourkela*. We are satisfied with the volume, quality, correctness, and originality of the work.

Raj Kishore Patel
Principal Supervisor

Akrur Behera
Member, DSC

Prasanta Kumar Bhuyan
Member, DSC

Garudadhwaj Hota
Member, DSC

Niranjan Panda
Chairperson, DSC

Sourav Chatterjee
Head of the Department

Department of Chemistry
National Institute of Technology Rourkela

Prof. Raj Kishore Patel
Professor

January 16, 2017

Supervisor's Certificate

This is to certify that the work presented in the dissertation entitled *Studies on the utilization of red mud for environmental application* submitted by *Manoj Kumar Sahu*, Roll Number 511CY605, is a record of original research carried out by him under my supervision and guidance in partial fulfillment of the requirements of the degree of *Doctor of Philosophy* in *Chemistry*. Neither this dissertation nor any part of it has been submitted earlier for any degree or diploma to any institute or university in India or abroad.

_____
Raj Kishore Patel

Dedicated to My Parents

Manoj Kumar Sahu

Declaration of Originality

I, *Manoj Kumar Sahu*, Roll Number *511CY605* hereby declare that this dissertation entitled *Studies on the utilization of red mud for environmental application* presents my original work carried out as a doctoral student of NIT Rourkela and, to the best of my knowledge, contains no material previously published or written by another person, nor any material presented by me for the award of any degree or diploma of NIT Rourkela or any other institution. Any contribution made to this research by others, with whom I have worked at NIT Rourkela or elsewhere, is explicitly acknowledged in the dissertation. Works of other authors cited in this dissertation have been duly acknowledged under the sections "Reference". I have also submitted my original research records to the scrutiny committee for evaluation of my dissertation.

I am fully aware that in case of any non-compliance detected in future, the Senate of NIT Rourkela may withdraw the degree awarded to me on the basis of the present dissertation.

January 16, 2017
NIT Rourkela

Manoj Kumar Sahu

Acknowledgment

First of all, I would like to express my profound gratitude to my supervisor Prof. Raj Kishore Patel, Department of Chemistry, National Institute of Technology, Rourkela for his excellent guidance, constant encouragement, continuous support, generous help and inspiration during the entire period of my research work. I would believe myself really fortunate to be associated with him at the important turn of my carrier.

I am grateful to Prof. A. Biswas, Director, National Institute of Technology, Rourkela for his inspiration and encouragement throughout the research work. I also acknowledge to Vedanta Alumina Ltd. for providing financial support during my research work. I sincerely thank to my DSC members Prof. A. Behera, Prof. G. Hota and Prof. P. K. Bhuiyan for their valuable suggestions during this programme.

I wish to thank all faculty members of the department of chemistry. I wish to place on record my thankfulness to numerous technical and nontechnical staffs of Chemistry Department, NIT, Rourkela, who have lent their expertise and cooperation at various stages of this endeavor. I am thankful to Kar sir, Swagatika didi, Samir bhai, Pratap bhai of Chemistry Department, for their help during this programme.

I am heartily thank to all my lab mates Sandip, Tapaswini didi, Kishore, Basanti, Uttam, Sumanta, Sraban, Mantu and Dibya for their help and cooperation.

I am wholeheartedly thankful to Jublie for her cooperation during last part of my work.

No words can convey my gratitude to my parents, brother and sister-in-law for their generous love and blessings, without which it would have never been possible on my part to reach so far.

I would like to thank all those people, who have directly or indirectly helped me at various stages of my research work Finally I thank to God for letting me through all the difficulties.

January 16, 2017
NIT Rourkela

Manoj Kumar Sahu
Roll Number: 511CY605

Abstract

Red mud is a waste by product generated from alumina processing industries which creates a number of environmental problems. Reports of the utilization of the red mud for the treatment of natural, industrial and domestic waste water are available in literature. Clean water and a clean environment are the today's requirements. The use of one waste for the removal of another waste is a challenging job. The present dissertation is an embodiment of the investigations for developing simple inexpensive adsorbents by the modification of red mud for waste water purification.

In laboratory scale, neutralization of highly alkaline red mud is carried out by acid and CO_2 gas treatment and modified by calcination. In another method, red mud adsorbent is prepared by surface modification with the impregnation of an anionic surfactant SDS. After modification, the red mud is called as Activated red mud (ARM) which is used as an adsorbent. The adsorbents (ARM) are used for the removal of Pb(II), Cd(II) ions and organic safranin-O dye separately from aqueous solutions in batch mode. The adsorbents, before and after treatment are characterized by XRD, SEM, EDX, TGA-DSC, FTIR, UV-Visible, BET surface area .The AAS analytical techniques is used to measure the residual metal ion concentration in treated water.

The activated red mud used for the removal of hazardous Pb(II) possess the rounded shape aggregate particles with surface area 67.10 m^2/g and particle size in the range of 0.1–150 μm . The maximum adsorption capacity as calculated from Langmuir isotherm model is found to be 6.0273 mg/g at *pH* 4. The pseudo-second-order kinetics describes the adsorption process. The adsorption process is described by ion exchange mechanism.

The maximum adsorption capacities of Cd(II) on activated red mud (ARM) are found to be 12.046 and 12.548 mg/g at temperature 293 and 303 K, respectively. The endothermic, spontaneous and feasible nature of adsorption is known from the thermodynamic parameters. The external mass transfer coefficient (k_f) is found to be 0.084 $\times 10^{-3}$, 0.012 $\times 10^{-3}$ at temperature 293 K and 9.9 $\times 10^{-3}$, 11.5 $\times 10^{-3}$ at 303 K which are evaluated by the McKay $et\ al.$ and Weber–Mathews equation respectively. The desorption efficiency of Cd(II) is found to be 91.29% with 0.2 $mol/L\ HCl$.

The BET surface area of the SDS/RM is found to be 67.10 m^2/g. The maximum adsorption capacity of modified red mud (SDS/RM) is found to be 8.94 mg/g at temperature 308 K and *pH* 4 obtained from Langmuir isotherm model. The external mass transfer coefficient (k_f) value as obtained from McKay $et\ al.$ equation is found to be 3.49 $\times 10^{-4}$

, 4.61 $\times 10^{-4}$ at temperature 308 K and 2.13 $\times 10^{-4}$, 3.11 $\times 10^{-4}$ at 328 K obtained from Weber–Mathews equation .These values indicate the faster adsorption of safranin-O on the surface of ARM at lower temperature.

The response surface methodology (RSM) is applied to examine the efficiency of the removal of safranin-O dye from aqueous solution by the activated red mud neutralized by CO_2 gas. A 2^4 full factorial central composite design (CCD) method is used to evaluate the effects of adsorption parameters. The operating parameters for maximum uptake capacity of 9.768 mg/g is; adsorbent dose (0.62 g), temperature (29.06 ℃), *pH* (8.3) and initial safranin-O concentration (37.3 mg/L). At this optimum condition, the adsorption of safranin-O from aqueous solution is found to be 94.5%.

***Keywords*: *Red mud*; *adsorption*; *Pb(II) removal*; *Cd(II) removal*; *Safranin-O dye removal*; *response surface methodology*.**

Contents

List of Figures

List of Tables

Chapter 1

Introduction

1.1 Background of the study

During the past few decades, industries have contributed to economy growth of the world but at the same time they have created severe environmental pollution. Most of the industries such as textile manufacturing and processing, paper, plastic, petroleum, cement, sugar and food industries are established as core industries for the progress of human society. The enhance industrial activities, specially transportation, consumption, processing and manufacturing process has not only degraded the natural biodiversity but also put stress to the environment due to accumulation of waste beyond its capacity. After globalization, the rapid economic growth by some of the developed countries has adversely affected the quality of the environment and has become a major threat to sustainable development. Since the awareness of environment started in late 80's there is a serious concern around the globe for public health due to environmental pollution. Due to vast population and developing trend in developing countries, the pollution prevention has not been taken care as per the international standard, as a result India is in the seventh position in the list of most environmentally hazardous country of the world [1].

The global water pollution due to increase in water pollutant by a number of anthropogenic activities, is a serious problem faced by the modern world. Almost all industries discharge wastewater containing heavy metals to the environment. The presence of heavy metals in surface and ground water is the most serious threat to human welfare, wild species and aquatic life. Heavy metal enters to the aqueous system from car radiator manufacturing, metal plating, tanneries, mining, painting and other such industries, also from fertilizers and pesticides used in agriculture [2]. The nonessential metals such as lead, cadmium, zinc, arsenic, etc are generally toxic and non-biodegradable in nature and create pollution in soil, water and atmosphere [3].

Lead enters into the different segments of environment and human food chain from various sources like lead-based gasoline, gunshot, paints, batteries and alloys. The increase of lead levels >0.5–0.8 $\mu g/mL$ into blood stream causes various abnormalities. The next metal which is targeted in this work is cadmium. Cadmium is also a non-essential toxic and carcinogen heavy metal [4]. The industrial process like electroplating, paint, pigment,

plastic, mining and metallurgical process uses cadmium in different form [5]. Cadmium is accumulated in the tissues of liver, kidney, pancreases and bones once it is ingested in to the human body. As a result the metabolic process are disrupted to cause disease like anemia, hypertension, neuralgia, nephritis and secretion disorder [6]. The textile industries is one of the largest and significant contributor for the economic growth of a country. The textile wastewater contains dissolved solid, toxic compound and organic dyes discharge continuously to the environment by untreated or partially treated which cause the accumulation of pollutants in soil as well as water bodies around the industries. The wastewater from dye industries not only change the chemical and biological oxygen demands of water, but also create problems to the aquatic animals and human life.

The by-product of industries exists as solid, liquid or gaseous wastes. Earlier it was not considered as a problem but now a days these materials are considered as a vexing problem to human society. The management of solid waste or by-product is one of the major concerned of the industries as well as the government. As a result of the new concept, industries and government are funding generously to utilize the by-product. Many value added product or process has been developed by utilizing the solid by-product. In this regard, red mud can be converted in to a low cost adsorbent besides its other uses. By using solid waste as suitable adsorbent it can address two most important pollution problem. (1) it will reduce the volume of waste materials generated (2) one waste can be utilized to reduce another pollutant. In past, many research are being carried out throughout the globe to utilize waste like red mud, fly ash, sludge and slag for the treatment of water and wastewater. Among all the waste, the red mud, a solid waste residue of alumina industries is one of the most potential candidates to be used as an adsorbent.

The extraction of alumina from bauxite by Bayer's process is economical and most used process. In this process, bauxite is digested with excess of sodium hydroxide at elevated temperature and pressure [7]. During the process, bauxite is converted in to soluble sodium aluminate and the insoluble component are called as 'red mud' or 'bauxite residue' [8]. The red color of the bauxite residue is due to the presence of high percentage of oxidized iron and thus termed as red mud. The *pH* of the red mud is in the range of 10.5-12.5 due to the presence of sodium hydroxide and change in the mineral composition of bauxite during Bayer's process. During the Bayer's process, the bauxite is converted in to sodium aluminate as per the following reaction:

$$2NaOH + Al_2O_3.3H_2O \rightarrow 2NaAlO_4 + 4H_2O + RedMud \tag{1.1}$$

Besides iron oxide, the other major constituents of red mud are silica, alumina and titanium oxide [9]. The general constituents of red mud (% w/w) are: Fe_2O_3 (30–60%), Al_2O_3 (10–20%), SiO_2 (3–50%), Na_2O (2–10%), CaO (2–8%) and TiO_2 (trace–10%). It is estimated that the red mud generation is in between 1–1.5 tones per tons of alumina produce depending on the quality of bauxite. In the year 2015 around 115 millions tons of

alumina are extracted which generates approximately 150 million tons of red mud [10–13]. Because of alkalinity constituent and volume of red mud generated, it possesses a severe environmental lode. Extensive researches are going on throughout the globe for utilization of red mud. The thrust area of this research is to develop an adsorbent by modification of red mud and used for the removal of hazardous inorganic and organic species from water.

Furthermore, red mud can be used as low-cost environment-friendly adsorbent for removal of hazardous inorganic metal ions and organic pollutants from water. It is reported that the adsorption capacity of red mud for heavy metal depends on the composition and procedure to prepare the adsorbent from red mud. These includes: removal of toxic substance like fluoride [14], Cr(VI) [15], arsenic [16], cadmium [17], lead [18], vanadate and molybdate [19], copper [2], phosphate [20, 21], nickel [22], organic dyes [23] from water and wastewater.

1.2 Motivation

In India, mining of ores is a major industrial process. Many ores are being exported to several other countries. Any industries for processing ores definitely produce waste or by-products. In earlier period, importance is not given for the management of waste as a part of industrial process. Due to environmental concerned several new regulation has been implemented by government. Because of that it is now becoming a practice to develop a new process on the principle of grave to cradle. The utilization of industrial waste to create any value added process or product, benefit the society both in terms of economy and environment. In last few decades, few research output has been successfully utilized one or other waste. Red mud is one such waste which has brought the attention of many researchers around the world. In present day context, recovery and purification of wastewater by another waste is a challenging job. The protection of environment by the treatment of wastewater utilizing red mud is an excellent idea. The research is carried out to explore the possibility of converting red mud to a suitable adsorbent which can be utilized for the treatment of wastewater by targeting some specific hazardous species.

These above idea motivated to undertake the present research "*Studies on the utilization of red mud for environmental application*". This work is appropriate in the present context of the solid waste utilization. The outcome of the present work will be a guiding information for future researcher in utilization of red mud.

1.3 Objective

It is reported that many industrial waste are successfully converted in to suitable adsorbent for the removal of heavy metals and organic dye from water. However, reports on modified red mud for adsorption of cation like lead, cadmium and safranin-O dye is not clarified. In

view of the above it is thought worthwhile to undertake the studies for the utilization of modified red mud adsorbent for the removal of above species from water.

The present research work is undertaken with the following objectives:

1. To prepare adsorbents by modifying the red mud after neutralization.
2. To establish the structure of modified red mud by using different instrumental and analytical techniques.
3. To study the removal efficiency of the adsorbent for the removal of Pb(II), Cd(II) and safranin-O dye separately.
4. To evaluate the mechanism of adsorption process based on the results of kinetics, thermodynamics and isotherms studies.
5. To study the effects of mass transfer for the removal process.
6. To optimize the process based on response (output variable) which is influenced by several independent variables (input variables) by Response surface methodology (RSM).

1.4 Thesis structure

The work for the thesis is organized into nine chapters. Chapter-1 represents the general introduction of the topic which includes generation, environmental problems associated, maintenance and neutralization of red mud. Chapter-2 represents the extensive literature review on utilization of red mud for environmental application specifically adsorption of hazardous metal ions and organic dye from aqueous solution. Chapter-3 describe the experimental procedure adopted for preparation of adsorbent and batch mode removal of the adsorbate. The description of instruments used for analysis and the theory used for discussion of the results has also been presented concisely. Chapter-4 describe the result and discussion for the removal of lead ions from aqueous solution using acid neutralized activated red mud. Chapter-5 represents the result and discussion with all relevant data about the adsorption capacity of acid activated red mud for removal of cadmium ions from aqueous solution. Chapter-6 describe the result and discussion of sodium dodecyl sulphate modified red mud for the removal of safranin-O dye from aqueous solution. Chapter-7 represent the details results and discussion for the removal of safranin-O dye from aqueous solution using CO_2 neutralized activated red mud by response surface methodology technique. Chapter-8 concisely represent the conclusion and summary. Chapter-9 contains the pathway towards possible future work. A complete record of references has been provided at the end of the dissertation.

Chapter 2

Literature reviews

This chapter provide the details information and discussion about the generation of bauxite residue and their harmful effects on environment. The problems for the maintenance of red mud are also discussed. To work as per the defined objective, it is necessary to know the work done in the related area. All relevant information as reported in the literature has been reviewed thoroughly and presented in brief the insight of the work. Specifically, it discusses the effect of heavy metals and organic dye on environment and human health. Further, available methods for the treatment of heavy metals and organic dye are also discussed. The utilization of red mud as adsorbent to remove the hazardous species are also presented for better understanding of the red mud utilization.

2.1 Bayer process of alumina production

The extraction of alumina from bauxite using Bayer's process by the treatment of concentrated $NaOH$ aqueous solution at high temperature (106–240 ℃) and pressure (1–6 atm) is wildly used, because of its economic viability. The Austrian chemist Karl Bayer invented the Bayer's process and patented in 1987. In this process the minerals of alumina in bauxite are converted in to tetrahydroxoaluminate $Al(OH)_4^-$ which is soluble in that solution. Subsequently it is converted to soluble sodium aluminate. The other minerals present in bauxite remain insoluble and separated as solid phase. After separation the solid phase is treated as waste and termed as "Red mud" (Figure 2.1). The details reactions involve during the process are represented below:

$$Gibbsite : Al_2O_3 \cdot 3H_2O + 2NaOH \xrightarrow{105\text{–}150^{\circ}C} 2NaAlO_2 + 4H_2O \tag{2.1}$$

$$Boehmite : Al_2O_3 \cdot H_2O + 2NaOH \xrightarrow{240^{\circ}C} 2NaAlO_2 + 2H_2O \tag{2.2}$$

$$Diaspore : Al_2O_3 \cdot H_2O + 2NaOH \xrightarrow{280^{\circ}C} 2NaAlO_2 + 2H_2O \tag{2.3}$$

The red mud generated is disposed in to red mud pond in the form of slurry which creates a number of environmental problems.

Figure 2.1: Red mud

2.2 Generation and important characteristics features of red mud/bauxite residues

2.2.1 Generation of bauxite residues

The generation of red mud depends on the quality of bauxite. It is reported that the red mud generated per tons of alumina extraction varies in the range of 0.3 tons (high-grade bauxite) to 2.5 tons (very low-grade bauxite) [8, 24]. In India, the annual capacity for the production of alumina is around 1.692 million tons, produces about 06 million tons of aluminum and 2 million tons of red mud [25]. The major alumina industries of India which generate red mud are presented in Table 2.1 [26].

Table 2.1: Estimated red mud generation in India

Name of Industries	Generation of red mud per annum (million tons)
ADITYA	1.82
JSW	1.82
RAYKAL	1.82
VEDANTA	1.82
UTKAL	1.95
HINDALCO	2.06
NALCO	2.70
Total	13.99

2.2.2 Chemical and mineral composition of red mud

Bauxite residue is highly alkaline having a pH of >12.5 and contains a complex mixture of the oxides and salts of six major elements like Fe, Al, Ti, Si, Na and Ca, along with a number of trace elements. There is high variation in the composition of red mud worldwide as it depends on the quality of bauxite. However, the typical chemical composition of red mud is presented in Table 2.2 [27].

Table 2.2: Typical composition of red mud generated worldwide

Composition	Percentage
Fe_2O_3	30-60 %
Al_2O_3	10-20 %
SiO_2	3-50 %
Na_2O	2-10 %
CaO	2-8 %
TiO_2	Trace- 10 %

Like the composition, there is also large variation in the particle size of red mud with a range of average particle size from 10 μm –20 μm [28]. Red mud is crystalline in nature having a high surface area in the range of 10–30 m^2/g depending on the magnitude of grinding of the bauxite before digestion with a true density of ~3.30 g/cm^3. The variation of chemical composition of red mud generated in different country of the world are presented in Table 2.3 [29].

Table 2.3: Variation of chemical composition of red mud (wt.%) in different country

Country		Major constituents of red mud (wt.%)				
		Fe_2O_3	Al_2O_3	TiO_2	SiO_2	Na_2O
India	MALCO	45.17	27.00	5.12	5.70	3.64
	HINDALCO	35.46	23.00	17.20	5.00	4.85
	BALCO	33.80	15.58	22.50	6.84	5.20
	NALCO	52.39	14.73	3.30	8.44	4.00
Hungary		38.45	15.20	4.60	10.15	8.12
Jamaica		50.90	14.20	6.87	3.40	3.18
Surinam		24.81	19.00	12.15	11.90	9.29
USA	ALCOA Mobile	30.40	16.20	10.11	11.14	2.00
	Arkansas	55.60	12.15	4.50	4.50	1.5-5.0
	Sherwon	50.54	11.13	Traces	2.56	9.00
FRG Baudart		38.75	20.00	5.50	13.00	8.16
Taiwan		41.30	20.21	2.90	17.93	3.80
Australia		40.50	27.70	3.50	19.90	1.2

The chemical composition of red mud in major Indian industries [30] are shown in Table 2.4.

2.3 Storage and disposal of red mud

Because of environmental awareness industries are continuously upgrading the process for the generation of cleaner residue in alumina. As per the norms the treatment, storage and disposal create a new challenge for the waste management. The important component of

Table 2.4: Chemical composition of (%) of red mud generated at different industry in India

Refinery	Al_2O_3	Fe_2O_3	SiO_2	TiO_2	CaO	Na_2O	LOI
HINDALCO Renukoot	21.9	28.1	7.5	15.6	10.2	4.5	12.2
INDAL Muri	24.3	24.5	6.2	18.0	-	5.3	-
BALCO Kobra	19.4	27.9	7.3	16.4	11.8	3.3	12.6
NALCO Damanjodi	14.8	54.8	6.4	3.7	2.5	4.8	9.5
INDAL Belgam	19.2	44.5	7.0	13.5	0.8	4.0	10.0
MALCO Mettur Dam	14.0	18.0	56.0	50.0	2.0-4.0	6.0-9.0	12.60

red mud which creates more problems to the environment are high alkalinity, heavy metals and radionuclide. The safe disposal and management of huge red mud residue is a global problem. This problem is partially addressed depending on the surrounding of the industry and facility available. As an industrial practice the red mud are stored either in the red mud ponds or use in dry landfills.

Some alumina processing plants disposing red mud by dry stacking which required less space as compared to red mud ponds. Seven alumina processing plants out of 84 are disposing red mud directly in to the sea water as these plants are located nearer to sea [31]. The disposal mechanism of major alumina processing plants of India are summarized in Table 2.5.

There are many probable uses of red mud but in most of the cases neutralization is required before it is used. The red mud storage by any of the methods adopted by industries not only creates a series of environmental problems to localities but also imparts economic problems for maintains to industries. Proper technology can solve this numerous environmental problems by utilizing the red mud either as a raw materials for some value added product or modification of red mud to reduce the toxicity, which will definitely gives some economic benefits. Extensive research are going on throughout the world for the management of red mud by safe disposal, utilization and storage [32]. The utilization of red mud require multiple approaches as there is a huge variation of the constituents [33]. The criteria for the utilization of red mud have the following important parameters.

1. Huge volume of red mud should be utilized.
2. The cost of the materials prepared from red mud should be comparable with the existing materials and performance should be more or at least same.
3. It should be economically viable.
4. There should not be any environmental impact during and after the use [33].

Table 2.5: Red mud disposal mechanism of major alumina processing plants in India

Name of the plant	Red mud (t/t) of alumina	Dumping process
INDAL, Muri	1.35-1.45	This plant disposed red mud as slurry in close cycle in red mud ponds without any liner.
NALCO, Damonjodi	1.2	This plant adopted the modified close cycle process to dispose the red mud as slurry. Before disposing the slurry is washed in six stages by counter current of pond return water (0.5 g/Na_2O). Subsequently it condensed from the evaporators. The washed red mud is wrapped and dispatch to disposal site. The bottom and sides of the ponds are provided with impervious and semi pervious clay with base filters.
Vedanta, Lanjigarh	1.3	Wet disposal as slurry
BALCO, Korba	1.3	The plant adopted the process of settling, four stage counter current washing and filtered. The filtrate is wrapped with the pond return water and disposed in the pond by using modified close cycle disposal (MCCD) system. The dykes of the currently used pond have stone masonry and well protected polythene liners and clay layer.
HINDALCO, Renukoot	1.4	The close cycle disposal method is adopted with five stages counter current washing and filtered. About 70% solid is disposed in to the ponds.
INDAL, Belgaum	1.16	The plant adopted the dry disposal mode. After clarification process in six stage counter current to washing and filtration it is disposes in to the ponds. The dry portion of the pond which covered with a 15 cm black cotton soil for vegetation.

2.4 Environmental concern associated with red mud

The environmental impacts of red mud can be locally severe and long-lived and can affect terrestrial and aquatic environments. Negative impacts can result from the residue. Red mud creates serious problem to the environment due to chemical composition and magnitude of generation. It cannot be disposed of easily because of its high alkali contained. Hence the slurry is stored in a large pond or reservoir, but that process of storing is also not free from problems like contamination of underground water by percolating through the soil and the alkaline dust spread in air which effect the plant life in dry condition. Due to instability of storage, dumping of red mud require vast area of land and even cannot prevent the mixing of dust in air to form suspended particulates matter at dry condition. Moreover, List of Waste Commission Decision (2014/955/EU) [34] categorically classified red mud as a hazardous waste, though earlier it is consider as non-hazardous. Even then, no technology has been developed so far which can utilize the red mud in large scale for commercial purpose with

an economic viability. There are many problems for the management of red mud slurry but few important problems are enlisted below:

1. Expensive maintenance of vast red mud pond.
2. Threat of alkaline pollutants to both plants and animals.
3. Percolation of alkaline slurry to contaminate the ground water.
4. Run-off contamination to surrounding environment especially in rainy session.
5. Mixing of dry dust of red mud in the atmospheric air which affects the leaving organisms [35, 36].

2.5 Red mud neutralization

As per the regulation, the *pH* of the red mud to be disposed should be around 9.2. At this *pH* the chemically adsorbed sodium is released which makes the toxic heavy metal insoluble [37]. Efforts are also being made to incorporate *pH* reduction steps at the time of disposal of red mud. The *pH* reduction steps includes acid neutralization, CO_2 treatment, sea water neutralization and sintering.

2.5.1 Acid neutralization

It is reported that minerals acid solutions, acidic industrial wastewater are used to neutralized the red mud. The carbonic acid can also be considered for same purpose. This process has a number of limitations: (1) large volume of acid are required even if spent acid are also used (2) the cost of the neutralization process will be also high (3) it will generate a large volume of impurities. (4) All these process will not be acceptable by pollution control board. Before neutralizing the red mud by 1 N HCl, the acid neutralizing capacity of red mud is evaluated and only the required amount of acid is used for the neutralization of red mud which addresses some of the disadvantages of acid neutralization process.

2.5.2 CO_2 treatment

The use of CO_2 either from industrial process or atmosphere is a promising potential for the neutralization of red mud. CO_2 gas or flue gas containing CO_2 are used for the neutralization of red mud [38]. The mechanism of the process is reported [39]. This process has also limitation. (1) Though the *pH* drops down to required level it bounce back to its original *pH* level after few days. (2) The rate of neutralization is slow, not acceptable to industries. Subsequently the use of high pressure liquid CO_2 is explored for the neutralization [40]. Researcher have also studied the use of CO_2 in multiple cycle for neutralization [41].

2.5.3 Seawater neutralization

Red mud can be neutralized by using sea water as it causes the precipitation of hydroxide, carbonate or hydroxycarbonate of calcium and magnesium present in sea water [19]. In this process, the hydroxide is not eliminated but convert the highly soluble and strongly caustic waste in to weakly alkaline and less soluble solid. The carbonate and bicarbonate alkalinity is removed with the formation of aragonite and calcite with the reaction of calcium [42]. This process has also few limitations: (1) the neutralization process is rapid initially but decreases rapidly as the *pH* approaches to 8.5 because of the formation of salt of carbonate of calcium and magnesium (2) the safe disposal of red mud is possible only when the red mud is separated at *pH* 9 with total alkalinity of less than 200 mg/L [43].

2.5.4 Sintering

Sintering is another option to fix all leachable soda, but it has also limitation: (1) the cost will be high, because of high energy consumption (2) to maintain high temperature required for sintering.

2.6 Utilization of red mud

Research are being carried out very actively for the utilization of red mud which can not only facilitated the alumina industry to manage red mud but also solve the environmental problems. The following methods are reported which may be implemented to reduce the menace of red mud [44].

- To be utilized as construction materials like bricks, blocks, gravels, aggregates and others such products.
- Can be used as raw materials in the manufacture of cement, special category of cement, as additive to cements, and for the construction of roads, dams and decorative pavements.
- Act as red pigment especially for painting of floors of industries and big buildings.
- As an additives in the pulp of paper and wood industries.
- For the manufacture of inorganic polymers and reinforced refractory products.
- As a raw materials in iron and steel industries to bind the iron ores flux.
- Rejuvenator and neutralizing agent for acidic soil.
- Extraction of valuable metals.

- To remove heavy metals from water.
- Can be used for development of catalysts as all the constituents are having catalytic properties.

2.7 Water pollution due to heavy metals

Water is not only a liquid but elixir of life. Living organism cannot sustain without water. Water are required for the domestic, agriculture and industrial purposes. It is also required for recreation, to maintain the heat balance of the atmosphere and so many other purposes. The water are getting polluted by different types of pollutants due to anthropogenic activity. Earlier it is considered as a natural abundance species and can be used in any ways but today it is not true. Water is becoming a precious natural resource. It is rightly told by Einstein in case there will be third world war it will be due to water only. Among the pollutants the metallic pollutants are very important as they are not bio-degradable and increases continuously in environment due to bio magnification. The metals like lead, cadmium, arsenic, copper, chromium, mercury, nickel, zinc etc. possesses more threat to the nature, because they enters to environment due to industrial activities [45]. Pollution due to the above metals remains for a long time and enters to food chain which causes peril issue for human health [46, 47]. There are three mechanism by which heavy metal enters to the environment such as: (1) as a by-product of mining and processing industries (2) by disposal of wastewater, sewage sludge and sewage effluents (3) by disposal of metal containing waste in open atmosphere [48]. The other sources includes the unscientific agricultural practices, forest fire and other natural calamity [49]. The local and central agencies of a country has fixed the permissible limit of all such metals to different component of environment.

2.8 Water pollution due to organic dyes

Organic dyes are essential constituents of today's lifestyle, but most of them are sustainable organic pollutants as it remains in the environment after it enters for a long periods. Hence dyes are considered as most serious environmental pollutants. The dyes reduce the penetration of light causes disruption in photosynthesis [50]. The presence of dyes in water causes the eutrophication and drastically reduced the aesthetic value. The other detrimental effects include to form toxic carcinogenic breakdown products. The ETAD (Ecological and Toxicological Association of the Dyestuff) has prescribed the LD_{50} values greater than 200 mg/kg for almost 90 of some 4000 dyestuff in use. The most toxic dyes are the basic and diazo direct dyes [51].

2.9 Conventional methods for treatment of water

A number of treatment option like precipitation [52, 53], ion exchange [54], solvent extraction [55, 56], reverse osmosis [57], dialysis/electro-dialysis [58], supported liquid membrane [59] and adsorption [60–62] are reported in the literature to remove inorganic and organic pollutants from water. All these methods have some advantages as well as disadvantages, hence they cannot be used in all conditions. These methods are not widely used because of some disadvantages which includes: difficulties in the preparation process, high cost, removal of pollutants under certain condition and generation of other waste or toxic sludge. Among the above mention methods, adsorption is one of the promising method, but it depends completely on the quality and cost of the adsorbent. Adsorption is a process where a solute is removed from the solution phase through contact with a solid matrix which has a tendency to attract the targeted solute. This process is very effective separation technique to remove organic and inorganic species from contaminated water. This process is also eco-friendly cost effective, simple operation process, easy to regenerate, and insensitive to other substances.

2.10 Utilization of red mud in environmental application

The population explosion put more stress to the environment. To full fill the requirement of growing population, industrialization, use of fertilizer and pesticides for batter crop production has increase many fold in last century. This practice generates a large number of pollutants which pollutes both surface and ground water constantly to deteriorate the environment and water. As a result, it seriously affect the existence of living organism. Thus it is very much essential to prevent the harmful effect of these pollutants for a batter environment. The heavy metals and organic dyes causes more damage than other pollutants.

Different natural and/or synthetic adsorbents can be effectively used for troubleshooting the waters contaminated with heavy metals and dyes. The adsorbent used have some disadvantages like, lower adsorption capacity, not very effective at high adsorbate concentration and low efficiency to cost ratio [63]. For instance, activated carbon is one of the most widely used materials for treatment of wastewater. However, the high cost of preparation and recovery of used material limits its application [64]. Different natural materials like clay minerals [65], zeolites [66], natural oxides [67], modified industrial waste (i.e. red mud, fly ash) have been reported as adsorbent to remove various hazardous species from polluted water. Red mud may be a suitable waste material which can be modified to prepare a good adsorbent to remove hazardous species from water. The red mud is chemically and mechanically stable having a suitable structural properties, but it requires proper modification. The utilization of red mud will benefit the environment, if the process will be economically viable. The utilization of red mud not only reduce the cost

of its management, but also prevent the contamination of soil and ground water. During modification, it can also form some value added product which can be used as a catalyst or other uses.

Different methods have been adopted for modification of red mud to enhance the adsorption properties such as acid activation [68–70], Heat and chemical treatment [71] and chemical modification using inorganic based materials [72]. Based on the published data, brief discussion is presented bellow about the adsorption capacity for different species of red mud as an adsorbent. The important findings and relevant discussion on the results are also presented.

Iron oxide is used to activate the red mud and used as an adsorbent to remove Cd(II) from aqueous solution [73]. The optimum condition for maximum adsorption of Cd(II) on to the above adsorbent is reported to be : pH of 6.0, adsorbent dose of 6.0 g/L, contact time of 90 min, initial Cd(II) concentration of 400 $\mu g/L$ and temperature of 300 K . The adsorption capacity are reported to be 117.64, 116.28, and 107.53 $\mu g/g$ by Langmuir isotherm and 3.83, 3.68, and 3.07 $\mu g/g$ by Freundlich adsorption isotherm at 293, 298, and 308 K, respectively. The adsorption process follows the pseudo-second order kinetics with film diffusion and intraparticle mechanisms. The effect on adsorption by initial Cd(II) concentration is presented in Figure 2.2.

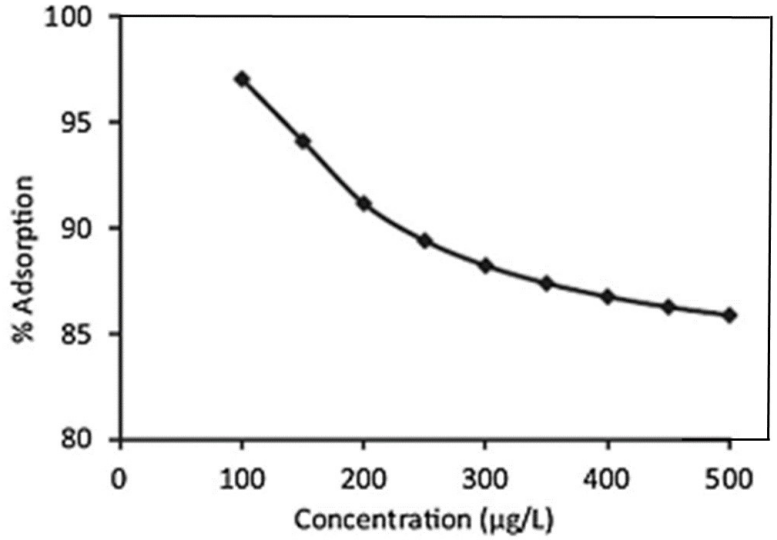

Figure 2.2: Effect of initial concentration on Cd(II) adsorption

Cd(II) is removed from water by the red mud neutralized with seawater (Bauxsol), acid treated Bauxsol (aBauxsol) and acid-heat treated Bauxsol (AB) [74]. The removal of Cd(II) decreases with increase in the concentration of cadmium and also depends on the contact time. The maximum sorption capacities is found to be 20.32, 22.48 and 24.73 mg/g for Bauxsol, aBauxsol and AB, respectively from Langmuir isotherm model indicates AB to be the best adsorbent. The overall sorption followed the second-order rate kinetics for all the

adsorbent. The negative value of ΔG indicates the spontaneity of the sorption of Cd (II) at room temperature.

Further Cd(II) is removed from the pollutant river water by bacteria-modified red mud and compared the result with results of removal of cadmium from $Cd(NO_3)_2$ solution by batch methods [75]. The red mud is modified by *Staphylococcus cohnii GC subgroup A* bacteria. The maximum adsorption capacity is reported to be 83.034 mg/g at optimum conditions (*pH* 4.0, contact time 60 min, adsorbent dose 1 mg/mL, and temperature 30 ℃) The adsorption process follows the pseudo-second-order rate equations. The negative value of $\Delta G°$ and positive value of $\Delta H°$ indicates the spontaneity and endothermic nature of the adsorption process. Moreover, the decrease in degree of freedom of the adsorbate is indicated from the positive value of $\Delta S°$.

A series of granular red mud adsorbent (GRM) are prepared by directly mixing red mud in the range of 2% to 8% mass fraction with cement, and is used to remove cadmium from aqueous solution [76]. The maximum adsorption capacity as calculated from Langmuir adsorption isotherm of GRM is reported as 9.4251, 10.1926 and 10.7887 mg/g at *pH* of 6.5 and temperature of 30, 40 and 50 ℃, respectively. The adsorption process follows the pseudo second order kinetic model. The adsorption is found to be endothermic indicated from the thermodynamic parameters.

Another heavy metal Pb(II) is removed by batch solid phase extraction (SPE) method by using red mud as an adsorbent [77]. The maximum adsorption takes place at adsorbent dose of 0.1 g for 1 h contact time with 10 mL of initial lead solution. Lead and chromium is also removed from water solution by red mud [78]. The effect of adsorbent dose, adsorbate concentration, *pH*, temperature, particle size on adsorption is also investigated. The experimental data are fitted to both Freundlich and Langmuir isotherms models. The maximum adsorption capacity of 64.79 mg/g for lead and 35.66 mg/g for chromium are reported. The results of column study indicate that it also can be used in industrial scale. The exhausted column after adsorption of metal ions could be chemically regenerated with 1% HNO_3. There is no significant effect on adsorption by other ions present in solution.

The efficiency of raw red mud (R_w), acid treated red mud (R_a) and heat treated rad mud (R_{ah}) as adsorbent to remove Pb(II) Cd(II), and Cu(II) is investigated [18]. The specific surface area is reported to be 14.2, 20.7 and 28.0 m^2/g for R_w, R_a and R_{ah} adsorbent. The order of adsorption capacity of the materials followed the sequence $Cu > Pb \geq Cd$, which is in accordance with the in solubility of corresponding metal hydroxides. The Cd, Zn, Cu and Pb ions are removed from aqueous solution by red mud in presence of 0.01 M $NaNO_3$ [79]. The maximum adsorption capacity for cadmium and zinc is reported to be 68 mg/g and 133 mg/g at *pH* 6 and 7, respectively. Both Langmuir and Freundlich isotherms models describes the adsorption process.

Cadmium is also removed from aqueous solution by granular red mud (GRM) [17]. The adsorption process follows the pseudo-second-order model at initial *pH* of 6.0 and 3.0. The

process is controlled by intraparticle-diffusion as confirmed from the mass transfer study for GRM-cadmium system at *pH* 6.0. The maximum adsorption capacity of 38.2 mg/g at 20 ℃, 43.4 mg/g at 30 ℃ and 52.1 mg/g at 40 ℃ is reported. The exhausted GRM is regenerated by 0.1 M HCl.

The feasibility of wastewater treatment by red mud aggregate of red mud and 8% (w/w) $CaSO_4$ is evaluated in both batch and column mode [80]. The maximum adsorption capacity of red mud aggregate is reported as 19.72 mg/g for Cu^{2+}, 12.59 mg/g for Zn^{2+} , 10.95 mg/g for Ni^{2+} and 10.57 mg/g for Cd^{2+} with a contact time of 48 h.

Red mud is activated by the treatment of red mud with hydrogen peroxide and used to remove cadmium and zinc from aqueous solution by both batch and column mode [81]. The red mud material was first treated with hydrogen peroxide at room temperature for 24 h to oxidize adhering organic matter and washed repeatedly with double-distilled water. The resulting material was dried at 100 ℃, cooled, and again activated in air in a muffle furnace at 500 ℃ for 3 h. Then the activated red mud was crushed into smaller particles and sieved and used for the adsorption process. At low concentration, the removal of both the ions is almost 100% at *pH* 4, but at higher concentration it is only 60-65% at *pH* 5 , adsorbent dose 10 g/L and an equilibrium time 8–10 h. The adsorption process is exothermic in nature. The maximum adsorption capacity from Langmuir model is reportedto be 1.16 $\times 10^4$ mol/g for Cd(II) and 2.22 $\times 10^4$ mol/g for Zn(II) at 30 ℃. The material is regenerated by using 1% HNO_3.

Pellet of different size are prepared by mixing in wt.% of 58.7, 25.2, 11.7, 2.9, 1.5 of red mud, kaolin, sodium silicate solutions, fly ash and magnesium chloride, respectively and calcined at 600 ℃, which is used to remove Pb^{2+}, Cu^{2+} and Cd^{2+} from aqueous solutions [82]. The experimental data indicate the fitting of Langmuir model. More than 95% of Pb^{2+}, Cu^{2+} and Cd^{2+} are removed after 24 h.

Raw red mud (RM_{nt}) and acid-treated red mud (RM_a) is used to remove Pb^{2+}, Cd^{2+} and Zn^{2+} form aqueous solution [83]. The adsorption capacity of RM_{nt} is in the order of $Zn \geq Pb > Cd$, but the adsorption capacity of RM_a is reported to decrease by 30%. The heat treated red mud is used for the removal of lead ions [84]. The adsorption data fits Langmuir isotherm model well and the maximum adsorption capacities of the heat activated red mud is 38.2 mg/g.

There are several model for analyzing the effect of different independent variable on the response but response surface methodology (RSM) is an unique model which is based on the series of mathematical and statistical method [85]. RSM is widely used for process design, optimization and enhancement in the existing design. This technique is more practical as it depends on the experimental methodology including interactive effects among the independent variables and depicts the overall effect on variable parameter of the process [86].

It is reported that both (ANN) artificial neural network and response surface methodology

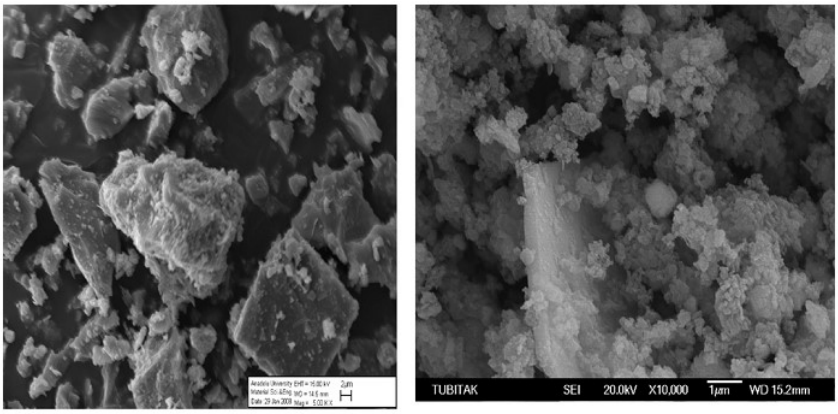

(a) (b)

Figure 2.3: SEM micrograph of the particle of red mud: (a) before adsorption and (b) after adsorption

(RSM) are applied to predict the removal of lead by red mud from leachate of industrial sludge [87]. The values of thermodynamic parameters indicate the endothermic and spontaneous nature of the adsorption process. Both the model are compared on the basis of (R^2 values) coefficient of determination, absolute average deviation (ADD) and root mean squared error (RMSE).The design matrix of RMSE by RSM and ANN model are 6.993 and 2.479 with R^2 values 0.672 and 0.898, and for ADD are 1.218 and 0.218, respectively. It is reported that the prediction by RSM model has a greater deviation than prediction by ANN model. The particles of red mud as shown in SEM micrograph before and after adsorption of lead is presented in Figure 2.3. The figure indicate that red mud contains par1ticles of different size and shape with a clear porous surface. It also contains some crystals. The pores of the surface are filled up with lead ions after adsorption.

Activated red mud (aBauxsol) is used to remove Cu(II) and Pb(II) from aqueous solution by batch mode [74]. The maximum adsorption capacity of the aBauxsol sorbent is 123.28 mg/g for Pb(II) and 21.56 mg/g for Cu(II) at *pH* 5.5 after 1 h of contact time. The adsorption process for both the ions are controlled by diffusion in the film fluid and diffusion within the particles. The adsorption process followed Langmuir model.

In India, the textile industries have grate economy significance by virtue of its contribution to overall industrial output and employment generation when compared to other industries such as leather, paper, pulp and food industries. But most of them lack effluent treatment plants. Instead, they directly discharge untreated colored and toxic effluent in to the nearby canals, rivers, lakes and streams. The discharge of industrial wastewater causes serious environmental problems due to their chemical structure which gives them a persistent and recalcitrant nature. The literature so far reviewed has shown a large number of conventional dye removal methods using low cost adsorbent involving physico chemical, chemical and biological process and some emerging techniques using low cost adsorbent. Different type of dye is removed by red mud. Some of the recent reported literature are

presented.

An anionic Congo red dye is removed by using red mud as an adsorbent from aqueous solution [23]. The adsorption process is described by first order rate kinetics. Both Langmuir and Freundlich isotherm models are fitted to equilibrium adsorption data. The maximum adsorption capacity is reported to be 4.05 mg/g at *pH* 2.0 and temperature 30 ℃ and explained by ion exchange mechanism.

Rhodamine B, fast green and methylene blue basic dyes are removed by H_2O_2-activated red mud from wastewater [88]. The removal percentages are 92.5% for rhodamine B at *pH* 1.0, 94.0% for fast green at *pH* 7.0 and 75.2% for methylene blue at *pH* 8.0. The adsorption for all the dyes are reported as exothermic in nature. Desorption of dyes are studied with a number of solvent but acetone is found to be best for dye desorption.

Activated red mud is used to remove acid blue 113 (AB113) and reactive black 5 (RB5) dyes from water solutions with the variation of different reaction parameters [68]. The red mud is activated (ARM) at a ratio of 1:2 of red mud and 1 N nitric acid (w/v) for 24 h and the material formed is activated in an oven for 4 h at 150 ℃. The removal efficiency for AB113 is better than RB5 due to smaller molecular size of AB113. Moreover, the binding site for AB113 and RB5 is also different. The Fruindlich isotherm model is in better agreement with experimental data. The pseudo second-order model describes the adsorption process.

Adsorbent is prepared by heat treatment of seawater neutralized red mud (SWRM) and used to remove the Reactive Blue dye 19 (RB19) [89]. The adsorption capacity of the adsorbent is found to increase due to the transformation of hydroxides to corresponding oxides which increase the surface area. The adsorption capacity of SWNRM400 (heated to 400 ℃) is 416.7 mg/g for RB19 in acidic medium which is greater than untreated SWNRM and SWRM500 (heated to 500 ℃). The pseudo-second-order reaction mechanism describes the adsorption process and electrostatic interactions is responsible for batter adsorption. It is reported that the adsorption potential of red mud in batch mode for Acid blue 15 dye from aqueous solutions is investigated [90]. The maximum adsorption capacity of 29.44 mg/g for AB 15 is reported.

Acid violet from wastewater is removed by red mud [91]. The adsorption capacity of 1.37 mg/g at *pH* 4.1 is reported from Langmuir isotherm model. Due to formation of aqua complex causes the dissociation of acid-base at solid/solution interface. The percentage of removal decreases with the increase in *pH* and the desorption of dye increases with increase in *pH*. The following mechanism is proposed for the removal in acidic solution.

$$\mathrm{O}\!-\!\mathrm{M}\!\begin{array}{l}\diagup\mathrm{O}\\\diagdown\mathrm{O}\end{array} + H - OH \xrightarrow{H^+} \mathrm{OH_2^+}\!-\!\mathrm{M}\!\begin{array}{l}\diagup\mathrm{O}\\\diagdown\mathrm{O}\end{array} + OH^- \tag{2.4}$$

$$\mathrm{Cl^-/OH_2^+}\text{—}\mathrm{M}\begin{matrix}\diagup\mathrm{O}\\ \diagdown\mathrm{O}\end{matrix} + Dye \longrightarrow \mathrm{Dye/OH_2^+}\text{—}\mathrm{M}\begin{matrix}\diagup\mathrm{O}\\ \diagdown\mathrm{O}\end{matrix} + Cl^- \tag{2.5}$$

The positive charge on the oxide solution interface decreases with increase in *pH* but when the *pH* is greater than pH_{zpc} of the adsorbent, the surface became negatively charged may be due to association of positively charge ions as represented bellow.

$$\mathrm{Na^+/O^-}\text{—}\mathrm{M}\begin{matrix}\diagup\mathrm{O}\\ \diagdown\mathrm{O}\end{matrix} \tag{2.6}$$

Two cationic dye, malachite green (MG) and crystal violet (CV) is removed from aqueous solution by the acid activated sintering process red mud (ASRM) [69]. The adsorption is most favorable for both the dyes at *pH* higher than 3.2. The maximum adsorption capacities are 336.4 mg/g for MG and 60.5 mg/g for CV at 25 ℃, as calculated from Langmuir isotherm model. The ΔH value indicates the endothermic nature of the adsorption for MG but exothermic in nature for CV. The adsorption process followed pseudo-second order kinetic model. The mechanism of adsorption for MG and CV on ASRM is explained by two different ways as shown below:

1. Due to electrostatic interaction between the positive charge (–N^+) on cationic dye and the negative charge on ASRM presented by ion exchange or Si–O–Si structures.

$$ASRM\text{–}OH + N^+((CH_3)_2)\text{–}Dye \longrightarrow ASRM\text{–}O\text{–}N((CH_3)_2)\text{–}Dye + H^+ \tag{2.7}$$

$$ASRM\text{–}Si\text{–}O^- + N^+((CH_3)_2)\text{–}Dye \longrightarrow ASRM\text{–}Si\text{–}O\text{–}N((CH_3)_2)\text{–}Dye \tag{2.8}$$

2. Due to hydrogen bonding between the nitrogen atom of dyes and OH on the surface of ASRM as suggested in Figure 2.4.

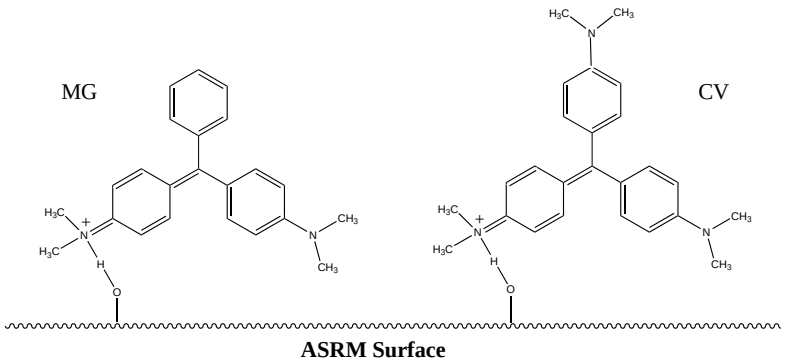

Figure 2.4: Proposed hydrogen bonding interaction for the adsorption of MG and CV on ASRM

2.11 Research gap

It is known from the literature that a number of research works has been carried out using red mud as an adsorbent to remove heavy metals and dyes. The activation of red mud are made by acid neutralization, calcination, and sea water neutralization or doping with the metal salts. However it is not clarified the specific changes in the structure of red mud by changing the process of neutralization by acid and subsequent activation. Similarly the use of surfactant and acid for neutralization of red mud adsorbent for safranin-O dye removal is not reported. This fact encourage to undertake the present work.

2.12 Aims and purposes

There are many objectives in this research which includes the neutralization of red mud and its modification, the characterization of the adsorbent material, the study of adsorption and desorption behavior of two heavy metals and a cationic dye from synthetic water solution separately. To be very specific, there are two main objectives of this research:

1. Modification of red mud
2. To know the adsorption capacity of the material for Pb(II), Cd(II) and safranin-O dye

The main purpose of this work is to fulfill the main objective which includes the research activity like neutralization by acid and CO_2 in gas phase. Then the neutralized red mud is modified by different process. The modified adsorbent materials are characterized before and after adsorption by XRD, SEM, EDX, TGA/DSC, AAS, UV-Visible, FTIR and BET techniques. The adsorption capacity of the adsorbent used to remove Pb(II), Cd(II) and Safranin-O dye from synthetic aqueous solution is evaluated by doing all relevant experimental methods. The structural properties and phase changes is determined by XRD. The pore volume, pore diameter and surface area of the adsorbent are analyse by BET-N_2 adsorption/desorption method. The surface functional group is determined by FT–IR analysis. The surface morphology of the adsorbent is examined by SEM and the percentage composition is found from the corresponding EDX analysis. The stability of the adsorbent is examined by TGA/DSC. The AAS and UV-Visible analytical techniques are used to measure the concentration of metal ions and dyes after adsorption, respectively. The adsorption efficiency of modified red mud is evaluated by using response surface methodology techniques with the help of Design Expert 7.0 software. The mechanism of the adsorption process is proposed best on the results of kinetics, thermodynamics and isotherms studies. The mass transfer for the removal process is also studied.

Chapter 3

Materials and methods

This chapter presents the details procedure of experiment conducted during the course of this research work. The details of chemicals and glassware used in this work are discussed. The preparation of adsorbent and instrumental technique used for characterization are included in this chapter. The details study to know the adsorption capacity in batch mode are elaborately presented. The theories which are used for explanation of the results are also discussed.

3.1 Reagents and Chemicals

AR grade chemicals were used in this study and acquired from Merck (Germany, and Mumbai (India)) and Rankem (New Delhi (India)). All glassware used were of Borosil or Tarson make. The cationic Safranin-O dye and the anionic surfactant used in this study were obtained from Sigma-Aldrich, Steinheim (Germany). CO_2 gas with 20% volume was procured from a local vender SKP enterprises, Rourkela and used as in where basis. The physiochemical properties of safranin-O are shown in Table 3.1.

Table 3.1: The physiochemical properties of the safranin-O dye

Molecular formula	$C_{20}H_{19}N_4Cl$
Molecular weight (g/mol)	350.85
IUPAC name	3,7-diamino-2,8-dimethyl-5-phenylphenazinium chloride
λ_{max} (nm)	520
Generic name	C.I. Basic Red 2

3.2 Adsorbate preparation

Stock solutions of Pb(II) ions, Cd(II) ions and safranin-O dye were prepared by dissolving 1.598 g of $Pb(NO_3)_2$, 2.736 g of $Cd(NO_3)_2 \cdot 4H_2O$ and 1 g safranin-O in 1 liter of double distilled water to form 1000 mg/L separately. Different concentrations (5–100 mg/L) of test solutions of Pb(II) and Cd(II) were prepared by proper dilution of the stock solutions. Different test solution of safranin-O were prepared by proper dilution and their concentration were measured using calibration curve. 0.1 M HCl and 0.1 M $NaOH$ were used to maintain the *pH* of the solution.

3.3 Adsorbent preparation

In this present study the used red mud was obtained from Vedanta Aluminum Industries, Langigarh, Odisha, India. The chemical compositions of dry red mud was examined and found to contain Fe_2O_3 (54%), Al_2O_3 (13%), SiO_2 (7%), Na_2O (8%) and TiO_2 (3.5%).

3.3.1 Preparation of adsorbent for removal of Pb(II) and Cd(II) ions

Acid dilution followed by ammonia precipitation method was used for the preparation of activated red mud (ARM). Approximately 10 g of red mud was taken in a 1000 mL beaker and 190 g of Millipore water was added to form slurry. Then 18 g of 31 wt.% HCl was added to the slurry and heated at 60 ℃ for 20 min with constant stirring. Than the solution was diluted with water to make a total volume of ~800 cm^3 and settle down for some time. After that, the acidic solution was removed by decantation. Than the liquid ammonia solution (specific gravity 0.880) was added slowly with constant stirring, until a *pH* of ~8 was reached for complete precipitation. Then the resulting precipitate mixture were heated at 50 ℃ for ~10 min with constant stirring. The precipitate obtained was separated by filtration, wash three times with distilled water and dried overnight in air oven at 110 ℃. Finally, calcined in air oven at 500 ℃ for 2 hours which was referred as activated red mud (ARM) and kept in an air tight container until used [92]. The basis for preparing acid activated red mud was to neutralize the highly alkaline red mud.

3.3.2 Preparation of adsorbent for removal of safranin-O dye

The red mud was modified and used for the removal of safranin-O dye by following two methods:

Method I

10 g of red mud was taken in a 500 mL conical flask. Then 30 mL of H_2SO_4 (16 mol/L) was slowly added and the reaction mixture was stirred for 2 h at 80 ℃. After that, 100 mL of deionized water was added into the flask to extract soluble compounds from the resultant mixture. The resulting solution was then centrifuged at 3000 rpm for 10 min to separate the solid product and washed three times with distilled water and dried at 100 ℃ in an oven for 24 h.

For the modification of the surface of the red mud, 0.1 g of the above chemically treated red mud was first dispersed in 50 mL of distilled water for 2 h at room temperature using a magnetic stirrer to swell and reach the homogeneity. The *pH* of the solution was maintained at *pH* 4 using 0.1 M hydrochloric acid. Then 1.0 mL of 5% (m/v) sodium dodecyl sulphate (SDS) surfactant was added and the mixture was stirred for 1 h. The SDS surfactant was added to the solution of red mud at a concentration lower than its critical

micelle concentration (CMC = 2.3 g/L) to modify the surface of the red mud. The mixture was separated by centrifugation and dried in an air oven at 30 ℃. The sodium dodecyl sulphate modified red mud (SDS/RM) was kept in an airtight container until used.

Method II

The alkaline red mud slurry was taken in a beaker and settle down for some time, than the supernatant liquid was removed from the solid red mud by decantation. In a 500 mL gas close-fitting plastic bottle with a bay for CO_2 gas and an opening to escape the pressure, approximately 10 g red mud was taken and mixed with 100 mL distilled water. The solution mixture was stirred with a mechanical stirrer with stirring speed (180 rpm) at room temperature. The CO_2 gas was passed into the red mud solution with a gas flow rate of 5 mL/min through a rotameter until the *pH* of the red mud suspension decreases from 12.8 to 7.37. After that the neutralized red mud was separated by centrifugation for 20 min at 3000 rpm and dried in an air oven at 110 ℃ for 2 h. The material was calcined at 500 ℃ for 2 h which referred as CO_2 neutralized activated red mud (ARM) and stored in an airtight glass bottle until used.

3.3.3 Leaching test of the red mud

All experiments were conducted in 500 mL Erlenmeyer flasks at 25 ℃ and at 200 rpm agitation. Deionized water (100 mL) was added to 10 g (dry weight) of red mud samples. 20 mL HCl and H_2SO_4 was added in the above conical flask separately for leaching test [93]. The samples were then brought to a final volume of 200 mL using deionized water. At the end of the leaching process, the mixture solution was centrifuge and the resulting super latent liquid was examined and found to contain mainly Al, Si, and Na bellow the permissible limit of WHO.

3.4 Characterization of the adsorbent

3.4.1 Density and porosity

The physical properties of red mud like specific gravity, bulk density, density and dry density were determined by using 10 mL capacity pyconometer. The following equations were used for the determination of densities.

$$Specific\ gravity(S) = \frac{weight\ of\ the\ sample}{weight\ of\ equal\ volume\ of\ water} \tag{3.1}$$

$$= \frac{(W_2 - W_1)}{[(W_4 - W_1) - (W_3 - W_2)]} \tag{3.2}$$

$$Bulk\ density(v) = Weight\ of\ density\ bottle + \frac{sample}{10\ mL} \tag{3.3}$$

$$Dry\ density(V_d) = \frac{v}{1 + W} \tag{3.4}$$

Where, W_1 = weight of the empty bottle. W_2 = weight of the bottle with the sample (1 g) W_3 = weight of the bottle containing 1 g of the sample and water W_4 = weight of the bottle with water W = weight of the water.

Porosity was determined from the specific gravity (S) and bulk density (v) values of the adsorbent by applying the following formula:

$$Porosity\% = \frac{(S - v)}{S \times 100} \tag{3.5}$$

3.4.2 Point zero charge (pH_{zpc})

The surface electrochemical properties of the adsorbent were carried out by comparing the *pH* value at the point zero charge (pH_{zpc}). The point zero charge is the *pH* of the suspension where the density of the surface charge is zero. The increase in pH_{zpc} value indicates the presence of acidic functional group due to release of H^+ ion and the decrease in pH_{zpc} value indicate the presence of basic functional group due to release of OH^- ion. In this study, the mass titration method was adopted, even though acid/base potentiometric titration method was convenient for pH_{zpc} evaluation.

In the mass titration method, three electrolytic solutions having *pH* 3, 6 and 11 were prepared by the addition of 0.1 M $NaNO_3$ and 0.1 M $NaCl$. The *pH* of the solution were adjusted to require value by using 0.1 M HNO_3 and 0.1 M $NaOH$. 0.05%, 0.3%, 0.5%, 1.0%, 3.0% and 5.0% concentration of the suspension of adsorbent were prepared by using 50 mL of the electrolytic solution at a definite *pH*. The bottles were scaled and shake at 150 rpm for 2 h in a rotary shaker to attain the equilibrium. After equilibrium, the final *pH* was measured. The difference in value between the final and initial *pH* was plotted against the final *pH*. In the graph the point of zero *pH* gives the point of zero charge value.

3.4.3 X-ray diffraction study

The powder X-ray diffraction (XRD) of sample was determined by using Philip's (Netherlands) PAN analytical X'Pert X-ray diffractometer with a Cu Kα radiations source generated at 35 kV and 30 mA. Scattering angle 2θ was ranged from 10 to 80° at a scanning rate of 2° min^{-1} and was analyzed using X'pert High score software provided with the

instrument. The samples were oven-dried at a temperature of 110 ℃ for 2 h before the analyses. The X-Ray pattern of the material and mineral composition of different phases are determined by using XRD.

3.4.4 Scanning electron microscope (SEM) and energy dispersive X-ray (EDX)

The surface micro-morphology of materials was investigated using scanning electron microscope (SEM) and corresponding qualitative element composition was analyzed using energy dispersive X-ray (EDX) operated at an accelerating voltage of $2\theta\ keV$, (JOEL model JSM-6480LV, Japan). The sample was coated with platinum for 30 to 90 seconds as required at a current strength of 50 mA at vacuum before obtaining the SEM micrograph.

3.4.5 FT–IR study

FT–IR spectra of the samples were obtained by using PerkinElmer FT–IR Spectrometer Spectrum RX-I (USA). The spectrum obtained at 4 cm^{-1} resolution spectra in the range of wave number 400–4000 cm^{-1} of the adsorbent before and after adsorption.

3.4.6 BET surface area

The BET surface area was measured at liquid N_2 temperature using the Brunauer–Emmett–Teller (BET) surface area analyzer (Quantachrome AUTOSORB-1, USA). The samples were degassed at 100–150 ℃ in vacuum. Helium was used as carrier gas and surface area was measured by N_2 adsorption–desorption method. The multipoint BET method was used to measure total surface area.

3.4.7 Particle size analysis

The particle sizes of the adsorbent were determined by wet method by particle size analyzer (Nano-ZS 90, MALVERN, UK). The sample powder was dispersed in a solvent (deionized water) and diluted to 100 mL in volumetric flask. The 10 mL of sample was taken in quartz cube for analysis.

3.4.8 Thermogravimetric analysis (TGA) and differential scanning calorimetric (DSC) analysis

The thermogravimetric (TG) analysis and differential scanning calorimetric (DSC) analysis of air dried samples were carried out using NETZSCH STA 449C, Germany. In this analysis, 40 mg of sample was used and alumina was used as reference. The sample was heated in an Al_2O_3 crucible at a heating rate of 10.0 ℃ min^{-1} from 25 to 900 ℃.

3.4.9 *pH* analysis

The *pH* measurements of aqueous solutions were made using a calibrated Orion 2 Star bench top *pH* meter and PHAN Lab India *pH* analyser.

3.4.10 Atomic absorption spectrometer (AAS)

After adsorption, concentration of Pb(II) and Cd(II) in the filtrate was determined by using VARIAN, AA240 atomic absorption spectrometer (AAS) using standard method. Calibration was made using proper concentration of standard solution prepared from stock solution by dilutions.

3.4.11 UV-visible spectrophotometer

The concentrations of safranin-O in water were determined from the calibration curve at λ_{max} = 520 nm using UV-visible spectrophotometer (PerkinElmer).

3.5 Batch experiment study

3.5.1 Adsorption study

Adsorption experiments were conducted using the batch method by varying the initial adsorbate concentration, initial *pH*, temperature, contact time and adsorbent dose. The experiments were carried in a 250 mL stopper conical flask containing a fixed amount of adsorbent with 100 mL of standard initial concentration of adsorbate. The ionic strength of the aqueous solutions were adjusted with $NaCl$. The flasks were shaken in an electrically thermostatic reciprocating shaker at 120 rpm for the desired contact time. The time required to reach the equilibrium condition was estimated by drawing samples at regular intervals till equilibrium was obtained. After stirring, the solutions were allowed to settle for 10 min and the samples were centrifuged (3000 rpm for 20 min) and filtered through a Whatman 42 filter paper (for safranin-O dye removal, filtration is not required). The filtrate was used for the analysis of residual Pb(II) and Cd(II) concentration.

In order to study the effect of *pH* on the adsorption rate, the *pH* of the adsorptive solutions were varied from 2 to 12 using 0.1 N HCl or 0.1 N $NaOH$ solutions keeping all other solution parameter constant. The *pH* measurements were done after standardizing the *pH* electrode. The effect of adsorbent dose on adsorption was studied with the variation of dose in the range of 0.1–1 g. The effect of temperature was carried out by varying the temperature in the range of 10–60 ℃. The effect of contact time was studied from 10 to 90 min. The experiments were conducted with the variation of initial concentration from 10 mg/L to 100 mg/L to know the adsorption efficiency of the adsorbent. The effects of each parameter were

evaluated in an experiment by varying the specific parameter, while keeping other parameters constant.

For each experiment, the adsorbate concentrations on before and after adsorption were determined by atomic absorption spectrophotometer (AAS) (in case of Pb(II) and Cd(II)) and UV-visible spectrophotometer by fixing the λ_{max} value at 520 nm (in case of safranin-O dye). The following equation was used to calculate the percentage of adsorbate in the surface of adsorbent:

$$\%Removal = \frac{(C_0 - C_e)}{C_0} \times 100 \tag{3.6}$$

$$q_e(mg/g) = \frac{(C_0 - C_e)}{m} \times v \tag{3.7}$$

where C_0 and C_e (mg/L) are the initial and final concentration of dye. V is the volume of the solution (L) and M is the mass of adsorbent (g).

3.5.2 Desorption study

After completion of the adsorption experiments, 0.5 g of metal loaded adsorbent was centrifuged at 3000 rpm for 30 min with 50 mL of distilled water with different *pH* by the addition of 1.0 M HCl and 1.0 M $NaOH$ solution. In case of safranin-O dye, the desorption experiment was carried out by taking 0.5 g dye loaded adsorbent with 50 mL of different solvents such as water, sulphuric acid (0.1 M), hydrochloric acid (0.1 M) and acetic acid (0.1 M) and centrifuged at 3000 rpm for 30 min. After 30 min of centrifugation the residual desorbed solution was analyzed by instrumental techniques as given in the adsorption studies.

3.5.3 Re-usability study

0.5 g of regenerated adsorbent were added to 100 mL of 10 mg/L adsorbate solution (Pb(II)) in a series of 250 mL beaker. The containers were shacked with rotary shaker for 2 h. The solid were separated by centrifugation and the residual solution was analyzed by instrumental techniques as described earlier.

3.6 Kinetic models of adsorption

Adsorption kinetics studies is undertaken to know the rate controlling step of the adsorption and the mechanism of adsorption. The mechanism of the adsorption process indicates the chemical interaction of functional groups present on the surface of the adsorbent and the adsorbate.

Various kinetics adsorption models were applied to know the order of interactions between adsorbent–adsorbate and the rate of adsorption of the adsorbate species. In this

present study, the following kinetic models were applied to study the mechanism of the adsorption of adsorbate on adsorbent.

3.6.1 Pseudo-first-order kinetic model

The pseudo first order equation developed by Lagergren in the year 1898 is used wildly in liquid phase adsorption process. The equation is represented as follows [94, 95]:

$$log(q_e - q_t) = logq_e - \left(\frac{K_1 t}{2.303}\right) \tag{3.8}$$

where q_e and q_t are the amount of lead adsorbed (mg/g) at equilibrium and at time t (min), respectively. K_1 is the pseudo-first order rate constant (min^{-1}). The K_1 and the correlation coefficient R^2 value can be calculated from the slope of the linear plot of $log(q_e - q_t)$ versus 't' at different time intervals.

3.6.2 Pseudo-second-order kinetic model

The assumption that developed the pseudo-second-order kinetic model is the rate of limiting step due to the chemical adsorption or adsorption involving valence forces either by exchange or sharing of electrons between absorbent and adsorbate.

The pseudo-second-order rate expression is:

$$\frac{t}{q_t} = \frac{1}{K_2 q_e^2} + \frac{t}{q_e} \tag{3.9}$$

where q_e (mg/g) and q_t (mg/g) are the quantity of the adsorbate adsorbed on the adsorbent at equilibrium time and at time t (min) respectively. q_e and K_2 (the pseudo-second-order rate constant ($g/mg \cdot min$)) can be calculated from the slope and intercept of the plot t/q_t versus time 't' respectively.

3.6.3 Elovich's model

The Elovich Model is represented [96]:

$$q_t = \frac{1}{\beta}\, ln\, (\alpha\beta) + \frac{1}{\beta} ln\, t \tag{3.10}$$

where α ($mg/g \cdot min$) = adsorption rate, β = magnitude of surface coverage. The Elovich constant α and β can be calculated from the slope and intercept of the linear plot of q_t versus lnt, respectively.

3.6.4 Bangham's Model

The slow step which occurs in the later stage of the adsorption process can be known from the kinetic data by using Bangham's equation [97] as represented bellow.

$$log\ log\left(\frac{C_0}{C_0 - q{\times}m}\right) = log\left(\frac{k_0{\times}m}{2.303{\times}V}\right) + \alpha\ log\ t \tag{3.11}$$

where, C_0 (mg/L) = initial concentration of the adsorbate , V (mL) = volume of solution , m (g/L) = adsorbent weight per liter of solution, q (mg/g) = amount of adsorbate retained at time t, α (<1) and k_0 (g) are constants. $log\ log[C_0/(C_0 - q{\times}m)]$ values are plotted against $log\ t$ in Bangham's plot.

3.6.5 Intra particle diffusion model

Adsorption occurs in multiple steps involving the transport of the solute from aqueous phase to the surface of the solid phase of the adsorbent followed by diffusion in to the matrix. The quantity adsorbed (q_t) is proportional to the $t^{1/2}$ when the rate is controlled by pore and intra particle diffusion.

The Weber-Morris rate constant for intraparticle diffusion model is represented as follows:

$$q_e = K_{ip}t^{0.5} + C \tag{3.12}$$

where q_t (mg/g) is the quantity of adsorbate adsorbed at time t. k_{ip} ($mg/g{\cdot}\,min$) is the intraparticle diffusion rate constant and C (mg/g) represents the thickness of the boundary layer which can be calculated from the slope and intercept of the plot q_t versus $t^{1/2}$ respectively at different initial concentration of adsorbate. The values of intercept give an idea about the thickness of boundary layer.

To predict the actual slow step involved, the kinetic data were analyzed by Boyd $et\ al.$ model to confirm both film and pore diffusion [98]:

$$F = 1 - \frac{6}{\pi^2}\sum_{m=1}^{\infty}\frac{1}{m^2}\ exp\left[\frac{-D_i\pi^2m^2t}{r^2}\right] \tag{3.13}$$

$$F = 1 - \frac{6}{\pi^2}\sum_{m=1}^{\infty}\frac{1}{m^2}\ exp(m^2\ B\ t) \tag{3.14}$$

where m = integer and F = fraction of solute adsorbed at time t which can be calculated by the following expression:

$$F = \frac{q_t}{q_\infty} \tag{3.15}$$

$$B = \frac{D_i \pi^2}{r^2} \tag{3.16}$$

where q_t (mg/g) = quantity of adsorbate adsorbed at time t (min) and q_∞ (mg/g) = quantity of adsorbate adsorbed at infinite time t . B = time constant (min^{-1}), r = radius of the adsorbent particle assumed to be spherical.

For every calculated value of F, corresponding values of B are computed from the following equations:

$$Bt = -0.4977 - ln\,(1 - F) \tag{3.17}$$

The plot between calculated Bt values versus time t are used to know the adsorption mechanism as film diffusion or particle controlled mechanism. If the graph is a straight line passing through the origin indicates the particle diffusion mechanism for adsorption [99]. The calculated B values are used to evaluate the effective diffusion coefficient, D_i (m^2/s) using the (Equation 3.16). The linear plot of lnD_i verses $1/T$ allow to use Arrhenius equation for the determination of D_0, E_a and $\Delta S^\#$ as per the following formula:

$$ln\ D_i = ln\ D_0 - \frac{E_a}{RT} \tag{3.18}$$

$$ln\ D_0 = ln\ 2.72 + ln\ D^2 + ln\left(\frac{K_B T}{h}\right) + \left[\frac{\Delta S^\#}{R}\right] \tag{3.19}$$

where D_0 = pre-exponential constant, E_a = energy of activation, $\Delta S^\#$ = entropy; D = distance between the active site of the adsorbent. K_B = Boltzmann constant, h = Planks constant and R = gas constant.

3.6.6 Mass transfer study

Mass transfer analysis is carried out to determine the surface mass transfer coefficient, k_f and adsorption of adsorbate on adsorbent by using the mass transfer model given by McKay and co-workers [100] as:

$$ln\left[\frac{C_t}{C_0} - \frac{1}{(1+mK)}\right] = ln\left[\frac{mK}{(1+mK)}\right] - \left[\frac{(1+mK)}{mK}\right] \times k_f S_s t \tag{3.20}$$

where C_0 (mg/L) = initial concentration of adsorbate, C_t (mg/L) = concentration of the adsorbate at time t, m (g/L) = mass of adsorbent per unit volume, K $(q_m b)$ (L/g) = Langmuir constant, k_f = mass transfer coefficient (cm/s), S_s (cm^{-1}) = specific particle surface area for mass transfer. The surface mass transfer coefficient k_f can be calculated from the linear plot of $ln[(C_t/C_0) - 1/(1+mK)]$ versus 't'.

The value of S_s is calculated by the following equation:

$$S_s = \frac{6m}{d_p \rho_p (1 - \varepsilon_p)} \tag{3.21}$$

where d_p (cm) = particle diameter, ρ_p (g/L) = density of the adsorbent particles and ε_p = porosity of the adsorbent particles.

Waber-Mathews equation [101] to determine k_f is represented as::

$$\frac{d\left(\frac{C_t}{C_0}\right)}{dt} = -k_f S_s \tag{3.22}$$

where C_0 (mg/L) = initial concentration of adsorbate, C_t (mg/L) = concentration of the adsorbate at time t and S_s = specific particle surface area of the adsorbent. From the Weber model k_f values can be calculated from the slope of the straight line obtained from the plot of C_t/C_o versus t.

3.7 Adsorption Isotherm study

The interaction of adsorbate molecules with adsorbent surface is described by the adsorption isotherms. The experimental isotherm data can be applied to different isotherm models to find the best fitted model to design a process. The equilibrium adsorption data were fitted to Langmiur, Frundlich, Temkin, Dubnin-Raduskevich, Elovich and Harkin-Jura isotherm models to ascertain the best fitted model. The correlation coefficients R^2 value were compared to find the best fitted isotherm model.

3.7.1 Langmuir isotherm model

Langmuir adsorption isotherm is most widely used for the adsorption of a salute from a liquid solution based on the assumption that the adsorption occurs at a suitable homogeneous site of the adsorbent. The theme of Langmuir model based on the ideal localized monolayer model are: (a) solute molecules are adsorbed at specific site on the surface of the adsorbent (b) only one molecule can accommodate in each site (c) the area of each site is a fixed quantity determine only by geometry of the surface (d) the energy of adsorption is same in all the site (e) the molecules once adsorbed cannot interact with neighboring molecules or migrate across the surface (f) adsorption is reversible.

The linearized Langmuir isotherm can be expressed as [102]:

$$\frac{1}{q_e} = \frac{1}{q_m b C_e} + \frac{1}{q_m} \tag{3.23}$$

or

$$\frac{C_e}{q_e} = \frac{C_e}{q_m b} + \frac{C_e}{q_m} \tag{3.24}$$

The non-linear form of Langmuir isotherm is:

$$q_e = \frac{q_m b C_e}{1 + bC_e} \tag{3.25}$$

where C_e = equilibrium concentration of adsorbate in solution (mg/L), q_e = amount adsorbate adsorbed at equilibrium (mg/g), q_m = theoretical maximum adsorption capacity (mg/g) and b = Langmuir constant (L/mg) corresponds to energy of sorption which can be calculated from the slope and intercept of the linear plot of Langmuir isotherm, respectively.

The adsorption efficiency and favorable or non-favorable adsorption process will be known from the dimensionless equilibrium parameter (r) calculated by using binding energy constant obtained from Langmuir adsorption isotherm. The value of 'r' is calculated from the following equation:

$$r = \frac{1}{(1 + bC_0)} \tag{3.26}$$

where C_0 (mg/L) is the initial concentration, b (L/mg) is the Langmuir constant. From the r values, the adsorption process can be described below: the process is unfavorable if r >1, the process is linear if r = 1, the process is favorable if 0 <r <1 and the process is irreversible if r = 0.

3.7.2 Freundlich isotherm model

Freundlich isotherm model describe the heterogeneous adsorption process, i.e., adsorption which takes place on a heterogeneous surface through a multilayer adsorption mechanism. The linearized Freundlich equation is represented as:

$$logq_e = logK_f + \frac{1}{n} logC_e \tag{3.27}$$

The non-linear form of the equation is represented as:

$$q_e = K_f C_e^{1/n} \tag{3.28}$$

Where K_f (mg/g) = Freundlich constant, $1/n$ = heterogeneity factor of adsorption, calculated from intercept and slope of lnq_e versus lnC_e linear plot, respectively. $1/n$ value should be less than unity for high adsorptive capacity [103]. q_e (mg/g) = amount of adsorbate adsorbed at equilibrium time 't', C_e (mg/L) = equilibrium concentration of adsorbate solution.

3.7.3 Dubinin-Radushkevich (D-R) isotherm model

Dubinin-Radushkevich isotherm model assumes that the characteristics curves of the adsorption are related to porosity of the adsorbent. The apparent free energy and characteristics of adsorption is estimated from this model. The mathematical equation of

D–R model is represented as:

$$lnq_e = lnq_m - K\varepsilon^2 \tag{3.29}$$

$$\varepsilon = RTln\left(1 + \frac{1}{C_e}\right) \tag{3.30}$$

where ε = polanyi potential, q_e = quantity of adsorbate adsorbed per unit mass of adsorbent, q_m = theoretical adsorption capacity, C_e = equilibrium concentration of adsorbate, K = constant related to adsorption energy, R = gas constant in $kJ/mol\cdot K$ and T = temperature in kelvin. A linear plot is obtained from the plot lnq_e versus ε^2 and the constant K and q_m can be calculated from slop and intercept, respectively.

3.7.4 Temkin isotherm model

The effect of indirect adsorbent–adsorbate interactions on adsorption can be known from Temkin isotherm. Due to the above interaction the heat of adsorption would decrease linearly for all the molecule because of the coverage of the surface [104]. The adsorption is known from the distribution of binding energy to reach a maximum binding energy.

The linearized Temkin isotherm is represented as:

$$q_e = B_1 lnK_T + B_1 lnC_e \tag{3.31}$$

The non-linear form of Temkin isotherm model is:

$$q_e = \frac{RT}{b} ln(K_T C_e) \tag{3.32}$$

where B_1 = Temkin adsorption constant describe the heat of adsorption (i.e. RT/b), K_T (L/mg) = equilibrium binding constant. The isotherm constant K_T and B_1 can be determined from the plot of q_e versus lnC_e.

3.7.5 Elovich isotherm model

The Elovich model is:

$$ln\left(\frac{q_e}{C_e}\right) = ln\left(K_E\, q_m\right) - \frac{q_e}{q_m} \tag{3.33}$$

where K_E is the Elovich equilibrium constant. The isotherm parameter is determined from the slope and the intercept of the plot $ln(q_e/C_e)$ verses q_e.

3.7.6 Harkin-Jura isotherm model

The Harkin-Jura [105] adsorption isotherm model is:

$$\frac{1}{q_e^2} = \frac{B}{A} - \frac{1}{A}\, log\, C_e \tag{3.34}$$

where A and B are constant and calculated from the linear plot $1/q_e^2$ versus, $logC_e$.

3.8 Thermodynamics study

The adsorption process depends on the kinetics and the rate of removal is significantly affected as a function of temperature of the system. In depth information about the inherent energy changes with respect to adsorption can be known from the thermodynamic parameter. To understand the process in a batter way ΔG = entropy change, ΔS = entropy change and ΔH = enthalpy change are evaluated accurately.

The ΔG of the adsorption process is calculated from classic Van't Hoff equation [106]:

$$\triangle G = -RTlnK_c \tag{3.35}$$

$$K_c = \frac{C_1}{C_2} \tag{3.36}$$

$$logK_c = \left(\frac{\triangle S}{R}\right) - \left(\frac{\triangle H}{RT}\right) \tag{3.37}$$

$$\triangle G = \triangle H - T\triangle S \tag{3.38}$$

where C_1 and C_2 = amount of metal ion adsorbed per unit mass of adsorbent and concentration of metal ion in aqueous phase, respectively. K_c = equilibrium constant, R = 8.314 $J/mol \cdot K$), T = temperature (K), ΔG, ΔS and ΔH are the changes in Gibb's free energy, entropy and enthalpy of adsorption respectively. The values of ΔH and ΔS are evaluated from the slope and intercept of the plot $logK_c$ versus $1/T$.

3.9 Response surface methodology (RSM) based central composite design (CCD)

To evaluate the optimum operating conditions and regression model equation, Response surface methodology (RSM) [107] was used. RMS is a mathematical and statistical techniques applied to optimize the adsorption process for the maximum uptake of the adsorbate. Design Expert 7.0 software was used for the statistical data analysis. The independent variables (factors): adsorbent dosage (X_1), temperature (X_2), solution *pH* (X_3) and Initial dye concentration (X_4) were used in the model. The Table 3.2 represents the actual and coded values of each variable. Three levels were used for the each variable: the lower (–1), the higher (+1) and the central point (0). A 2^4 full-factorial experimental design, having eight axial points and six replicates at the center point was employed. In total 30 experiments were performed in this study.

The experimental results were obtained by using the second-order polynomial equation as represented bellow;

$$Y = \beta_o + \sum_{i=1}^{n} \beta_i X_i + \sum_{i=1}^{n} \beta_{ii} X_i^2 + \sum \sum_{i<j=1}^{n} \beta_{ij} X_i X_j \tag{3.39}$$

where Y = predicted response (% removal), β_o = offset term, β_i = linear effect, β_{ij} = first-order interaction, β_{ii} = quadratic effect and X_i, X_j are the independent variables of the model.

Table 3.2: Factors and levels used in the central composite design study

Factors	Factor code	Level of factors		
		-1	0	+1
Adsorbent dose (g)	X_1	0.1	0.55	1
Temperature (℃)	X_2	10	35	60
pH	X_3	2	7	12
Initial concentration (mg/L)	X_4	10	30	50

Analysis of variance (ANOVA) was applied to the response and the corresponding parameters to analyse the modelled and finding the optimum level, also evaluate the statistical parameters by means of response surface methods.

Chapter 4

Removal of Pb(II) from aqueous solution by acid activated red mud

4.1 Introduction

Lead is released to the water, air and soil environment due to different industrial and natural process, resulting in damage of the ecosystems and human health. Lead is one of the common and most toxic pollutants among the different heavy metals and comes into the water bodies through the activities like combustion of fossil fuels, smelting of sulfide ore, acid mine drainage and various industrial activities such as metal plating, oil refining and battery manufacturing [108]. The lead is non-biodegradable in the environment and once enters to human body it accumulate mainly in bones, brain, kidney and muscles which may cause serious diseases such as nervous disorders, anaemia, sickness, kidney disease and even death [109, 110]. The presence of lead in natural or industrial wastewater is one of the most serious environmental problems worldwide and hence significant attention has been drawn by researcher throughout the globe for its removal. The limit of total lead of 50 ppb in drinking water is considered safe by the World Health Organization (WHO) in 1995 [111], which is decreased to 10 ppb in 2010 [112]. Also the permissible limit of lead in drinking water proposed for drinking, as set by European Union (EU), United States Environmental Protection Agency (USEPA) [113] and Guidelines for Canadian Drinking Water Quality [114] are 10 ppb, 15 ppb and 10 ppb, respectively. However, more recently an EPA document recommends a zero lead value in national primary drinking water standard [115]. Due to toxic properties of lead, the removal of lead from water and wastewater is essential in terms of safety of public health and environment [116]. Various materials used for the removal of different metal ions from water and wastewater have been reported [70, 78, 117–127], but they are not very popular due to a number of limitations.

Red mud is a highly alkaline waste material formed by the Bayer process of alumina production in the aluminum industries [80]. An estimated of 120 million tons of red mud are produced annually worldwide [128]. The red mud contains silica, aluminum, iron, calcium, titanium, sodium and minor constituent of potassium. The red mud has a great potential for water treatment with zero price and it is an efficient adsorbent because of its chemical

and mechanical stability associated with structural properties. The use of acid activated red mud has been explored as an adsorbent for the removal of Pb(II) from its aqueous solution in batch mode. In this work the red mud was neutralized by acid and excess of acid was removed by NH_4OH. The removal efficiency of the adsorbent was studied as a function of adsorbent dose, contact time, *pH* of the solution and initial lead concentration.

4.2 Results and discussion

4.2.1 Characterization of adsorbent

Particle size of the activated red mud is in the range of 0.1–150 μm. The $BET - N_2$ surface area of red mud and activated red mud are found to be 33.5 m^2/g and 67.10 m^2/g respectively as represented in Figure 4.1a. The surface area of activated red mud is more than the red mud, due to the removal of volatile materials after the thermal treatment at 500 ℃.

The results of TG and DSC analysis of activated red mud are presented in Figure 4.1b. The first weight loss is found to be 4.86% with corresponding endothermic peak in DSC at 162 ℃ due to the physically adsorbed water on the activated red mud. The second weight loss is found to be 6.11% with corresponding endothermic peak at 323 ℃. This may be due to loss of loosely bound water, and strongly bound water. The third weight loss is 1.00% which may be due to the remaining evolution of H_2O and volatile constituent present in the red mud. The results of the TG analysis are compared with literature data [129–132] in Table 4.1.

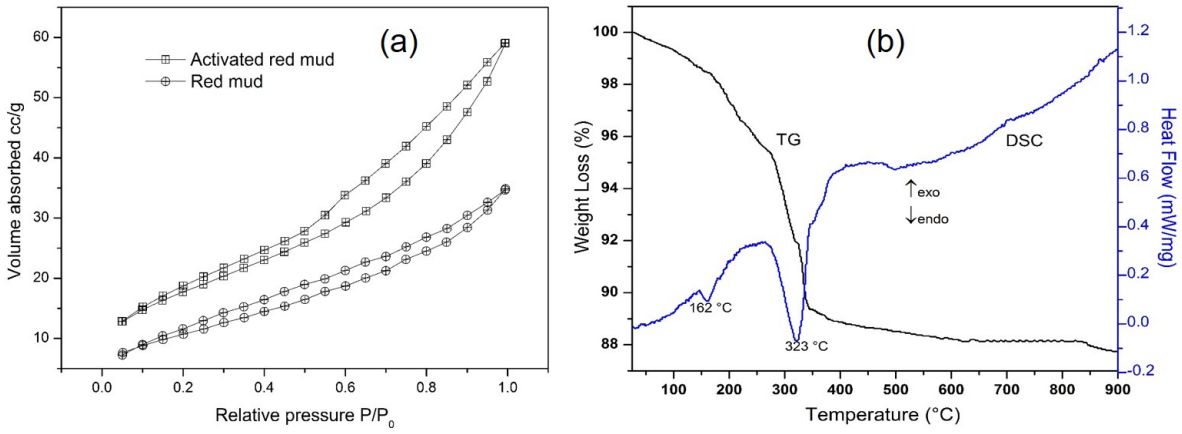

Figure 4.1: N_2 adsorption-desorption isotherm of red mud and activated red mud (a), thermogravimetric analysis and differential scanning calorimetric of activated red mud (b)

Figure 4.2 shows the particle size distribution of activated red mud. The horizontal axis denotes the radius of the particles distributed over the range from 0.2 to 5000 nm, with volume based peaks at about 61.46 nm and 537.4 nm.

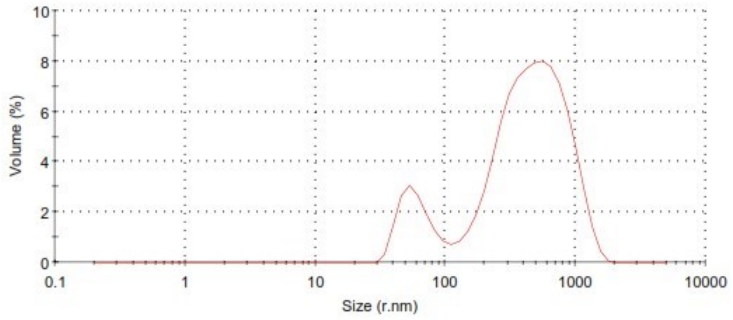

Figure 4.2: Particle size distribution of activated red mud

Table 4.1: Comparison study of TG analysis of acid activated red mud and red mud sample

Sample	Mass loss (%)	Temperature (℃)	References
Activated Red mud (Vedanta)	4.86	0-187.5	In this study
	6.11	187.5-345.9	
	1.00	345.9-900	
Total	11.97	0-900	
Red mud (Aughinish)	1.3	0-230	[129, 130]
	1.7	230-280	
	2.5	280-360	
	1.3	360-480	
	0.8	480-550	
	2.1	550-1150	
	0.2	1150-1200	
	0.3	T<1200	
Total	10.2	0-1200	
Red mud (Seydisehir)	5	0-150	[131]
	4	150-260	
	2	260-300	
	2	300-530	
	1	530-580	
	1.5	580-700	
	1.5	700-780	
	1	780-980	
	1	980-1200	
Total	19	0-1200	
Red mud (Zhengzhou Changcheng)	3	20-150	[132]
	3.6	105-450	
	4.3	560-720	
Total	10.9	20-880	

SEM images with corresponding EDX are shown in Figure 4.3. The SEM image of red mud before adsorption clearly indicate the rounded shape aggregate particles (poorly-crystallized/amorphous forms) due to the presence of some mineral phases mainly calcite and sodalite. These mineral phases are more soluble in an acidic environment. The

EDX data also indicate the elemental composition of activated red mud. SEM images of activated red mud after adsorption clearly indicate the presence of shiny patches over the rounded shape aggregates confirmed the adsorption of lead in the activated red mud which is further confirmed by the presence of lead in the corresponding EDX data.

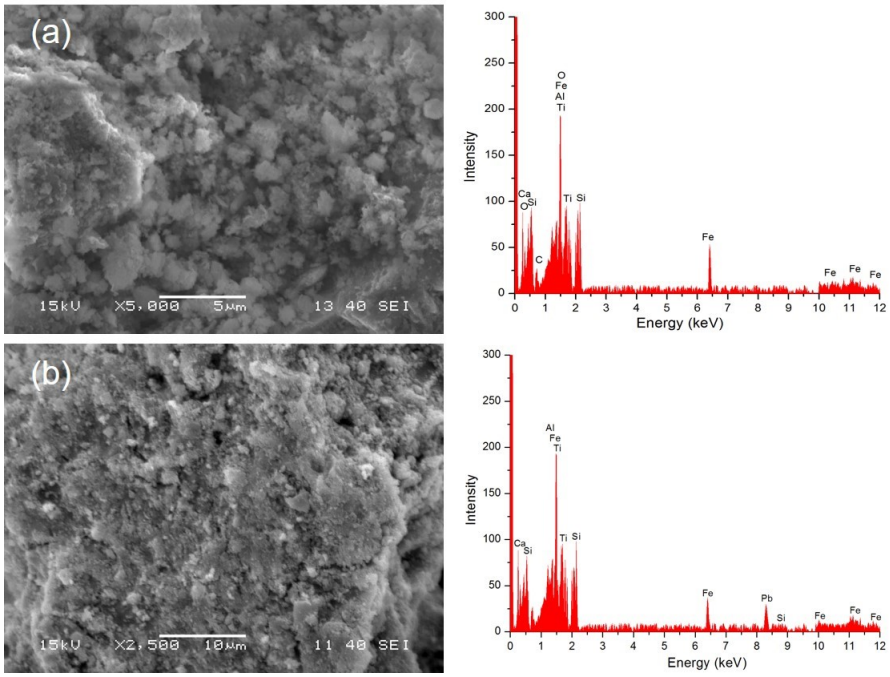

Figure 4.3: SEM micrograph and EDX spectrum of activated red mud: (a) before adsorption and (b) after adsorption

The XRD peaks of activated red mud confirms the following: hematite ($\alpha - Fe_2O_3$), goethite ($\alpha - FeO(OH)$), gibbsite ($\gamma - Al(OH)_3$), calcite ($CaCO_3$), rutile/anatase (TiO_2), and quartz (SiO_2), as referred from JCPDS (Joint Committee of Powder Diffraction Standards) file of X'Pert High Score software. XRD pattern of activated red mud after adsorption revealed that the intensity of gibbsite peak decreased prominently whereas the peak intensities of other mineral phases remain constant. Also, appearance of phases confirmed the formation of new mineral ilmenite ($FeTiO_3$). This may be due to dissolution of mineral phases during long period of adsorption. The dissolution of sodium aluminum silicate ($Na(AlSiO_4)$) is also responsible for increase of intensity of the gibbsite in activated red mud after adsorption. There is a new peak of lead at a d-spacing value 3.12068 Åwhich confirms the adsorption of lead in to the activated red mud as represented in Figure 4.4. The exact mineral morphology of lead is very difficult to abstraction from XRD but however it is confirmed the presence of Pb^{2+} species. The H^+ is a hard ion as compared to Pb^{2+}. In acidic medium the Pb^{2+} is replaced by H^+ and the process becoming faster with more concentration of H^+.

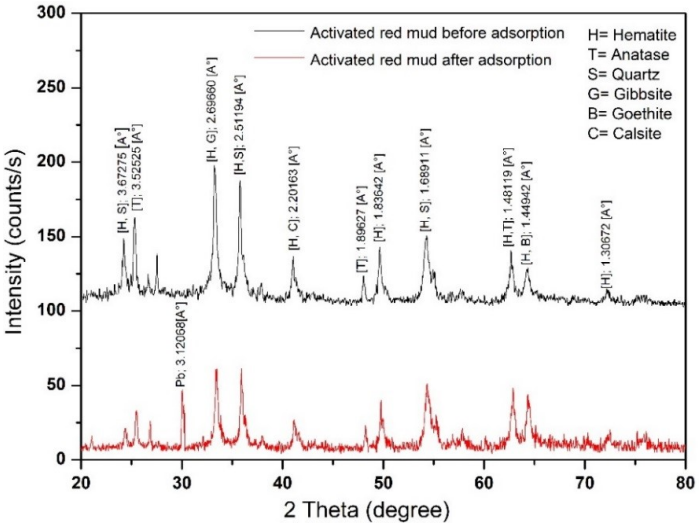

Figure 4.4: XRD of activated red mud before and after adsorption

The FT–IR spectrum of activated red mud before and after adsorption are shown in Figure 4.5. The position of absorption bands in both the spectra are almost similar except the peaks are more intense in the activated red mud before adsorption. The broad band at ~3398.33 and a weak peak at ~1633.04 cm^{-1} of activated red mud before adsorption are due to the stretching vibrations of O–H bonds and H–O–H bending vibrations of interlayer adsorbed H_2O molecule respectively. In an infrared spectrum, the hydroxyl-stretching vibrations of water are intense because of large change in dipole moment. The next band appears at 1021.82 cm^{-1}, assigned to Si–O–Si stretching vibrations (asymmetric), stretching vibration (symmetric) of T–O–Si (T=Si or Al) and bending vibrations (symmetric) of Si–O–Si and O–Si–O. The stretching vibrations of Fe–O bonds bands appear at 593.37 cm^{-1} in red mud. The O–H stretching vibration of activated red mud after adsorption is shifted to ~3413.71 cm^{-1}. This shift is due to existence of the shorter O–H bonds as it increases in the electrostatic attraction of the red mud layer in red mud than lead loaded red mud. The peak at 2352.96 cm^{-1} in red mud after adsorption is due to carbon dioxide gas in the measurement system. The new absorption bands at ~1563.89 and ~1427.64 cm^{-1} in the lead loaded activated red mud are due to stretching vibrations of C=O, confirmed the presence of carbonate groups. This may be due to chemisorbed CO_2 in activated red mud loaded with lead. Characteristic bands correspond to Si–O vibration are detected at 1366.78 and ~1030 cm^{-1} proved the presence of silicate groups. The band at 560.39 cm^{-1} is probably due to lead adsorbed over red mud.

4.2.2 Adsorptive removal of lead ions from aqueous media

Effect of adsorbent dose and *pH*

Adsorption of lead at different adsorbent dose and pH was studied to know the equilibrium data with initial lead concentration of 10 mg/L. The results of the experiments are presented

in Figure 4.6. The % removal of Pb(II) is increased to 80.7, 82.2, 83.7 and 94.1% with an increase the adsorbent dose 0.1, 0.2, 0.3 and 0.4 g respectively at a temperature of 27 ℃ and pH 7.2, due to increase in active sites for adsorption. However there is no significant change in % removal of Pb(II) after dose of 0.4 g, may be due to the facts that the active sites are overlapped. The adsorption capacity of the material is found to be 6.023 mg/g for Pb(II). Moreover the experimental data are best fitted to Langmuir isotherm which indicate the monolayer adsorption. Thus, 0.4 g/100 mL is considered as optimum dose and is used for further study.

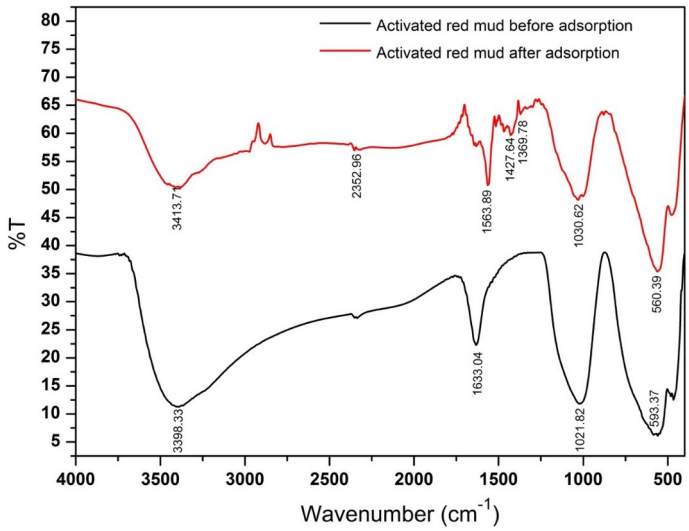

Figure 4.5: FT–IR spectra of activated red mud before and after adsorption

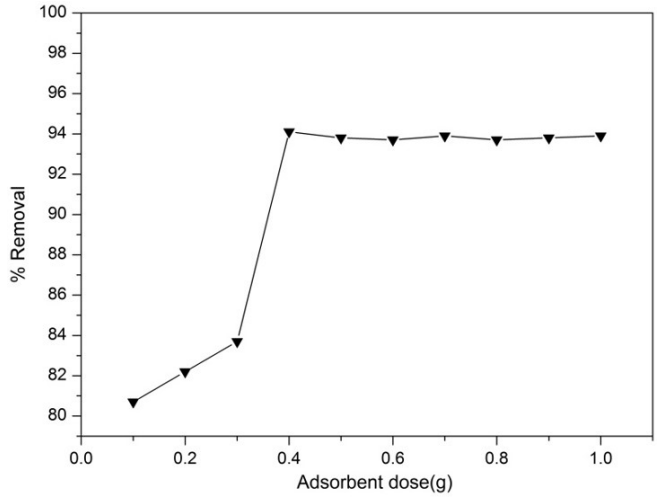

Figure 4.6: Adsorbent dose versus percentage removal of Pb(II) by activated red mud with initial concentration of 10 mg/L, temperature 27 ℃ and pH 7.2

The effect of pH on Pb(II) adsorption on activated red mud is summarized in Figure 4.7. The initial pH of the Pb(II) solution is maintained in the range of 2–12 by the addition of required amount of 0.1 M HCl or 0.1 M $NaOH$. The percentage removal of lead by ARM

decreased from 93.8% to 82% with increase in *pH* from 4 to 12, for initial lead concentration of 10 mg/L. This may be due to the fact that with increase in *pH*, OH^- concentration in the solution increases which makes partial dissolution of red mud in the aqueous solution. The reduction in percentage removal of lead may also due to the precipitation and coating phenomena at around the neutral and higher *pH* due the presence of sodium hydroxide which has been confirmed in the study of the effect of competitive ions. The above results suggest that the optimum *pH* for removal of lead is 4. The effect of *pH* on the adsorption of Pb(II) on activated red mud is compared with the result of the other authors given in Table 4.2.

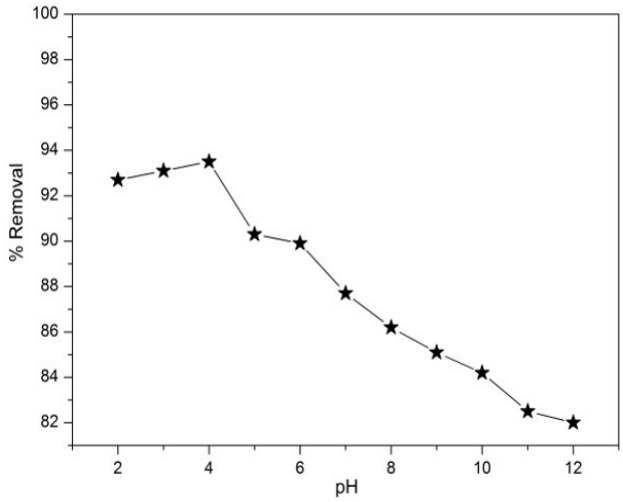

Figure 4.7: *pH* versus percentage removal of Pb(II) by activated red mud with initial concentration of 10 mg/L and adsorbent dose 0.4 g

Table 4.2: Summary of impact of *pH* on the adsorption of lead on activated red mud

Adsorbent	*pH*	Adsorption capacity	Reference
HCl treated activated red mud	4	6.2073 $mg/g.$	present study
H_2O_2 treated activated red mud	4	64.79 mg/g	[78]
Water treated red mud (R_w)	6	165.8 mg/g	[18]
HCl treated activated red mud (R_a)	4.4	117.3 mg/g	[18]
HCl treated heat activated red mud (R_{ah})	5.7	138.8 mg/g	[18]
HCl treated activated red mud	5	0.838 $mmol/g$	[18]
Pallet-type red mud	4	-	[133]
Pallet-type red mud	5.6	22.0 mg/g	[82]
Red mud	6	-	[79]
Red mud coagulant	6.3	-	[134]
Red mud coagulant	7	98.69 mg/g	[135]
H_2SO_4 treated red mud coagulant	8	-	[136]
Red mud coagulant	7	-	[137]
Non treated red mud	5.5	1.88 $mmol/g$	[83]
HCl treated red mud	5.5	0.77 $mmol/g$	[83]
Modified red mud	8.9	-	[138]
Sea water treated red mud (Bauxsol)	5.5	-	[74]

The zeta potential of the activated red mud before and after adsorption is presented in the Figure 4.8. Zeta potential is one of the fundamental parameter known to affect stability as the value indicate the magnitude of the electrostatic or charge repulsion or attraction between particles. Samples with zeta potential of between –30 mV and +30 mV typically tend to aggregate [139], although the precise stability threshold will vary according to particle type. In the present study, the zeta potential of activated red mud appears on –25 mV with higher intensity but the zeta potential after adsorption appears on –28 mV with lower intensity which clearly indicate that the charges on the surface of the adsorbent reduces after the adsorption of metal ions onto the material. The adsorption of metal ions depends on the charge of the surface of the adsorbent. The zeta potential remain in the negative site even after adsorption but the intensity decreases which clearly indicate that the lead ion is adsorbed on the adsorbent. The zeta potential is –14.7 at *pH* 4. In acidic medium the *pH* increases during adsorption and in the alkaline medium the *pH* decreases and the corresponding change in the zeta potential is in the range –10.3 to –22.3 mV at *pH* 2 to 12. The above results clearly indicate the exchange of H^+ with the Pb^{2+} ions.

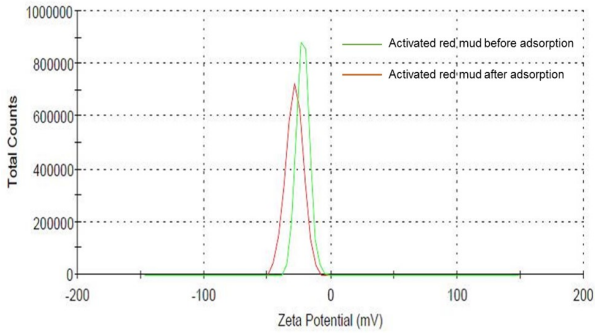

Figure 4.8: Zeta potential of activated red mud before and after adsorption

Effect of contact time and adsorption kinetics

Adsorption of lead at different contact times was studied for initial lead concentration of 10 mg/L with an adsorbent dose of 0.4 g and *pH* 4 of the solution. The result is presented in Figure 4.9. The percentage removal is found to increase from 88.5 to 93.8% for a contact time of 10 to 30 min. It is clear from the figure that the Pb(II) adsorption rate is high at the beginning of the adsorption, may be due to the adsorption sites are open and Pb(II) interact easily with these sites. A larger amount of Pb(II) is removed (~88% removal) in the first 10 min of contact time, and Pb(II) uptake becomes almost constant after 30 min, this indicates the possible monolayer formation of Pb(II) ions on the outer surface and that can be considered as equilibrium time of Pb(II) adsorption.

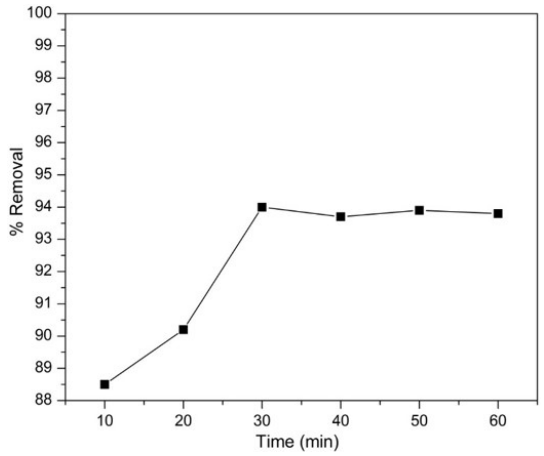

Figure 4.9: Time versus percentage removal of Pb(II) by activated red mud with initial concentration of 10 mg/L, adsorbent dose 0.4 g and *pH* of the solution 4

The values of K_{ad}, K_2 and R^2 were calculated from their respective kinetics plot and given in Table 4.3. The pseudo-first-order rate constant (K_1) and their correlation coefficient (R^2) are found to be 0.0822 and 0.8823 respectively. The pseudo-first-order and pseudo-second-order kinetics plot are given in Figure 4.10. The low value of pseudo-second-order rate constant (K_2) and high value of correlation coefficient (R^2) indicates that the adsorption of Pb(II) onto ARM followed pseudo-second-order kinetics.

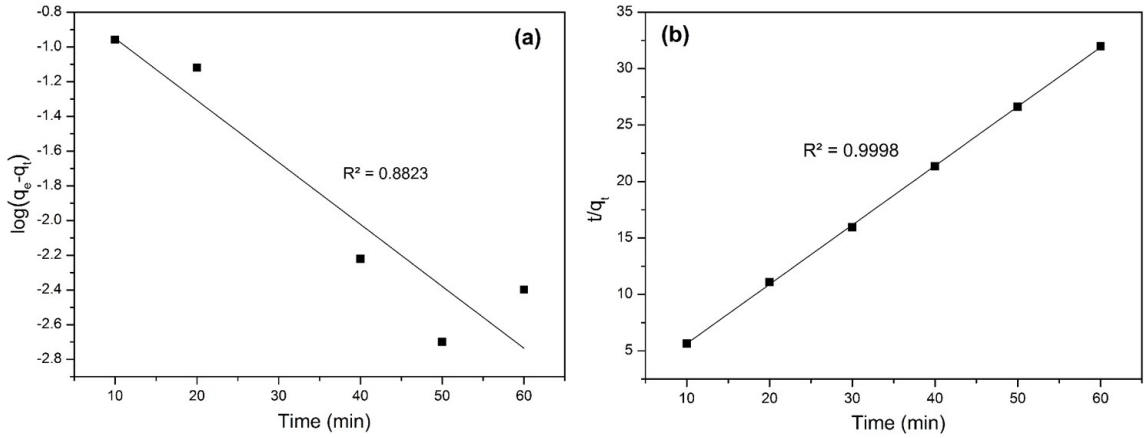

Figure 4.10: Pseudo-first-order (a) and pseudo-second-order (b) kinetics model for Pb(II) adsorption

Table 4.3: Pseudo-first-order and pseudo-second-order kinetics data for Pb(II) removal

Pseudo 1^{st} order		Pseudo 2^{nd} order	
K_{ad}	0.0822	K_2	0.6437
R^2	0.8823	R^2	0.9998
		q_e	1.9054

Effect of temperature and thermodynamic study

The adsorption capacity of the adsorbent is effected with the change in temperature. The effect of temperature for adsorption of Pb(II) on to the activated red mud has been studied in the temperature range of 10 to 80 ℃. The effect of temperature and the percentage removal of lead with initial concentration of 10 mg/L are shown in Figure 4.11. It is observed that the percentage removal of lead increases from 90.1 to 95.9% with the increase in temperature from 10 ℃ to 80 ℃ which indicates the endothermic nature of the process and maximum adsorption 94.9% of lead ions are found at 30 ℃ which is the equilibrium temperature of the solution. The increase in mobility of the metal ions is due to increase in temperature causes the decrease in the retarding forces of diffusing ions. Because of that there is an increase in the adsorption capacity of the adsorbent [140].

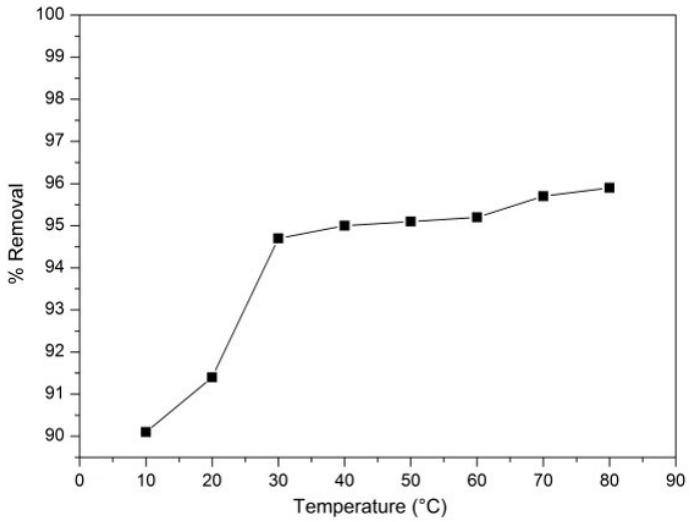

Figure 4.11: Temperature versus percentage removal of Pb(II) by activated red mud with initial concentration of 10 mg/L, adsorbent dose 0.4 g, pH of the solution 4 and time 30 min

The results of thermodynamic study are given in Table 4.4. The negative values of ΔG at all temperature confirm the spontaneous nature of adsorption. The positive values of ΔH confirm the feasibility of the reaction and indicate the endothermic nature of adsorption. The decreasing value of ΔG with increase in temperature shows the reaction is more feasible.

Table 4.4: Thermodynamic parameters of Pb(II) adsorption onto the ARM

Lead Concentration		10 (mg/L)				
ΔH (kJ/mol)	ΔS $(kJ/K \cdot mol)$	ΔG (kJ/mol)				
		20 ℃	30 ℃	40 ℃	50 ℃	R^2
0.30263	11.34362	–226.57	–340.00	–453.44	–566.87	0.785

Effect of initial lead (II) concentration and adsorption isotherm

Batch experiments were performed to investigate the effect of initial lead concentration from 10 mg/L to 100 mg/L with optimum adsorption dose on lead adsorption onto activated red mud. When the initial concentration of lead is 10 mg/L the removal percentage is 91%, it means the removal is 9.1 mg whereas, when the initial concentration is 100 mg/L the percentage removal is 12.91%, it means the removal is only 12.91 mg out of 100 mg. Hence it is evident from the result that the percentage removal of Pb(II) ions decreased from 91% to 12.91% with increasing the initial Pb(II) concentration from 10 to 100 mg/L as shown in Figure 4.12. The reduction in lead adsorption is due to the lack of available active sites required for the high initial concentration of lead. The higher uptake of lead at low concentration may be attributed to the availability of more active sites on the surface of the adsorbent for lesser number of adsorbate species.

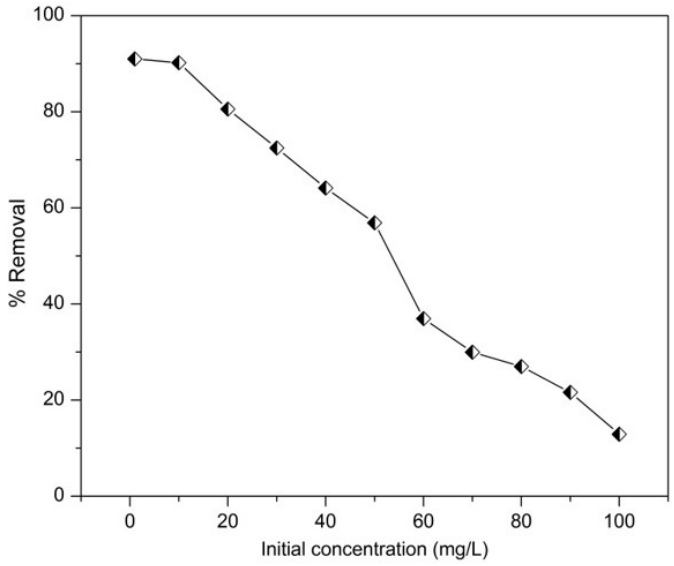

Figure 4.12: Initial concentration versus percentage removal of Pb(II) by activated red mud with adsorbent dose 0.4 g, *pH* of the solution 4, temperature 30 ℃ and time 30 min

The adsorption isotherm data were calculated from their respective isotherm plot and the data are given in the Table 4.5. The maximum adsorption capacity (q_m) and binding energy constant (b) of activated red mud for adsorption of lead is found to be 6.2073 mg/g and 2.0434 L/mg respectively according to Langmuir model. The calculated r values found in this study are between 0.0467 and 0.0049 for 10 to 100 mg/L concentration of Pb(II) representing favorable adsorption process. The values of Freundlich isotherm constant K_f, n, and R^2 are found to be 0.1160 mg/g, 2.3469, 0.2123 respectively. The Langmuir adsorption isotherm model better fit to the experimental data with high correlation coefficient (R^2) value of 0.9938 as shown in Figure 4.13. This indicates a monolayer adsorption of lead onto the adsorbent surface.

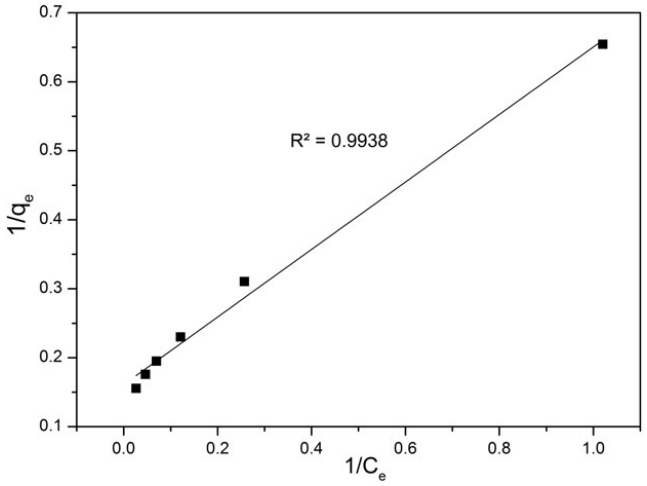

Figure 4.13: Langmuir adsorption isotherm plot for Pb(II) adsorption on the activated red mud

Table 4.5: Langmuir and Freundlich isotherm data

Langmuir isotherm		Freundlich isotherm	
q_m	6.0273	n	2.3469
b	2.0434	K_f	0.1160
R^2	0.9938	R^2	0.2123

4.2.3 Regeneration and re-usability of the adsorbent

Regeneration and re-usability studies gives an idea about the nature of adsorption. Chemisorption exhibits poor desorption. The regeneration of the adsorbent may be important for keeping the process cost down and recovering the metals extracted from the liquid phase [141]. In this study different *pH* (*pH* 2 to *pH* 12) of the solution was selected by using 1.0 M HCl and 1.0 M $NaOH$ as an eluent to desorb the Pb(II) ions from metal-loaded activated red mud. The result shows that 91.2% of regeneration occurs at *pH* 2, because under acidic conditions the adsorbent surface is protonated by H_3O^+ ions to make possible desorption of positively charged metal ions from the adsorbent surface. The effects of *pH* on regeneration of the adsorbent or desorption of Pb(II) is presented in Figure 4.14a. The re-usability of the adsorbent was study by taking number of cycle (cycle 1 to cycle 7) and after each cycle of adsorption, desorption was carried out with adsorbent dose 0.4 g/100 mL at temperature 27 ℃ and *pH* of the solution is 2 as shown in Figure 4.14b. The result shows that the percentage removal of Pb(II) decreases with increase the number of cycle and the maximum percentage removal of Pb(II) takes place in cycle 1 that is 95.8%.

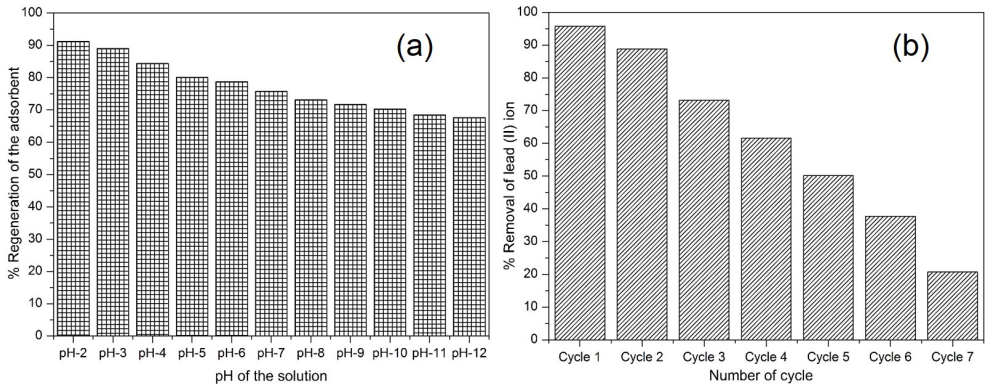

Figure 4.14: (a) Percentage desorption of the adsorbent versus pH of the solution plot (b) percentage removal of the Pb(II) ion versus number of cycle plot at temperature 27 ℃

4.2.4 Effect of competitive ions

Waste water contains many cations. Therefore, it is thought worthwhile to study the effect of competitive ions like sodium, potassium, calcium, and magnesium on the adsorption of lead. Varying concentration of these solutions was prepared from their chloride salts. The initial concentration of lead was fixed to 10 mg/L while the initial concentration of other cations varied from 10 to 100 mg/L. The results of these studies are given in Figure 4.15. It is clear from the figure that presence of these cations reduced the adsorption of lead appreciably i.e. 73.1 to 56.8% for sodium, 72.68 to 57.22% for calcium, 72.07 to 55.57% for magnesium and 71.45 to 55.98% for potassium with increase in initial concentration of different cations from 10 to 100 mg/L, respectively [142]. The cations reduced the lead adsorption in the order, potassium >magnesium >calcium >sodium.

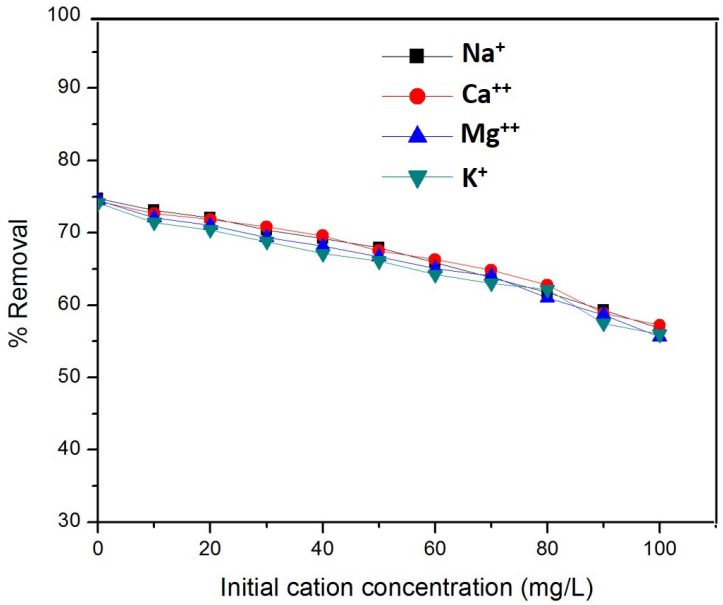

Figure 4.15: Percentage removal versus initial cation concentration of solution with initial lead ion concentration of 10 mg/L

4.2.5 Mechanism of adsorption and desorption of Pb(II) on ARM

The adsorption and desorption of the metal ion on the adsorbent surface strongly depend upon the *pH* value of the solution [143, 144] and is demonstrated by Figure 4.16. The adsorption of Pb(II) ions on the activated red mud is 94.1% in acidic medium i.e. at *pH* 4. Because, among the various constituents of red mud, the point zero charge (ZPC) of silica is ~2.3 and the composite ZPC of the adsorbent is found to be 3.1 but the surface has high positive charge density at *pH* less than 3.1 and due to electrostatic repulsion the adsorption capacity is quite low under these condition. the negative charge density increases when the *pH* is more than ZPC value resulting in a sudden enhancement in metal adsorption at *pH* 4.

On the other hand the desorption of Pb(II) ions on the lead loaded activated red mud surface is 91.2% at *pH* 2. Because, at lower *pH*, the process of regeneration predominates over the process of adsorption and hence the process of conversion of adsorbent into its H^+ plays an important role leaving behind Pb(II) in the aqueous solution. The hydroxylated surface i.e., $Al(OH)_3$ and $FeO(OH)$ present in activated red mud helps to absorbed H^+.

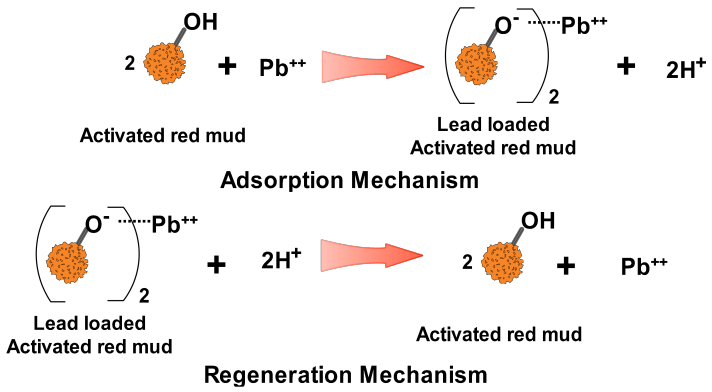

Figure 4.16: Mechanism of adsorption and regeneration of Pb(II) on ARM

4.3 Conclusions

The results of the above work indicated that the adsorbent prepared after neutralization and activation by thermal treatment is suitable for the removal of Pb(II) from aqueous solution. The material has not only a high adsorption capacity for the lead ion but also capable of lowering the metal ion concentration to a great extent. The metal ion concentration gradient is a fundamental force that transfers metal ion from solution to adsorbent surface and diffuses metal ion into the matrix of the adsorbent. The adsorption process followed pseudo-second-order kinetics with an equilibrium time of 30 min. The adsorption isotherm is better described by the Langmuir isotherms. The maximum adsorption capacity of ARM is 6.2073 mg/g. The adsorption of lead by ARM is accomplished by ion exchange. This acid neutralized red mud can be used as low cost adsorbent for adsorption of Pb(II) from wastewater.

Chapter 5

Equilibrium and kinetic studies of Cd(II) ion adsorption from aqueous solution by activated red mud

5.1 Introduction

Cd(II) is another toxic metal ranked in 7^{th} position in the priority list of hazardous substances with a permissible limit of 5 –10 ppb. Hence in this chapter, activated red mud prepared by same procedure as in the previous chapter is used to remove Cd(II) from its aqueous solution.

Water contamination by heavy metals including cadmium is one of the most spartan environmental issues, and it is exceptionally hard to solve the problem. Cadmium occurs in air, water, soils and foodstuffs because of natural phenomenon such as erosion, abrasion of rocks and soils, forest fires and volcanic eruptions. Besides the natural process, cadmium enters to environment by various anthropogenic pathways like, by-product from smelting, refining and mining of sulfide ores of zinc [145, 146]. The manufacturing industries like pigments, cadmium-nickel batteries, alloy, electroplating, plastic, dyes, pesticides, fertilizers, textile and processing industries such as mining, smelting and refining also generate cadmium containing waste [55, 147–150]. Like other metals, cadmium is also non-degradable and can be accumulated effectively in living tissue and easily adsorbed into the human body. Cadmium and its compounds are extremely poisonous and long-term exposure can harm to human endocrine system, kidney and bones [151, 152]. Therefore, several organizations such as World Health Organisation (WHO) [112], American Water Work Association (AWWA) [153], Canadian drinking water quality guideline [114] and United States Environmental Protection Agency (USEPA) [115] have recommended 0.005 mg/L as the maximum permissible limit for Cd(II) in drinking water. According to Indian Standard Institution (ISI) and Central Pollution Control Board (CPCB) [154], 0.01 mg/L is the desirable limit of cadmium in drinking water. In view of the above, the removal of cadmium ions from the water and wastewater is necessary for safety of public health and environment.

There is a growing interest for the development of low cost materials and methods to remove Cd(II) ions from drinking water or industrial effluents. Although many different

methods such as chemical precipitation [52, 53], ion exchange [54], solvent extraction [55, 56], reverse osmosis [57], dialysis/electro-dialysis [58], supported liquid membrane [59] and adsorption [60–62] are reported to remove heavy metal ions, the process based on adsorption methods is promising, because of high removal efficiency and low cost [155]. Many low-cost materials [156–165] have been reported for Cd(II) removal from water and wastewater systems, but they are not very popular because of various limitation like cost, removal efficiency and maintenance.

In this work, attempts have been made to utilize red mud, a highly alkaline (pH >12) and undesirable by-product of alumina processing industries. the high surface reactivity of red mud is due to its major constituents: oxides and hydroxides of aluminum, iron, silicon, titanium [166]. The storage and maintenance of highly caustic red mud are a challenging environmental problem in the alumina industry. The utilization of red mud in bulk make an environmental benefit and enhance the socio-ecological and economic value of alumina industries [35]. Only a limited number of studies have been made for the removal of Cd(II) ions from aqueous solution by using red mud as a low cost adsorbent. Gupta $et\ al.$ used red mud modified with hydrogen peroxide to increase the removal of Cd(II) ions from aqueous solution [81]. Zhu $et\ al.$ and Shao-hua $et\ al.$ reported that, after modification of red mud to granular red mud and red mud granulated with cement, the Cd(II) adsorption capacity is reported to increase [17, 76]. Ma $et\ al.$ reported that, the adsorption of water-borne Cd(II) ions increased on treatment with $CaCO_3$-dominated red mud [167].

However, reports about the adsorption of Cd(II) ions from aqueous solutions by acid activated red mud are not clarified. The aim of this study is to find out the mass transfer of Cd(II) adsorption on acid activated red mud. Furthermore, this work investigates the percentage removal of Cd(II) ions from the aqueous solutions by batch experiment. The effect of various parameters were examined on the adsorption of Cd(II) ions on ARM from aqueous solutions.

5.2 Results and discussion

5.2.1 Characterization of adsorbent

The BET surface area of the red mud is 33.5 m^2/g which is increased to 67.10 m^2/g on activation. Red mud contains the following mineral phases: hematite (Fe_2O_3), goethite ($FeO(OH)$), gibbsite ($Al(OH)_3$), calcite ($CaCO_3$), rutile/anatase (TiO_2) and quartz (SiO_2) which are identified by XRD analysis. These are in agreement with its chemical composition of red mud (Fe_2O_3 - 43.82%, Al_2O_3 - 46.89%, SiO_2 - 12.51%, TiO_2 - 3.90%, CaO - 2.31%, Na_2O - 9.87%, loss of the ignition - 7.69%). XRD of activated red mud before and after cadmium adsorption is presented in Figure 5.1. The results obtained from the analysis indicate that there are remarkable changes between the ARM and Cd-loaded ARM, which suggest that a phase transformation has taken place due to the formation of new mineral

ilmenite ($FeTiO_3$). The appearance of this mineral (Ilmenite) influences the cadmium sorption mechanism. $FeTiO_3$ consist of two simple oxides: TiO_2 and Fe_2O_3 which changes the surface properties of the adsorbent and help for Cd(II) adsorption.

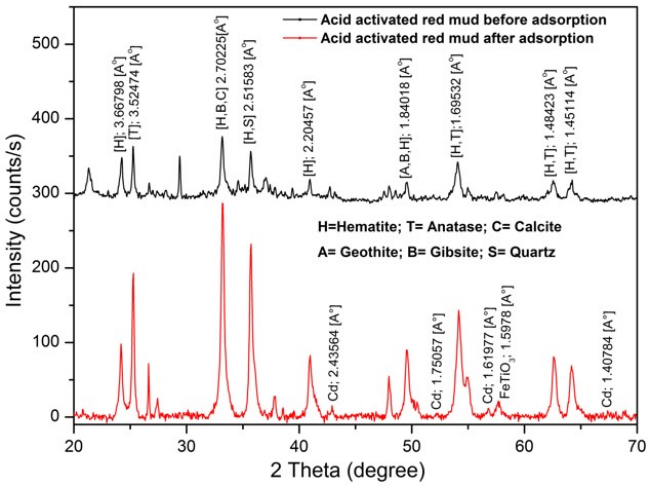

Figure 5.1: XRD of acid ARM before and after cadmium adsorption

The EDX spectra and SEM images of activated red mud before and after adsorption are illustrated in Figure 5.2. It is observed that it contains irregular shapes of black particle before adsorption which changes to shiny bulky particles spread all over the material before adsorption. It clearly indicates the presence of cadmium in the surface which is confirmed by the corresponding EDX.

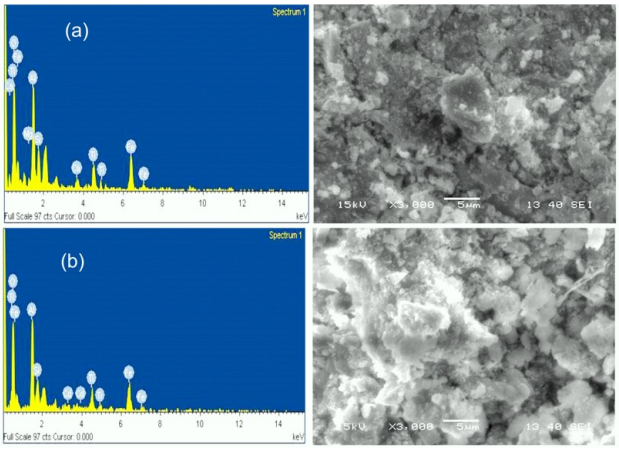

Figure 5.2: EDX spectrum and SEM micrograph of ARM: before adsorption (a) and after adsorption (b)

5.2.2 Batch adsorption study for the removal of Cd(II) ions from aqueous media

Effect of adsorbent dose and *pH*

The effect of adsorbent dose on the adsorption of Cd(II) on ARM was investigated at *pH* 7, ambient temperature (298 K) and contact time of 60 min with initial Cd(II) concentration of 10 mg/L shown in Figure 5.3a. The removal efficiency of Cd(II) increases gradually from 67.11 to 92.90% for 0.1 g –1.0 g/100 mL of activated red mud. As expected, removal capacity of cadmium ions increases with increase in the adsorbent dose and there is no significant change in percentage removal of cadmium after adsorbent dose of 0.5 g/100 mL, may be due to aggregation or overlapping of adsorption site. Hence 0.5 g/100 mL is considered the optimum dose and is used for further study.

Hydrogen ion concentration is one very significant parameter that control the adsorption behaviour of metal ions in aqueous solution [168]. Figure 5.3b depicts the effect of *pH* on Cd(II) removal with activated red mud. The removal efficiency of Cd(II) increased gradually with increase in *pH* and is nearly constant above *pH* 6. It is evident that the adsorption of Cd(II) onto the activated red mud is highly *pH* dependent, with maximum removal efficiency of 96.89% at *pH* 6. However, with increase in the *pH* values, adsorbent surfaces are more negatively charged due to protonation of adsorbent and becomes more accessible for the adsorption of metal ions (positive charged) through electrostatic force of attraction [169, 170]. The pH_{zpc} (zero point charge) value of the adsorbent is determined by reported method. The pH_{zpc} is found to be 4.8 where $\triangle pH$ = 0. This may be explained by considering the pH_{zpc} for the activated red mud. At *pH* <pH_{zpc}, the surface charge is positive, at *pH* = pH_{zpc}, the surface charge is neutral and at *pH* >pH_{zpc}, the surface charge is negative. The point of zero charge of ARM is 4.8 which is less than the *pH* value (*pH* 6). The maximum adsorption capacity of the material in this study comparable with other adsorbent at different *pH* is shown in Table 5.1.

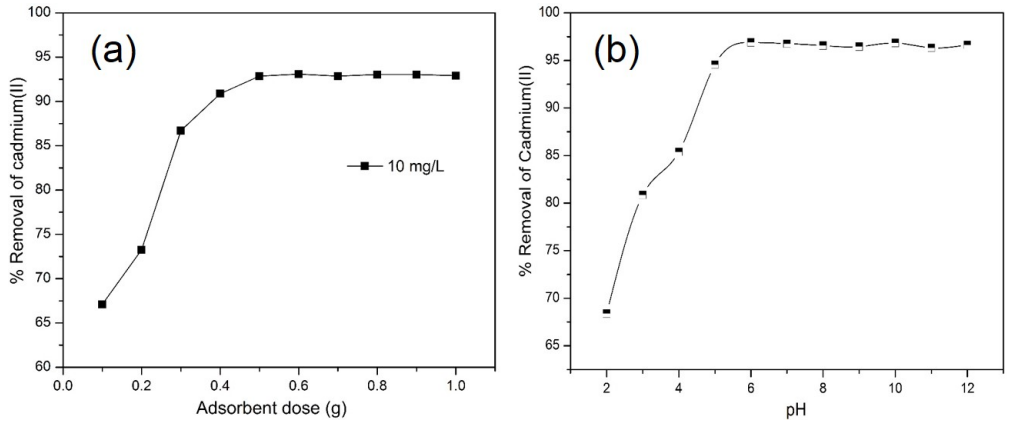

Figure 5.3: (a) Effect of adsorbent dose and (b) effect of *pH* for Cd(II) removal on ARM (initial concentration: 10 mg/L, adsorbent dose: 0.5 g, contact time: 120 min, temperature: 298 K)

Table 5.1: A comparison of maximum adsorption capacities for cadmium ions by different adsorbents at different *pH*

Adsorbent	*pH*	Adsorption Capacity (mg/g)	References
Bamboo charcoal	8.0	12.08	[171]
Coffee grounds	7.0	15.65	[172]
Rice straw	2.0–6.0	13.9	[173]
Chitosan/bentonite	6.5	120.5	[174]
Snail shell dust	6	16.66	[175]
Acid activated red mud	6	12.54	Present study

Effect of contact time and adsorption kinetics

The effect of contact time in the range of 10–60 min is depicted in Figure 5.4a. The equilibrium adsorption is established after 40 min of contact time and the maximum removal percentage is 94.38%, 92.07% and 87.50% for initial cadmium concentration 10 mg/L, 50 mg/L and 100 mg/L respectively. After equilibrium is reached, the contact time has no longer any influence on the cadmium ion adsorption and the removal efficiencies remained constant over the time period of 60 min. The adsorption rate increased rapidly in the first 10–30 min because of more number of available adsorption sites on the surface at the beginning of the adsorption process, whereas a further increase in contact time decreases the number of available adsorption site. The result obtained implies that the sorption mainly took place at the surface of the sorbent during the initial stage. The adsorption time of 40 min is used for the rest of the study.

Different kinetics of Cd(II) onto activated red mud are shown in Figure 5.4b, 5.4c and 5.4d. The values of intraparticle diffusion rate constants (K_{ip}), pseudo first-order (K_1) and second-order (K_2) rate constants are tabulated in Table 5.2 for the different experimental parameters. From the data it is concluded that the pseudo-second-order model shows excellent linearity with a high correlation coefficient (R^2 >0.99) in comparison to other kinetic models. The calculated q_e values from the model are also in good agreement with the experimental values. The pseudo-second-order kinetic model is formulated based on the concept of chemisorption in the limiting rate step, which is associated with the valence forces due to sharing or electron exchange between the adsorbate and the adsorbent [176]. The results are consistent with previous literatures in which adsorption kinetic of Cd(II) ion by different adsorbent are fitted with pseudo-second order model [177, 178].

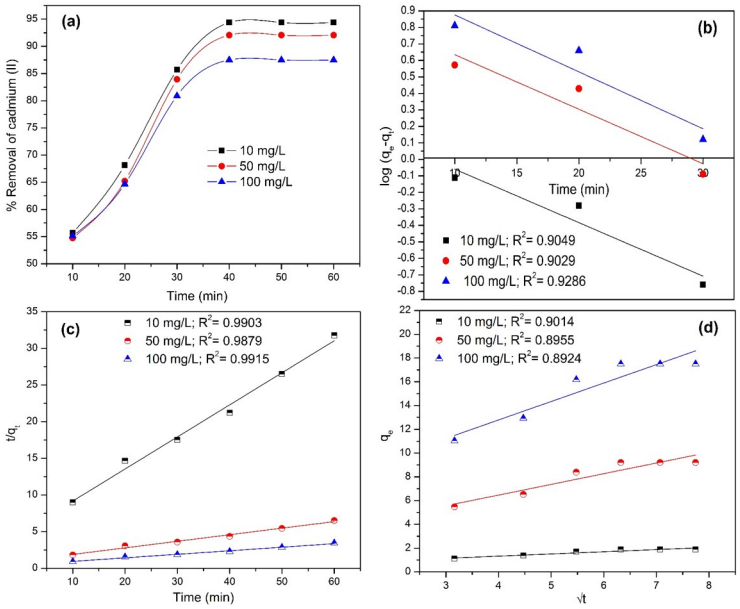

Figure 5.4: Effect of contact time (a), kinetic study of pseudo-first-order (b), pseudo-second-order (c) and intraparticle diffusion models (d) for removal of Cd(II) onto ARM (adsorbent dose: 0.5 g/100 mL, pH 6 and temperature: 298 K)

Table 5.2: Kinetics of Cd(II) ions adsorption onto ARM at different initial Cd(II) concentration

Kinetics models	Parameters	Initial Cd(II) concentration (mg/L)		
		10	50	100
Pseudo-first-order model	q_e (mg/g)	0.9681	0.9672	0.9660
	K_1	0.0747	0.0761	0.0795
	R^2	0.9286	0.9029	0.9049
Pseudo-second-order model	q_e (mg/g)	2.2853	11.1776	20.6232
	K_2	0.0400	0.0080	0.0052
	R^2	0.9903	0.9879	0.9915
Intraparticle diffusion model	k_{ip}	0.1841	0.9003	1.5525
	C	0.5915	2.8622	6.5785
	R^2	0.9014	0.8955	0.8924

Effect of temperature and thermodynamic studies

To determine the effect of temperature on Cd(II) adsorption from aqueous solutions, batch experiments were performed at different temperature (283–363 K) with initial concentration of 10 mg/L, 50 mg/L and 100 mg/L with optimum adsorbent dose and the results are represented in Figure 5.5a, that shows the increase in temperature increases the uptake capacity of metal ions. Higher temperature favors adsorption of metal ions, which reveal the endothermic nature of adsorption. An increase in percentage removal can be explained in terms of an increase in the number of active sites with increasing temperature due to some breakage of bonds near active sites.

The standard entropy change (ΔS) and the values of the standard enthalpy change (ΔH) were determined from the intercept and the slope of the Van't Hoff plot of log K_c versus $1/T$ depicted in Figure 5.5b. The thermodynamic parameters for the adsorption process are summarized in Table 5.3. The negative values of (ΔG) indicated the spontaneous and feasibility nature of the adsorption process. More over the decrease in ΔG values with an increase in temperature, indicates the increased trend in the degree of spontaneity and feasibility of cadmium adsorption. Generally, 0 to –20 kJ/mol for free energy change is reported to be the physical adsorption, and –80 to –400 kJ/mol is reported to be the range for chemical adsorption [179]. ΔG value is in the range of –188.582 to –233.669 kJ/mol and –283.41 to –351.09 for temperature 293 K and 303 K respectively, indicating chemical adsorption. The ΔH parameter is found to be 1.1723, 1.1545 and 1.0728 kJ/mol for initial concentration 10 mg/L, 50 mg/L and 100 mg/L respectively. the endothermic nature of the adsorption process is confirmed from the positive values of ΔH. The ΔS values are found to be 11.7420, 10.3922, 9.4827 $J/K\ mol$ for initial concentration of 10 mg/L, 50 mg/L and 100 mg/L respectively. The positive value of ΔS suggested a higher randomness tendency at the solid/solution interface during the adsorption of Cd(II) on the adsorbent.

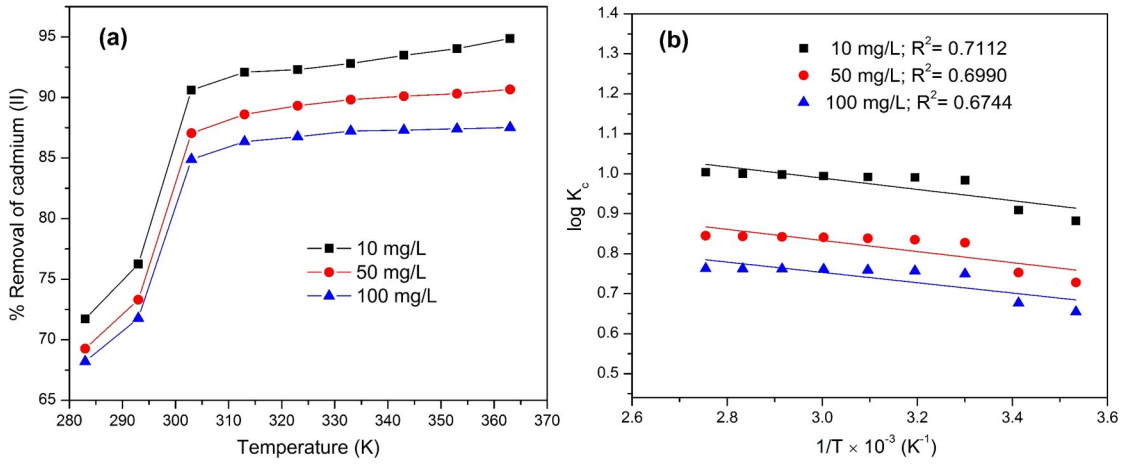

Figure 5.5: Effect of temperature (a) and van't Hoff plots of (b) for the adsorption of Cd(II) by ARM

Table 5.3: Thermodynamic parameters of cadmium adsorption onto the ARM at different initial cadmium concentration

Initial Cd(II) concentration (mg/L)	ΔH (kJ/mol)	ΔS ($J/K\cdot mol$)	ΔG (kJ/mol)		R^2
			293 K	303 K	
10	1.1723	11.7420	-233.669	-351.09	0.7112
50	1.1545	10.3922	-206.690	-310.613	0.6990
100	1.0728	9.4827	-188.582	-283.41	0.6744

Adsorption isotherm

The Langmuir parameter q_m and b were calculated from the slopes and intercepts of the plots of C_e/q_e versus C_e respectively, and are represented in Figure 5.6a. The result obtained from the different adsorption model are reported in Table 5.4. From the Langmuir plot the values of q_m for the removal of Cd(II) at 293 K and 303 K are found to be 12.05 mg/g and 12.55 mg/g respectively. It is observed that the value of 'r' in between the range of 0–1, for initial Cd(II) concentration of 10 mg/L, 50 mg/L and 100 mg/L, confirmed the favorable uptake of the Cd(II) [180].

The Freundlich constants K_f and $1/n$ were determined by intercepts and slopes of linear plot of $logq_e$ versus $logC_e$ plot (Figure 5.6b). From the Freundlich plot the values of K_f at 293 K and 303 K are found to be 0.3055 mg/g and 0.3200 mg/g respectively and are shown in Table 5.4. If the slope $1/n$ is less than 1, then the adsorption process is favorable. The values $1/n$ obtained are 0.3790 and 0.3692 at temperature 293 K and 303 K respectively, which indicates that the cadmium adsorption onto activated red mud is favorable. The value of K and q_m were obtained from the slope and intercept from the Dubinin–Radushkevich plot of lnq_e versus ε^2 and is shown in Figure 5.6c and the values of K and q_m for the removal of Cd(II) at 293 K and 303 K are found to be (2.3999 mol/kJ and 7.4574 mg/g) and (8.4969 mol/kJ and 7.9382 mg/g), respectively and presented in Table 5.4. The constant K_T and B_1 can be determined by the linear plot of q_e versus lnC_e shown in Figure 5.6d and the calculated parameters are presented in Table 5.4. The Temkin constant B_1 showed that the heat of adsorption of cadmium ions onto activated red mud showed a slight increase in value at higher temperatures indicating an endothermic process [105].

Table 5.4: Isotherm parameters for cadmium adsorption onto ARM at temperature 293 and 303 K

Isotherm models	Parameters	Temperature (K)	
		293	303
Langmuir	q_m (mg/g)	12.0464	12.5482
	b (L/mg)	0.0826	0.1090
	R^2	0.9967	0.9977
Freundlich	K_f (mg/g)	0.3055	0.3200
	$1/n$	0.3790	0.3692
	R^2	0.9956	0.9694
Dubinin–Radushkevich	K $(mol/k \cdot J)$	2.3999	8.4969
	q_m (mg/g)	7.4574	7.9382
	R^2	0.8094	0.7865
Temkin	K_T (L/mg)	0.7894	1.2140
	B_1	2.6666	2.6320
	R^2	0.9958	0.9898

Comparing the isotherm models results (Table 5.4) it is concluded that the Langmuir isotherm model is the best fitted with the equilibrium data (R^2 >0.99) than the Freundlich,

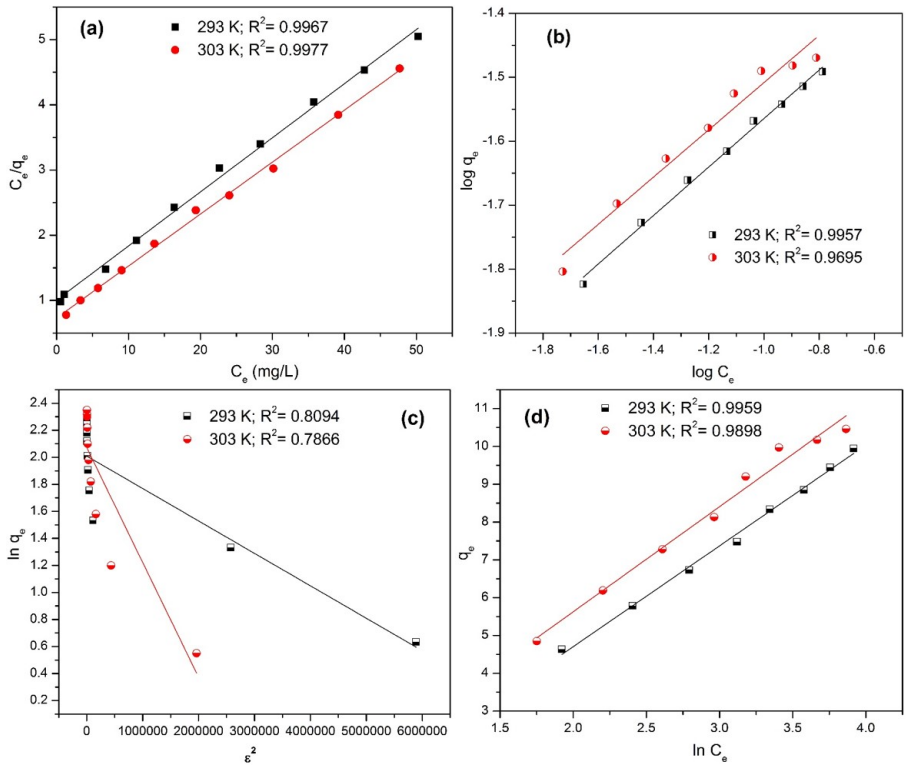

Figure 5.6: Isotherm models of Langmuir (a), Freundlich (b), Dubinin–Radushkevich (c), and Temkin models (d) for the adsorption of Cd(II) onto ARM at temperature 293 and 303 K (adsorbent dose: 0.5 g/100 mL, pH 6 and contact time: 40 min)

Dubinin-Radushkevich and Temkin models. It may be due to homogeneous distribution of active sites on adsorbent surface [181].

Table 5.5 provides a comparison of maximum adsorption capacity of Cd(II) on different adsorbents. The maximum adsorption capacity of present activated red mud is higher than most adsorbents presented in Table 5.5. Therefore, the activated red mud of present work is a suitable material for the removal of Cd(II) from aqueous solutions.

Table 5.5: Comparison of adsorption capacities of Cd(II) ions with some low-cost adsorbents

Adsorbent q_m (mg/g)	Adsorptioncapacity	References
Activated red mud	12.54	In this work
Areca waste	1.32	[182]
Bentonite	9.30	[183]
Saw dust	5.37	[120]
Saw dust	0.29	[184]
Rice husk	0.89	[184]
Modified sewage sludge	14.7	[185]
Peanut hulls	5.96	[186]
Bagasse fly ash	2.00	[187]
Kaolinite clay	0.88	[188]
Pre-treated rice husk	8.58	[189]
Modified steel-making slag	10.16	[190]

5.2.3 Mass transfer study

The linear plot between $ln[(C_t/C_0) - 1/(1 + mK)]$ versus t obtained from McKay $et\ al.$ equation is shown in Figure 5.7a. The value of k_f can be determined from the slope of the plot. The mass transfer coefficient values suggest that the transport velocity of adsorbate from the bulk to the surface of the solid phase is quite rapid which reveals the effectiveness of red mud for the treatment of cadmium bearing wastewater. The k_f value can be calculated from the slope of the straight line obtained from the plot of C_t/C_0 versus t from the Weber model and is represented in Figure 5.7b.

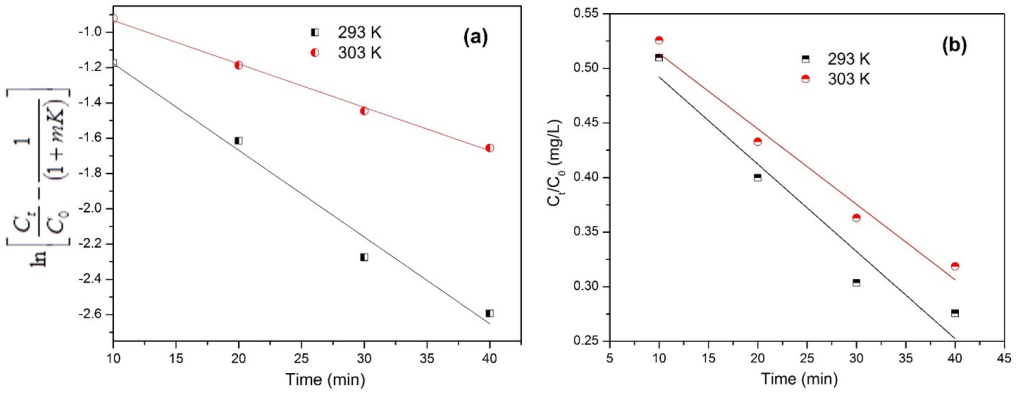

Figure 5.7: Mass transfer plot MeKay $et\ al.$ (a) and Waber–Mathews (b) for the adsorption of cadmium on ARM

The k_f values of McKay $et\ al.$ equation and Waber-Mathews equation are given in Table 5.6, which shows that the mass transfer coefficient rate ranges from 0.084 $\times 10^{-3}$ to 0.012 $\times 10^{-3}$ for McKay $et\ al.$ equation and 9.9 $\times 10^{-3}$ to 11.5 $\times 10^{-3}$ for Waber-Mathews equation for temperature 293 K and 303 K respectively. It can be understood from the k_f value that activated red mud adsorbed cadmium ions faster at lower temperature by McKay $et\ al.$ equation and at higher temperature by Waber-Mathews equation.

Table 5.6: External mass transfer coefficients k_f calculated from the equations of McKay $et\ al.$ and Weber–Mathews related to the adsorption of cadmium on ARM from aqueous solution

Temperature (K)	McKay $et\ al.$ equation $k_f(cm \cdot min^{-1})$	Weber-Mathews equation $k_f(cm \cdot min^{-1})$
293	0.084×10^{-3}	9.9×10^{-3}
303	0.012×10^{-3}	11.5×10^{-3}

5.2.4 Desorption study

The applicability of activated red mud as a potential adsorbent depends on properties of desorption and reusability. For regeneration, HCl solution was selected as the regenerating agent. Figure 5.8a shows the effect of HCl concentration on desorption efficiency. The

regeneration efficiency reached 76.75 to 91.29% when the concentration of HCl reached 0.1 mol/L to 0.2 mol/L respectively. A comparative experiment of ARM and ARM after regeneration was carried out as an effect of adsorbent doses to investigate the removal of Cd(II). As seen in Figure 5.8b, the adsorption capacity of adsorbent after regeneration is equal to the ARM unused.

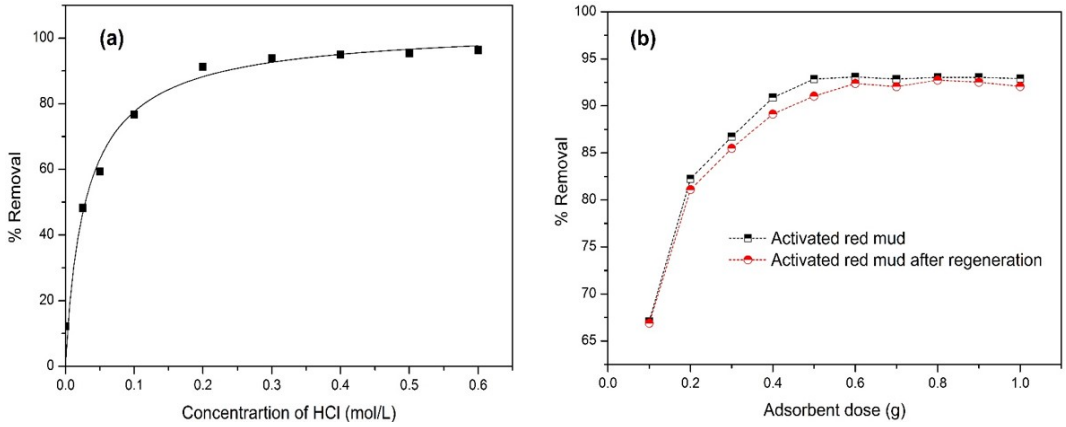

Figure 5.8: Effect of HCl concentration on desorption of cadmium (a) and effect of the dosage on cadmium removal using ARM and ARM after regeneration (b) (room temperature, pH 6, initial concentration: 10 mg/L)

5.2.5 Mechanism of Cd(II) adsorption

The mechanism of any adsorption process is an important component to understand the process as well as to know the characteristics of the material which help to design a new adsorbent for the future applications. Electrostatics interaction between the positively charged Cd(II) and the negative charge on activated red mud (ARM) presented by ion exchange (Equation 5.1) or Si–O–Si structures (Equation 5.2).

$$2(ARM - OH) + Cd^{2+} \longrightarrow (ARM - O^{-})_2Cd + 2H^{+} \tag{5.1}$$

$$2(ARM - Si - O^{-}) + Cd^{2+} \longrightarrow (ARM - Si - O^{-})_2Cd^{+2} \tag{5.2}$$

The adsorption of Cd(II) ions on activated red mud is maximum at pH 6, because when the pH value of the solution is greater than the pH_{zpc} value, the surface of the minerals is negatively charged while the number of H_3O^{+} ions decreases. Therefore, the positively charged Cd(II) ions are adsorbed onto activated red mud surface via chemical ion exchange or electrostatics attraction [191] as suggested in Figure 5.9.

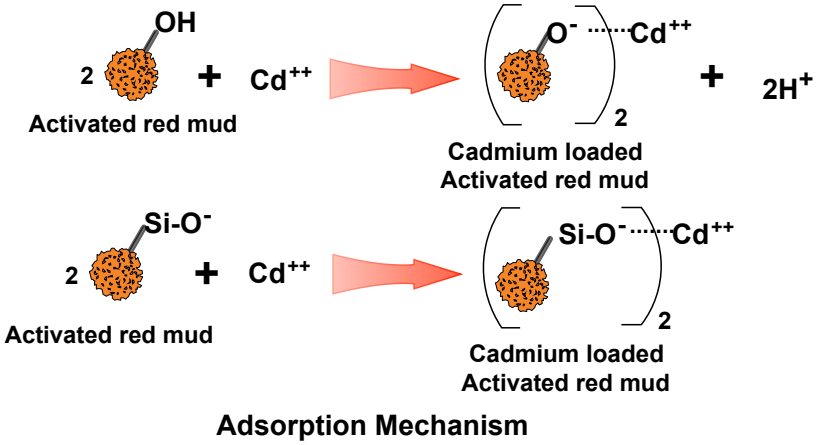

Figure 5.9: Mechanism of adsorption of Cd(II) on ARM

5.3 Conclusions

Activated red mud is an excellent adsorbent for the treatment of wastewater containing Cd(II) ions. The adsorption kinetics is found to follow pseudo-second-order rate equation and equilibrates within 30 min. The adsorption data fit very well to the Langmuir model and the maximum removal of Cd(II) is found to be 12.046 mg/g and 12.548 mg/g at temperature 293 K and 303 K, respectively at pH 6. The thermodynamics of cadmium adsorption onto activated red mud confirmed the endothermic and spontaneous adsorption process. Cadmium can be desorbed from ARM with HCl and the removal efficiency reaches 91.29% when the concentration of HCl is 0.2 mol/L. The adsorption capacity of adsorbent after regeneration is equal to the ARM untapped. Thus, the activated red mud can be considered as a low cost adsorbent for adsorption of Cd(II) from water. Also activated red mud can be used for potential application for wastewater remediation since it has not been tested on samples from industry.

Chapter 6

Removal of safranin-O dye from aqueous solution using modified red mud: kinetics and equilibrium studies

6.1 Introduction

Organic dyes are widely used in different industries to colour their products but it is one of the major group of water pollutant [192]. The wastewater discharged from the industries like textile, leather, cosmetics, paper, printing, plastic, pharmaceutical and food without treatment, affects the photosynthetic aquatic life due to the lack of light perception [193, 194]. Dyes are responsible for the genetic mutation in human beings and can be easily accumulated in the living tissues [195]. In addition, many dyes and their by-products are harmful to human and animal life [196, 197]. In view of toxic properties of dyes, it requires immediate attention to develope suitable methods for the removal of dye from wastewater. Various process are available in literature to remove dyes from wastewater [198–205], but due to different limitations the process are not very efficient. Researchers are striving hard to develop suitable methods and process to remove dyes from water. Recently, many low-cost and effective adsorbents [206–212] have been used for the removal of dye from water.

Huge amount of red mud, a caustic by-product of the alumina refinery are being generated annually worldwide [128]. As discussed red mud is a serious pollutant to the environment. It can't be disposed of easily because of its high alkali contained. There are many problems for the management of red mud slurry. Therefore, it is necessary to develop an effective utilization of bins red mud. In addition, red mud has a high potential for water treatment as it is an efficient adsorbent due to its chemical and mechanical stability and structural properties.

There is growing interest in research on both natural untreated and modified red mud minerals, including attempts to improve the characteristics of the materials regarding the removal of hazardous dye from industrial wastewater. To enhance the dye adsorption properties of red mud, different techniques of modification have been applied: acid activation [68–70], heat and chemical treatment [71] and chemical modification using inorganic based materials [72]. To the best of our knowledge, the investigation of sodium

dodecyl sulphate (SDS) surfactant modified red mud as an adsorbent for the removal of safranin-O dye has not been reported before. The surface modification using SDS surfactant represents an environmentally friendly and inexpensive method in comparison with other methods. A list of low-cost adsorbents for the adsorption of safranin-O from aqueous solutions is given in Table 6.1.

Table 6.1: Comparison of adsorption capacities of safranin-O dyes onto different adsorbents

Adsorbent(s)	*pH*	Adsorption Capacity (mg/g)	References
Calcined mussel shells	Above 9.2	154.34	[213]
Pineapple peels	6-8	21.7	[214]
Calcined bones	6.2	135.32	[208]
$NaOH$ treated rice husk	8	37.97	[215]
Alkali-treated rice husk	8	9.77	[216]
SDS/RM	4	8.94	present study

In the previous chapter, activated red mud have been prepared by acid dilution followed by ammonia precipitation method. The prepared adsorbent materials were found to be efficient adsorbents for removal of metal ions like Pb(II) and Cd(II) from aqueous media. This chapter describes the neutralization of red mud using H_2SO_4 and the surface modification of the neutralized red mud was carried by the addition of an anionic surfactant sodium dodecyl sulphate and used to remove the safranin-O dye from aqueous solution. The sodium dodecyl sulphate was chosen for the surface modification of the neutralized red mud due to the following reason: (1) prevent the agglomeration of a large ratio of surface area and volume which reduces the surface energy (2) for its admicellar sorption properties (3) highly biodegradable. The surfactant molecule adsorbed on the surface of the red mud by hydrophobic bonding and created surface aggregates on the hydrophilic adsorbent surface. Thus the surface charge of the adsorbent (SDS/RM) becomes negative due to the $-SO_3^-$ anion of the surfactant. In this condition, the cationic dye can be adsorbed onto the surface of the SDS/RM adsorbent. Therefore, in this work cationic dye (safranin-O) was chosen for adsorption in to modified red mud.

the effectiveness of the proposed for dye removal and the factor influencing the adsorption process were investigated in details. The kinetics and equilibrium data of the adsorption process were studied to understand the adsorption characteristics. Finally, safranin-O removal mechanism of SDS/RM was discussed.

6.2 Results and discussion

6.2.1 Physicochemical characterization of the SDS/RM adsorbent

The $BET - N_2$ surface area of the red mud and SDS/RM are found to be 33.5 and 67.10 m^2/g, respectively. The surface area of the SDS/RM increased significantly, which is helpful for the adsorption of safranin-O dye from aqueous solution. Figure 6.1 shows the XRD patterns of SDS/RM and safranin loaded SDS/RM. From the XRD data, the following important mineral phases are identified: hematite ($\alpha - Fe_2O_3$), goethite ($\alpha - FeO(OH)$), gibbsite ($\gamma - Al(OH)_3$), rutile/anatase (TiO_2) and quartz (SiO_2). From the XRD figure, some new peaks are appear and some parent peaks are disappear after the adsorption of safranin-O dye. Also some peaks of SDS/RM before adsorption are shifted form there original position after the adsorption which suggested that the safranin-O dye is loaded on the SDS/RM adsorbent surface.

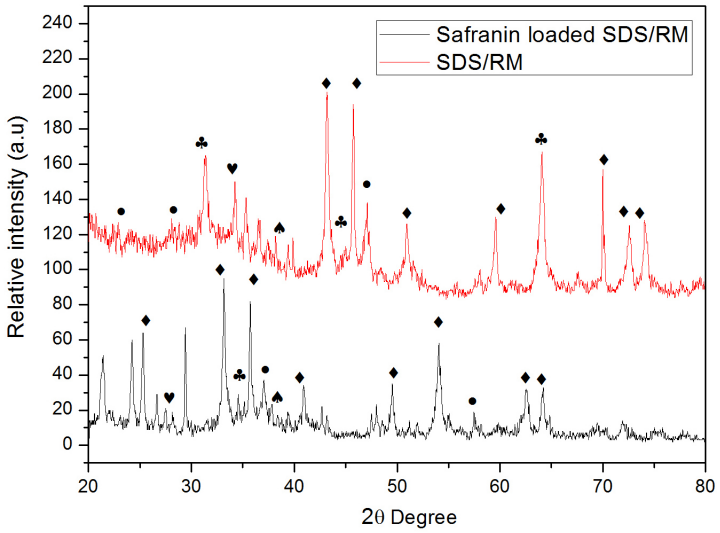

Figure 6.1: XRD of SDS/RM and safranin loaded SDS/RM showing ♠ TiO_2, ♣ $FeO(OH)$, ♥ SiO_2, ♦ Fe_2O_3, • $Al(OH)_3$

The SEM micrographs of SDS/RM and safranin loaded SDS/RM are shown in Figure 6.2. From the SEM images, significant difference are observed between the SDS/RM and safranin loaded SDS/RM. This may be due to that, after chemical treatment the surface of the SDS/RM becomes coarser. These properties should facilitate the adsorption of safranin-O to the surface of SDS/RM, implying high adsorption and rate.

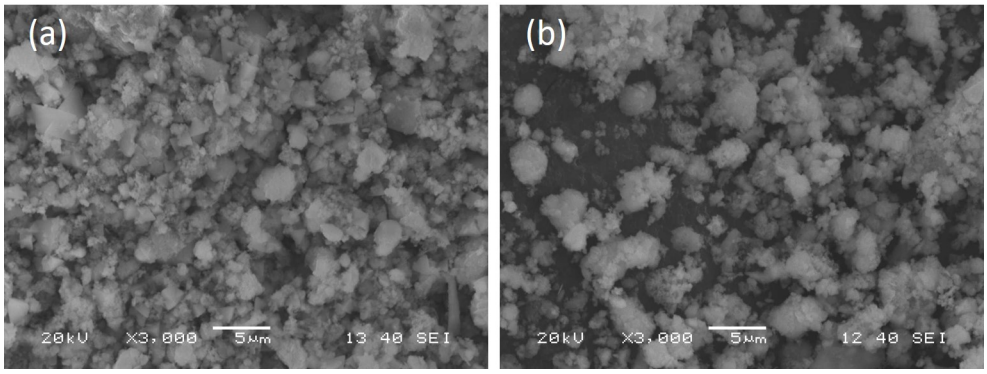

Figure 6.2: Scanning electron micrograph of (a) SDS/RM (Scale bar equals 5 μm) and (b) safranin loaded SDS/RM (Scale bar equals 5 μm)

FT–IR spectra of the SDS/RM, safranin-O and safranin-O loaded SDS/RM are presented in Figure 6.3. A broad adsorption at 3338 cm^{-1} in safranin-O and safranin-O loaded SDS/RM shows the presence of the $-OH$ and $-NH_2$ groups, respectively. The peak at 3183 cm^{-1} is due to $N-H$ group. The presence of the main peaks of safranin-O on safranin-O loaded SDS/RM in IR spectra indicates that, the safranin-O is unchanged on the surface of the adsorbent.

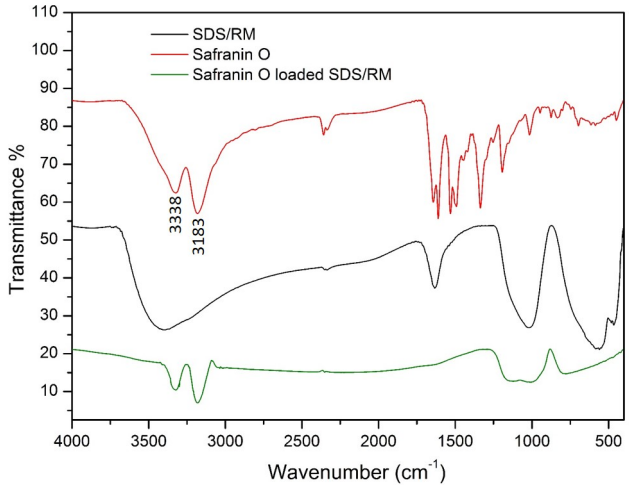

Figure 6.3: FT–IR spectra of SDS/RM, safranin-O and safranin-O loaded SDS/RM

6.2.2 Batch adsorption study for the removal of safranin-O dye by SDS/RM

Effect of *pH*

The *pH* is one of the most significant environmental factors influencing the chemistry of the safranin-O adsorption. The effect of *pH* on the adsorption of safranin-O onto SDS/RM was studied at a *pH* range of 2 to 12 with initial dye solution (50 mg/L). The obtained results are shown in Figure 6.4. From the figure it is clear that the adsorption decreases with an

increase in *pH*. In the *pH* range from 2 to 4 the uptake capacity increases smoothly, then decreases sharply with increase in *pH* values from 4 to 12.

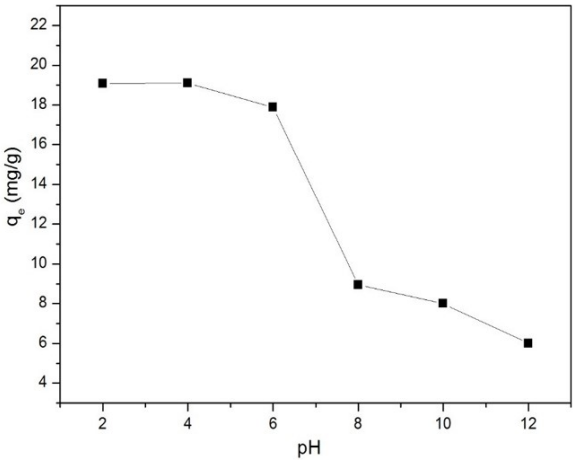

Figure 6.4: Effect of initial *pH* on the adsorption of safranin-O dye on SDS/RM (initial dye concentration = 50 mg/L, weight of the adsorbent = 0.25 g, contact time = 45 min, temperature = 303 K)

The variation in uptake capacity of the safranin-O dye with *pH* depend on the surface charge of the adsorbent. At acidic *pH*, the surfactant molecule adsorbed on the surface of the red mud by hydrophobic bonding and create surface aggregates (hemimicelles, mixed hemimicelles or admicelles) on the hydrophilic adsorbent surface. Thus the surface charge of the adsorbent (SDS/RM) becomes negative due to $-SO_3^-$ anion of the surfactant. In this condition, the cationic dye can be adsorbed to the surface of the SDS/RM adsorbent via electrostatic interactions. On the other hand, at alkaline *pH*, surface of red mud is negatively charged and the surfactant is negative too. So, the density of $-SO_3^-$ groups on the outer surface of the adsorbent decreases and consequently the adsorption capacity decreases [215]. The maximum adsorption capacity of the safranin-O takes place at around acidic *pH* 4, thus *pH* 4 is selected for all further adsorption experiments. The mechanism of the adsorption capacity at different *pH* is illustrated in Figure 6.5.

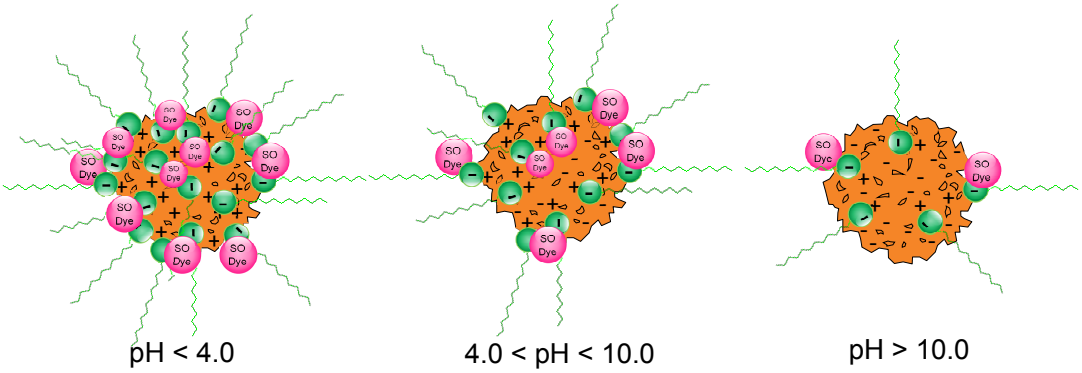

Figure 6.5: Proposed mechanism for the safranin-O adsorption on SDS/RM

Effect of contact time and adsorption kinetics

The effect of contact time on the adsorption of safranin-O on SDS/RM with different initial concentrations (20 to 50 mg/L) is represented in Figure 6.6a. The adsorption increased initially and attained the equilibrium at 45 min. The equilibrium adsorption of safranin-O is found to rise from 4.83 to 8.69 mg/g by changing the initial concentration from 20 to 50 mg/L at 45 min. It is clear that, at higher initial concentration, the adsorption of safranin-O increases, due to enhance driving force [208] or may be due to the availability of the uncovered surface area and the active sites of the SDS/RM.

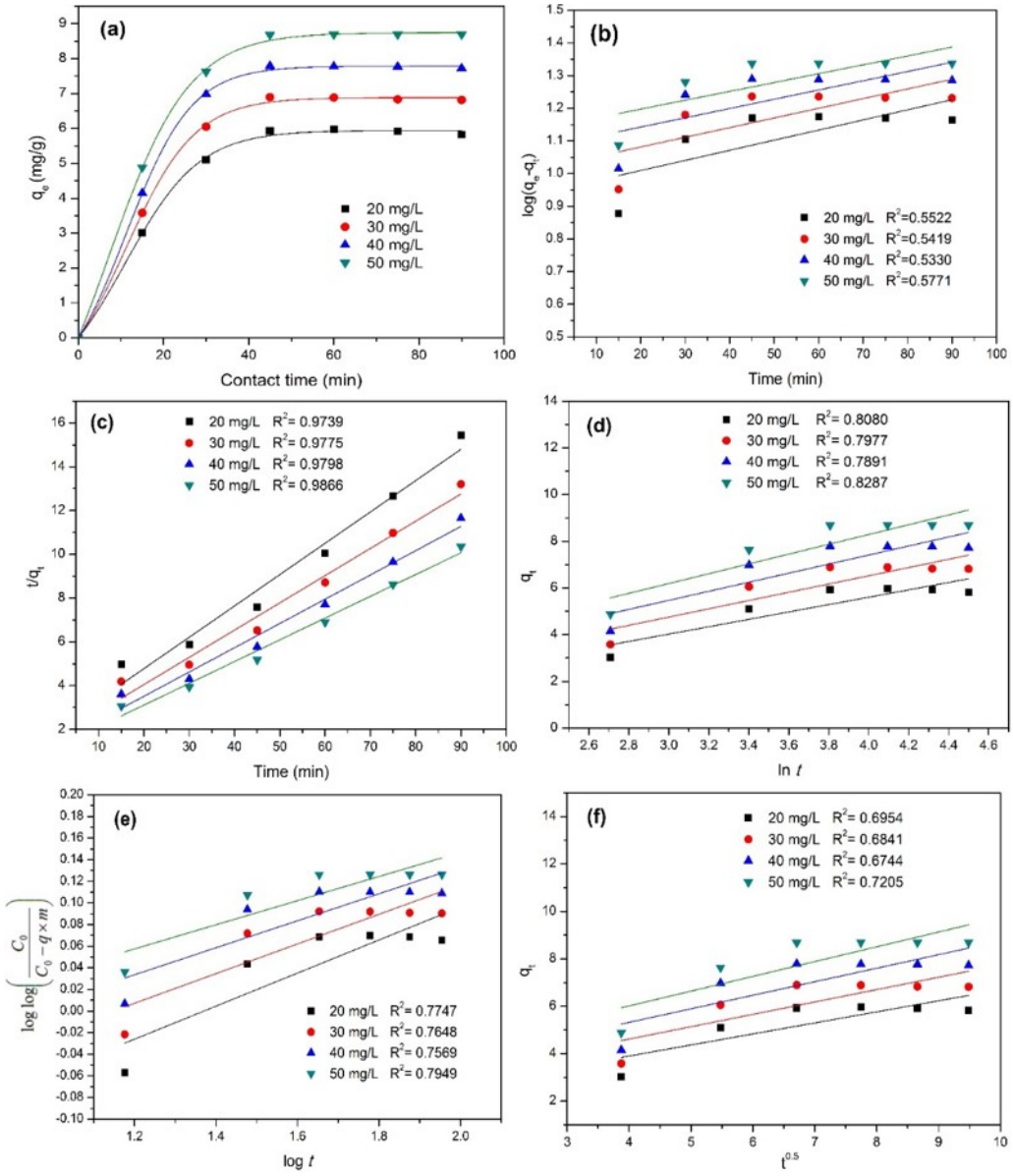

Figure 6.6: (a) effects of contact time for safranin-O dye adsorption on SDS/RM at different concentration (b) Pseudo-first order, (c) Pseudo-second order, (d) Elovich (e) Bangham's (f) intraparticle diffusion model for the adsorption of safranin-O dye on SDS/RM

The different kinetic model are shown in Figure 6.6, and the values of kinetic parameters as obtained from the plot represented in Table 6.2. From the Table 6.2 it is clear that, the pseudo second order model with the correlation coefficients (R^2 >0.97) is best fitted, signifying the dominating role of chemisorption. It means that the overall rate of safranin-O adsorption process seems to be controlled by the chemical process via electrostatic attraction [211]. Satisfactory linear curves are not obtained for Bangham's equation and intra particle diffusion model which indicates that the rate controlling parameter are not only due to diffusion of the adsorbate into pores of the adsorbent.

Table 6.2: Kinetic parameters for the adsorption of safranin-O onto SDS/RM at different initial concentration

Kinetic models	Parameters	Initial concentration (mg/L)			
		20	30	40	50
Pseudo-first-order	q_e (mg/g)	8.8614	10.5291	12.1916	13.9123
	k_1	0.0071	0.0068	0.0065	0.0062
	R^2	0.5522	0.5419	0.5330	0.5771
Pseudo-second-order	q_e (mg/g)	6.9836	8.0358	9.0197	10.0594
	k_2	0.0107	0.0099	0.0095	0.0088
	R^2	0.9739	0.9775	0.9798	0.9866
Elovich Model	α ($mg/g\cdot min$)	1.0057	1.2926	1.6201	1.9901
	β (g/mg)	0.6334	0.5651	0.5156	0.4761
	R^2	0.8080	0.7977	0.7891	0.8287
Bangham's	k_0 (g)	0.5685	0.6410	0.7048	0.7724
	α	0.1529	0.1372	0.1248	0.1118
	R^2	0.7747	0.7648	0.7569	0.7949
Intraparticle diffusion	k_{ip}	0.4661	0.5214	0.5706	0.6232
	C	2.0358	2.5302	3.0402	3.5218
	R^2	0.6954	0.6841	0.6744	0.7205

6.2.3 Mass transfer study

Different plot of mass transfer studies are shown in Figure 6.7 and the values of D_i, D_0, E_a and $\Delta S^{\#}$ are given in Table 6.3. A perusal of Table 6.3 indicates that, the diffusion coefficient decreases with an increase in temperature because with increasing temperature the adsorption of SDS surfactant on red mud surface decreases. The negative values of $\Delta S^{\#}$ obtained by the system reveal that the internal structure of the red mud does not go through any significant internal change during the adsorption of the safranin-O dye. The mass transfer coefficient (k_f) values indicate that the transition took off significantly and conspicuously from a bulk liquid phase to a solid phase to trap safranin-O onto SDS/RM [99]. The k_f values of McKay $et\ al.$ equation and Waber-Mathews equation are found to be 3.49×10^{-4}, 4.61×10^{-4} and 2.13×10^{-4}, 3.11×10^{-4} at temperature 308 and 328 K respectively. It could be understood from the k_f value that SDS/RM adsorbed safranin-O faster at lower temperature for both McKay $et\ al.$ equation and Waber-Mathews equation.

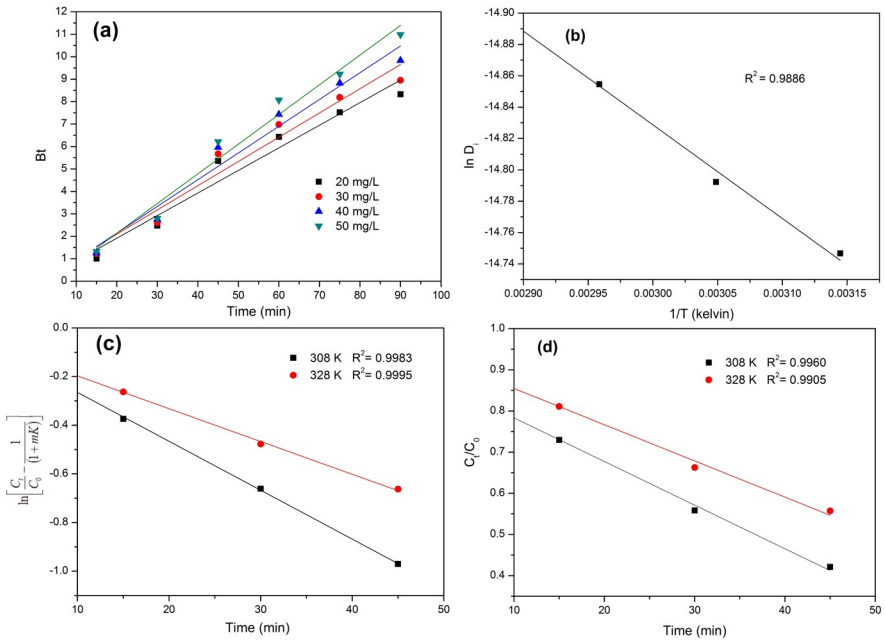

Figure 6.7: (a) Boyed plot (b) lnD_i vs. $1/T$ plot (c) McKay plot and (d) Waber-Mathews plot for the adsorption of safranin-O dye on SDS/RM

Table 6.3: Values of D_i, D_0, E_a, and $\Delta S^{\#}$ and k_f for safranin-O removal on SDS/RM from aqueous solution at different temperature

Dye	$D_i \times 10^{-7}$ (m^2/s)		$D_0 \times 10^{-8}$	$-E_a$	$-\Delta S^{\#}$
	308 K	328 K	(m^2/S)	$(kJ/mole)$	$(J/K \cdot mole)$
Safranin-O	3.95	3.55	6.4	4.81	73.64
McKay equation k_f (cm/min)	3.49×10^{-4}	2.13×10^{-4}			
Weber–Mathews equation k_f (cm/min)	4.61×10^{-4}	3.11×10^{-3}			

Effect of initial safranin-O concentration and adsorption isotherm

The effect of initial safranin-O concentration on the adsorption was studied in the range of 10 to 50 mg/L at temperature 308, 318 and 328 K by keeping the other parameters (*pH* 4, adsorbent dose 0.25 g, time 45 min) constant. The effect of safranin-O concentration on adsorption is shown in Figure 6.8a. The uptake capacity of SDS/RM increased initially and reached a constant after a certain concentration. This may be due to the lack of the active site for the adsorption of high initial concentration of safranin-O dye.

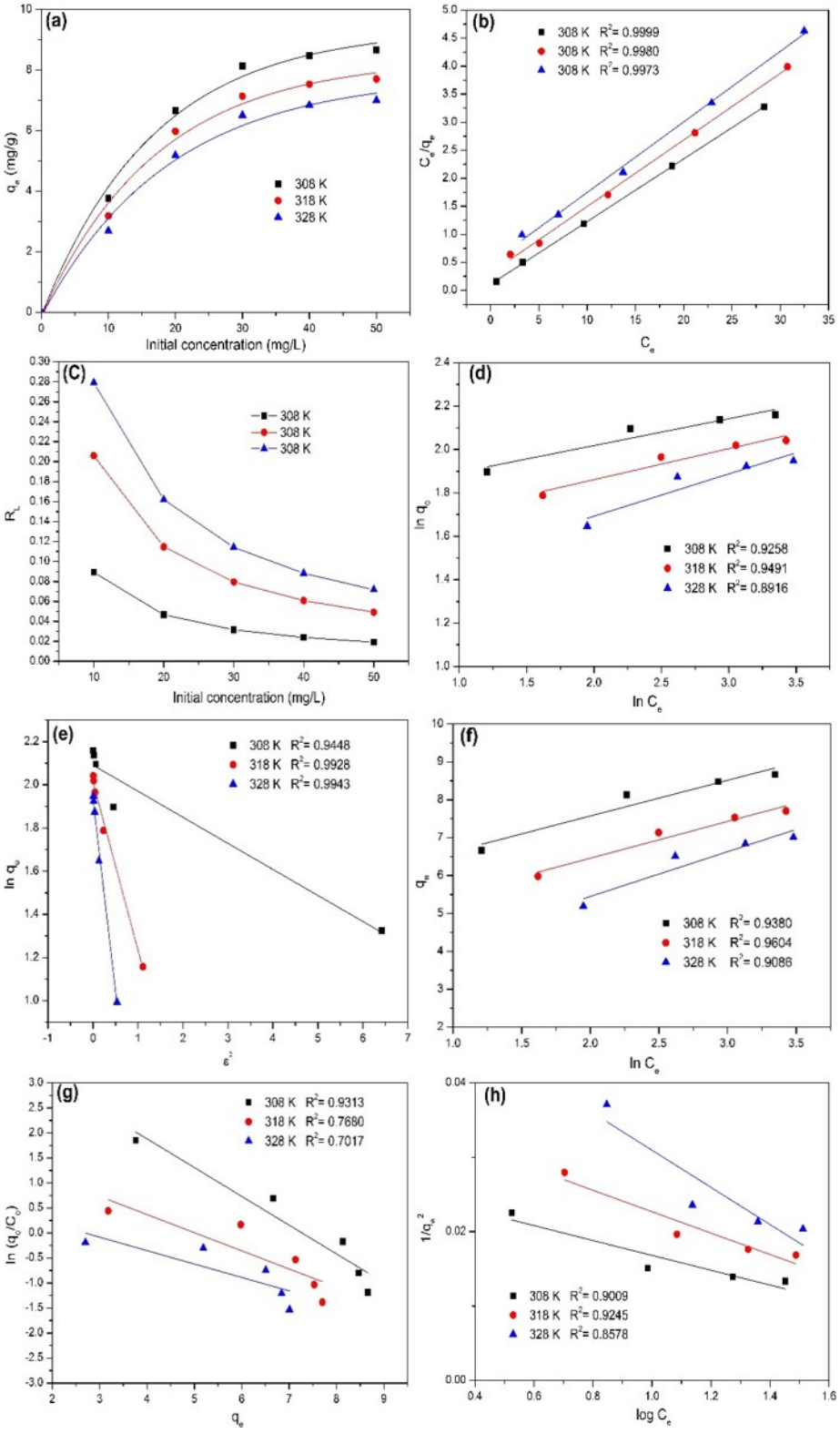

Figure 6.8: (a) Effect of initial concentration for safranin-O dye adsorption on SDS/RM at different temperature (b) Langmuir, (c) Dimensionless parameter, (d) Freundlich, (e) Dubinin-Radushkevich, (f) Temkin, (g) Elovich, (h) Harkin-Jura isotherm model for the adsorption of safranin-O dye on SDS/RM

The isotherms are shown graphically in Figure 6.8 (b, d, e, f, g, h) and the isotherm parameters are listed in Table 6.4. From the Table 6.4, the value of R_L is in between 0 to 1 confirmed the favourable uptake of the safranin-O. The calculated R_L values at different initial safranin-O concentration and different temperature are shown in Figure 6.8c. From the Freundlich isotherm, the values of $1/n$ is less than 1 represent a favourable adsorption [105]. With the increase in temperature, the Freundlich constant decrease shows the adsorption process is favourable at low temperature and exothermic in nature [215]. Smaller the value of the Temkin constant (B_1) suggested that adsorption of safranin-O on SDS/RM is favourable. Comparison of coefficients indicates that the Langmuir isotherm fitted more precisely (R^2 = 0.99) than the Freundlich isotherm (R^2 = 0.92), Dubinin-Radushkevich isotherm (R^2 = 0.94), Temkin isotherm (R^2 = 0.93), Elovich isotherm (R^2 = 0.93) and Harkin-Jura isotherm (R^2 = 0.90). The result indicate that the adsorption of safranin-O onto SDS/RM generates monolayer formation [215].

Table 6.4: Isotherm parameters for the adsorption of safranin-O dye onto SDS/RM at different temperature

Isotherm model	Parameters	Temperature (K)		
		308	318	328
Langmuir	q_m (mg/g)	8.9471	8.4193	7.9423
	b (L/mg)	1.0265	0.3859	0.2585
	R_L	0.0891	0.2057	0.2789
	R^2	0.9999	0.9980	0.9973
Freundlich	K_f	58.9604	37.7345	20.0975
	$1/n$	0.1237	0.1422	0.1948
	R^2	0.9258	0.9491	0.8916
Dubinin-Radushkevich	q_m (mg/g)	8.0927	7.4890	6.9254
	β (mol^2/KJ)	0.1207	0.7795	1.7856
	E	2.0352	0.8008	0.5291
	R^2	0.9448	0.9928	0.9943
Temkin	K_T (L/mg)	417.9285	106.8732	13.6380
	B_1	0.9423	0.9682	1.1813
	R^2	0.9380	0.9604	0.9086
Elovich	q_m (mg/g)	1.7397	2.7571	3.7230
	K_E	37.6249	2.2383	0.5532
	R^2	0.9313	0.7680	0.7017
Harkin-Jura	A	100.0207	69.5651	40.0643
	B	2.6810	2.5776	2.2395
	R^2	0.9009	0.9245	0.8578

6.2.4 Desorption study

Desorption experiments were carried out by batch method using different solvents such as water, sulphuric acid (0.1 M), hydrochloric acid (0.1 M) and acetic acid (0.1 M). The comparison of desorption efficiency is shown in Figure 6.9. The desorption by distilled

water is only 6% indicates that physical adsorption is not dominant factor while acetic acid confirmed thin desorption efficiency (64%) showing the presence of chemical-complexation type dye-adsorbent interaction routed. On the other hand, HCl and H_2SO_4 show the maximum desorption efficiencies of 93 and 71% respectively, because the anionic surface, i.e. sodium dodecyl sulphate present in the red mud helps to absorbed H^+ of acids not the dye molecules. However, the crest desorption by hydrochloric acid approved chemisorption of dyes on SDS/RM.

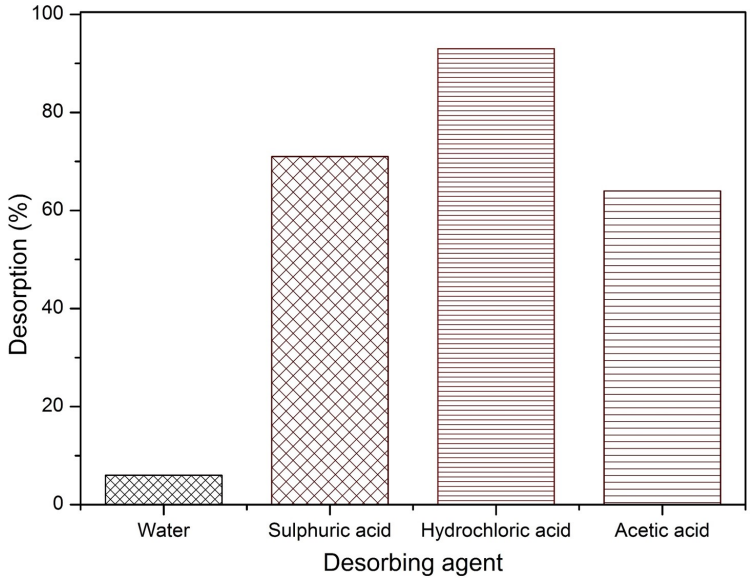

Figure 6.9: Desorption of safranin dye using various desorbing agent

6.3 Conclusions

Red mud modified with sodium dodecyl sulphate (SDS) is an excellent adsorbent for the treatment of safranin-O dye from aqueous solution. The solution *pH* is a critical parameter for the removal of safranin–O dye. Generally, adsorption capacity of safranin-O by modified red mud decreases with an increase in the solution initial *pH*. The maximum adsorption of safranin-O occurs at *pH* 4 with an equilibrium time of 45 min. Pseudo second order kinetic model describe the adsorption process. The maximum adsorption capacity of 8.9471 mg/g is calculated from the Langmuir isotherm model. The adsorption of safranin-O on SDS/RM is determined to be faster at lower temperature, and the process is regulated by mass transfer. The results represent a fundamental study of the adsorption of safranin-O dye from aqueous solutions by SDS modified red mud. The study shows that the modified red mud is an economical and efficient adsorbent for application in the treatment of dyes contaminated wastewater. Further investigations will be directed toward applications to real samples and the enhancement of the adsorption properties of the studied red mud.

Chapter 7

Adsorption of safranin-O dye on CO_2 neutralized activated red mud waste: Process modelling, analysis and optimization using statistical design

7.1 Introduction

In the previous chapter (Chapter 6) the removal of safranin-O dye by sodium dodecyl sulphate modified red mud is reported. In this chapter, the waste red mud was neutralized by passing CO_2 gas into the red mud. The neutralized red mud was activated by calcining and used as an adsorbent to remove safranin-O from aqueous solution. Central composite design (CCD) was employed to determine the relationship between experimental variables and optimum adsorption conditions for the removal of safranin-O dye on activated red mud.

Dyes are usually used to colour materials such as leather, plastics, textiles, food, paper, and cosmetics in many industries [192]. Among various industries, textile industry used large variety of dyes for coloration of fibre. As a result, a substantial amount of coloured wastewater is generated from these industries which create serious environmental problem not only because of its toxicity, but also due to its visibility problem [193, 194]. Therefore, the dyes should be removed from industrial effluent before discharge to the environment is an important aspect for both artistic sense and health point of view.

Various conventional methods were reported for the removal of dyes from the industrial wastewater [198–205]. Among them adsorption process is preferred widely to treat wastewater containing different class of dyes. Recently, many low-cost and effective adsorbent have been used by the researchers for the adsorption of dye from water [206–212]. However, some disadvantages like poor regeneration capacity, expensive and less adsorption capacity are associated with the adsorbent. Attempts are being made to prepare alternative adsorbent to overcome the disadvantages.

Red mud is one of the main waste material in alumina industries worldwide. The quantity of red mud generated, depends upon the quality of bauxite processed. A huge amount of red mud released by these industries is an economical and environmental problem which has led

researchers to develop new uses of red mud [128]. Red mud requires neutralization before it is used. The *pH* of neutralized red mud should be around 8.0 as in this *pH* the chemically adsorbed sodium present in the red mud is released and makes the toxic metals insoluble [32]. The global climate change due to increase in anthropogenic (CO_2) concentrations in the atmospheric air constructing a challenging issue for future generations [217]. The energy sector is a major contributor of CO_2 emissions, with estimates placing their current levels above 30 Gt [218]. The issues of climate change can be minimize by reducing the carbon emission from the industries and use it by capturing and storing. Thus, in this study, carbon dioxide gas is used to neutralize the alkaline red mud. Also, utilization of industrial waste as an assets to resolve the problem of another waste provide commercial profit.

Among different class (anionic, cationic and non-ionic) of dyes, cationic dye (safranin-O) was chosen as the target because it is more toxic and has harmful effects on living organisms during short period of exposure. Table 7.1 listed some of the reported adsorbent used to remove safranin-O from water. However, to the best of our knowledge, the applications of red mud on the adsorption of safranin-O has not been reported before. Therefore, it will be significant to study the interaction between the efficient, cheap and easily available red mud and safranin-O dye.

The aim of this study was to evaluate the removal efficiency of hazardous safranin-O from its aqueous solution by using CO_2 neutralized activated red mud. In this study, three-level, four-factor central composite design (CCD) was employed to determine the relationship between experimental variables (adsorbent dose, temperature, *pH* and initial safranin-O concentration) and optimum adsorption conditions for activated red mud. Meanwhile, characteristics of the adsorption isotherm was studied through the adsorption experiments.

Table 7.1: Adsorption capacities of safranin-O dyes onto different adsorbents

Adsorbent(s)	*pH*	Removal capacity (%)	References
Calcined mussel shells	>9.2	87.56	[213]
Pineapple peels	6-8	43.3	[214]
Calcined bones	6.2	96.78	[208]
NaOH treated rice husk	8	98.02	[215]
Alkali-treated rice husk	8	93.28	[216]
Corncob activated carbon	5-9	99.8	[219]
CO_2 neutralized activated red mud	8.3	95.5	Present study

7.2 Results and discussion

7.2.1 Adsorbent characterization

Particle size and BET surface area of the activated red mud is in the range of 0.1 to 150 μm and 67.10 m^2/g, respectively. SEM images of the CO_2 neutralized activated red mud

(Figure 7.1) shows that the surface view of the activated red mud is changed after the dye adsorption and the pores are completely filled with safranin-O and appeared puffy due to heterogeneity.

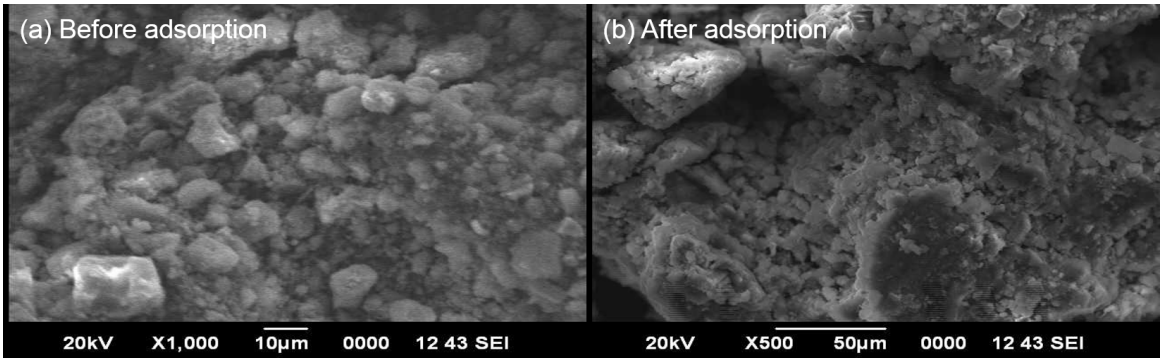

Figure 7.1: SEM images of CO_2 neutralized activated red mud (a) before adsorption and (b) after adsorption

The XRD pattern of activated red mud before and after adsorption is shown in Figure 7.2. The main phases identified in the CO_2 neutralised activated red mud are hematite (α $-Fe_2O_3$), goethite (α $-FeO(OH)$), gibbsite (γ $-Al(OH)_3$), anatase (TiO_2) quartz (SiO_2) and calcite ($CaCO_3$). Activated red mud after adsorption shows similar XRD patterns with activated red mud before adsorption. However, the intensity of diffraction peaks increases conspicuously whereas calcite ($CaCO_3$) mineral peak intensity is vanish, this may be due to the phase transformation.

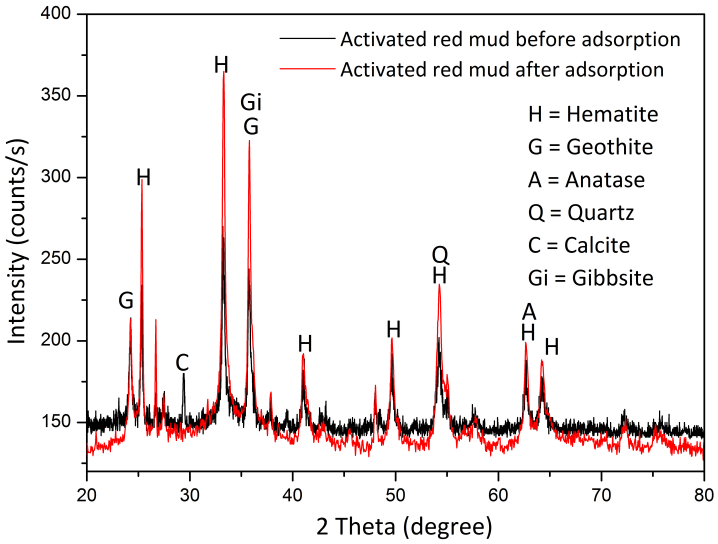

Figure 7.2: XRD pattern of CO_2 neutralized activated red mud before and after adsorption of safranin-O dye

Figure 7.3 shows the FT–IR spectra of the safranin-O dye, CO_2 neutralised activated red mud before and after safranin-O adsorption. CO_2 neutralized activated red mud shows a broad peak at 3087 cm^{-1} and a weak peak at 1634 cm^{-1}, due to the stretching vibration

of O–H and CO_3^{2-} groups respectively. After adsorption, some new absorption bands are occurred on dye loaded activated red mud. The bands at 1603 and 1634 cm^{-1} are assigned to aromatic ring. The band at 1424 cm^{-1} is due to $-CH_3$ bending vibration. The peaks at 1335 and 1338 cm^{-1} represented the aromatic–N. However, these newly appeared peaks after adsorption of dye, indicated the dye adsorbed onto CO_2 neutralised activated red mud. Additionally, the band at 3292 cm^{-1} is attributed to N–H group of safranin–O dye adsorbed on the surface of the red mud [220]. According to the FT–IR spectra the adsorption of safranin-O dye on activated red mud (ARM), the mechanism of adsorption can be illustrated in Figure 7.4.

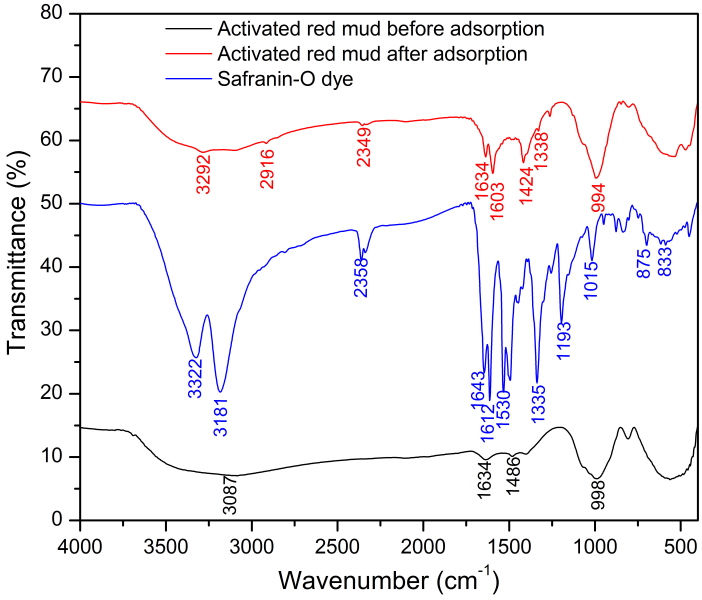

Figure 7.3: FT–IR spectrum of safranin-O dye and CO_2 neutralised activated red mud before and after adsorption of dye

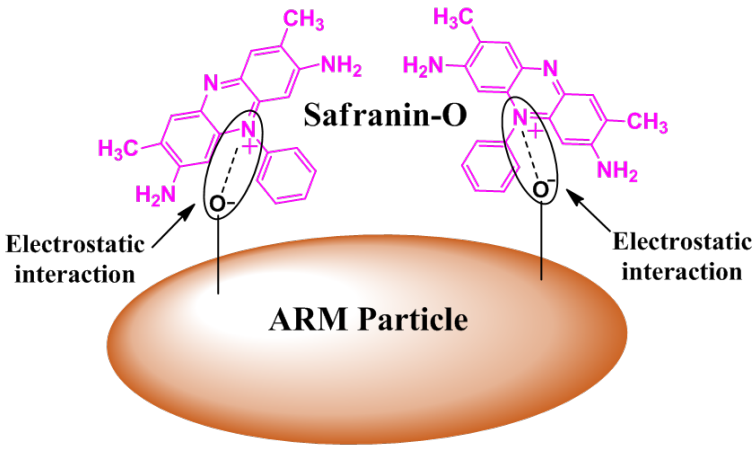

Figure 7.4: Schematic representation of adsorption mechanism of safranin-O dye onto activated red mud

7.2.2 Model determination

The model statistics for each model was output by Design Expert 7.0 software. Table 7.2 display the different tests to select an adequate model to be fitted for the adsorbate removal. A quadratic model is suggested, even though the R^2 and adjacent R^2 values of quadratic model is lower than the cubic model. This is because the cubic model is aliased, which means that the effects of each variable become indistinguishable due to different signals. For linear model and 2FI model, the R^2 and adjacent R^2 values are found to be 0.1962, 0.0676 and 0.3303, -0.0222, respectively, which shows both the models are not adequate for the experimental data. Therefore the quadratic model (R^2 = 0.9655 and adjacent R^2 = 0.9333) is selected to fit the experimental data. The experimental design matrix and their results are represented in Table 7.3.

Table 7.2: Selection of adequate model for the CO_2 neutralized activated red mud system

Source	Std. Dev.	R^2	Adj $-R^2$	Predicted R^2	PRESS	Remarks
Linear	8.57	0.1962	0.0676	-0.0057	2298.43	Not adequate
2FI	8.98	0.3303	-0.0222	-0.3174	3010.66	Not adequate
Quadratic	2.29	0.9655	0.9333	0.8339	379.70	Suggested
Cubic	2.20	0.9851	0.9383	-0.0650	2433.93	Aliased

7.2.3 Development of regression model equation

CCD was used to build a relationship between four independent variables for the removal of safranin-O dye from aqueous solution by second-order polynomial equation. Based on the model analysis, a quadratic model is chosen in terms of coded factor and actual factor for adsorption of safranin-O (% Removal) and the equation obtained is shown in Equation 7.1:

$$\begin{aligned} Y = {} & 93.3867 + 2.3642X_1 - 1.0650X_2 + 2.2025X_3 + 2.6658X_4 \\ & - 0.9875X_1X_2 + 0.5725X_1X_3 - 3.3913X_1X_4 - 0.4413X_2X_3 \\ & - 2.4800X_2X_4 - 0.1000X_3X_4 - 4.5304X_1X_1 - 4.7429X_2X_2 \\ & - 4.3317X_3X_3 - 3.6579X_4X_4 \end{aligned} \tag{7.1}$$

The positive sign and the negative sign of the term indicates the synergetic and antagonistic effect respectively.

Table 7.4 represents analysis of variance (ANOVA) results for safranin-O adsorption by activated red mud. Analysis of variance (ANOVA) is applied for the model to examine the fitness of the model, accuracy of the model, effects of single variables and interaction effects on the response [221]. The model F value is found to be 29.97 with lower probability (<0.0001) indicates the model is significant. There is only a 0.01% possibility that the model F value could happen due to noise. It is observed that among the four variables studied, initial concentration (X_4) has the largest effect on the removal of safranin-O due to the

maximum F value followed in order by adsorbent dose (X_1), *pH* (X_3) and temperature (X_2). The lack of fit for F value of 1.78 implies this terms is not significant relative to the pure error. There is only 27.20% chance that the lack of fit F value could occur due to noise [222]. The predicted determination coefficient (R^2) value is 0.9655.

Table 7.3: Experimental design matrix and response

Run	Coded values				Actual values				% Removal		Residual
	X_1	X_2	X_3	X_4	X_1	X_2	X_3	X_4	Observed	Predicted	
1	-1	-1	-1	-1	0.1	10	2	10	59.68	63.13	-3.45
2	1	-1	-1	-1	1	10	2	10	76.26	75.47	0.79
3	-1	1	-1	-1	0.1	60	2	10	70.05	68.82	1.23
4	1	1	-1	-1	1	60	2	10	75.69	77.21	-1.52
5	-1	-1	1	-1	0.1	10	12	10	67.51	67.47	0.039
6	1	-1	1	-1	1	10	12	10	83.59	82.10	1.49
7	-1	1	1	-1	0.1	60	12	10	70.38	71.39	-1.01
8	1	1	1	-1	1	60	12	10	79.91	82.07	-2.16
9	-1	-1	-1	1	0.1	10	2	50	81.96	80.40	1.56
10	1	-1	-1	1	1	10	2	50	78.52	79.18	-0.66
11	-1	1	-1	1	0.1	60	2	50	73.01	76.17	-3.16
12	1	1	-1	1	1	60	2	50	70.35	71.00	-0.65
13	-1	-1	1	1	0.1	10	12	50	84.19	84.35	-0.16
14	1	-1	1	1	1	10	12	50	83.57	85.41	-1.84
15	-1	1	1	1	0.1	60	12	50	76.95	78.35	-1.40
16	1	1	1	1	1	60	12	50	77.24	75.46	1.78
17	-1	0	0	0	0.1	35	7	30	72.57	70.54	2.03
18	1	0	0	0	1	35	7	30	80.24	79.99	0.25
19	0	-1	0	0	0.55	10	7	30	76.52	76.55	-0.025
20	0	1	0	0	0.55	60	7	30	74.59	72.28	2.31
21	0	0	-1	0	0.55	35	2	30	73.44	71.66	1.78
22	0	0	1	0	0.55	35	12	30	80.96	80.47	0.49
23	0	0	0	-1	0.55	35	7	10	74.58	73.42	1.16
24	0	0	0	1	0.55	35	7	50	85.21	84.09	1.12
25	0	0	0	0	0.55	35	7	30	96.38	93.39	2.99
26	0	0	0	0	0.55	35	7	30	92.72	93.39	-0.67
27	0	0	0	0	0.55	35	7	30	92.18	93.39	-1.21
28	0	0	0	0	0.55	35	7	30	91.71	93.39	-1.68
29	0	0	0	0	0.55	35	7	30	92.35	93.39	-1.04
30	0	0	0	0	0.55	35	7	30	94.98	93.39	1.59

In Table 7.5, the estimated regression coefficients, *t*-values and *p*-values are given. Significance of each model term is check using *p*-value. The *p*-values smaller than 0.05 indicates that the model is statistically significant, whereas the values greater than 0.1000 indicates the model terms are not significant. In this case all the linear model terms (X_1, X_2, X_3, and X_4) and quadratic model terms (X_1X_1, X_2X_2, X_3X_3 and X_4X_4) are significant, whereas only X_1X_4 and X_2X_4 are significant for the interaction model terms. Other

variables such as X_1X_2, X_1X_3, X_2X_3 and X_3X_4 are not significant effect for the removal of safranin-O due to the *p* value more than 0.05.

Table 7.4: Analysis of variance (ANOVA) for the selected quadratic model

Source	Sum of Squares	*df*	Mean Square	*F* Value	*p*-value Prob >*F*	
Model	2206.50	14	157.61	29.97	<0.0001	#
X_1	134.14	1	134.14	25.51	0.0001	#
X_2	27.22	1	27.22	5.18	0.0380	#
X_3	116.42	1	116.42	22.14	0.0003	#
X_4	170.56	1	170.56	32.43	<0.0001	#
X_1X_2	15.60	1	15.60	2.97	0.1055	*
X_1X_3	5.24	1	5.24	1.00	0.3338	*
X_1X_4	184.01	1	184.01	34.99	<0.0001	#
X_2X_3	3.12	1	3.12	0.59	0.4535	*
X_2X_4	98.41	1	98.41	18.71	0.0006	#
X_3X_4	0.16	1	0.16	0.030	0.8639	*
X_1X_1	562.96	1	562.96	107.05	<0.0001	#
X_2X_2	617.01	1	617.01	117.33	<0.0001	#
X_3X_3	514.65	1	514.65	97.86	<0.0001	#
X_4X_4	367.00	1	367.00	69.79	<0.0001	#
Residual	78.88	15	5.26			
Lack of Fit	61.60	10	6.16	1.78	0.2720	*
Pure Error	17.29	5	3.46			
Cor Total	2285.38	29				
R^2 = 0.9655	Adj R^2 = 0.8339					
# = significant	* = not significant					

Table 7.5: Estimated regression coefficients, *t*-values and *p*-values.

Terms	Removal of safranin-O		
	Coefficient	*t*-value	*p*-value
Constant	93.3867	99.750	0.000
X_1	2.3642	5.051	0.000
X_2	-1.0650	-2.275	0.038
X_3	2.2025	4.705	0.000
X_4	2.6658	5.695	0.000
X_1X_2	-0.9875	-1.722	0.106
X_1X_3	0.5725	0.999	0.334
X_1X_4	-3.3913	-5.915	0.000
X_2X_3	-0.4413	-0.770	0.453
X_2X_4	-2.4800	-4.326	0.001
X_3X_4	-0.1000	-0.174	0.864
X_1X_1	-4.5304	-10.346	0.000
X_2X_2	-4.7429	-10.832	0.000
X_3X_3	-4.3317	-9.893	0.000
X_4X_4	-3.6579	-8.354	0.000

Figure 7.5a shows the comparison of predicted and experimental % removal of safranin-O dye, where the points bunch nearby the diagonal line, showing good fitness of the model, because the value of predicted R^2 of 0.8339 is in logical agreement with the adjusted R^2 of 0.9333. Figure. 7.5b shows the relationship between the normal probability (%) and the internally studentized residuals. The straight line means that neither response transformation is required nor apparent problem with normality [223]. Adequate precision measures the signal-to-noise ratio of 18.660 shows an adequate signal because when the ratio is greater than 4, the model is a desirable one [224]. Thus, this model can be used to navigate the design space.

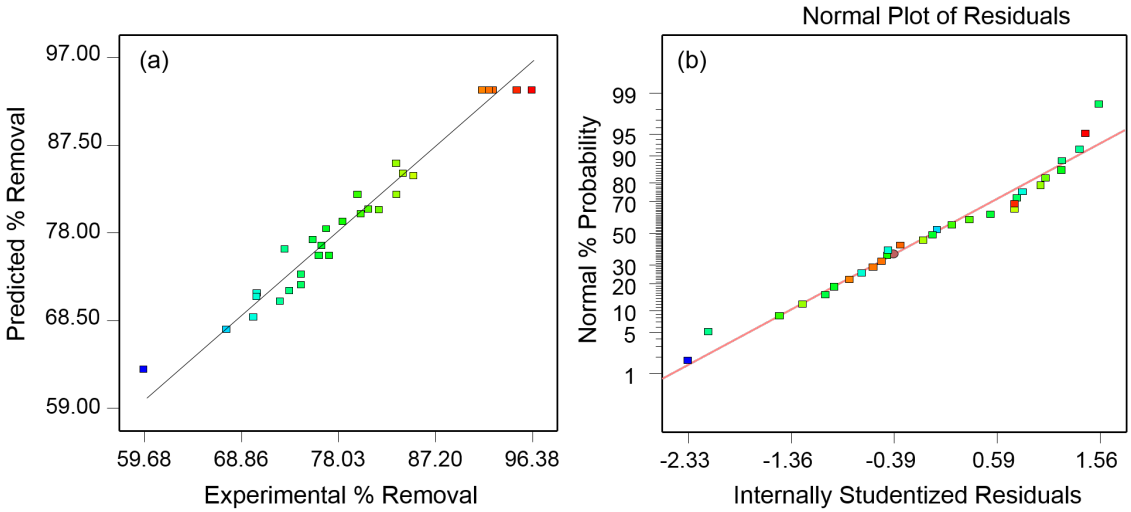

Figure 7.5: (a) Comparison of predicted and experimental % removal safranin-O dye, (b) Normal plot of residuals showing the relationship between normal probability (%) and internally studentized residuals

7.2.4 Model modification

After the evaluation of parameters significance, the model can be improved by excluding the terms that are not significant. The final model for describing the relationship between the adsorbent dose (X_1), temperature (X_2), *pH* (X_3) and initial concentration (X_4) is shown in Equation 7.2:

$$\begin{aligned} Y = {} & 93.3867 + 2.3642X_1 - 1.0650X_2 + 2.2025X_3 + 2.6658X_4 \\ & - 3.3913X_1X_4 - 2.4800X_2X_4 - 4.5304X_1X_1 - 4.7429X_2X_2 \\ & - 4.3317X_3X_3 - 3.6579X_4X_4 \end{aligned} \tag{7.2}$$

After elimination of the non-significant term, the R^2 (0.9549) and adjusted R^2 (0.9312) values decreases slightly whereas the predicted R^2 and adequate precision increases from 0.8339 to 0.8808 and 18.660 to 20.783, respectively.

7.2.5 Effects of variables on the removal of safranin-O dye

To understand the effects of interaction between the process variables and treatment outputs, the three dimensional (3D) response surface plots and there corresponding two dimensional (2D) counter plots of the model were constructed by using the statistical software. The response surface plots better visualizes the interaction effects of each factor to influence the percentage removal of dye from the aqueous solution. The shape of the contour plot shows the natures and extents of the interactions effects between the experimental factors on the response [225]. The circular and elliptical or saddle nature of the contour plots shows the negligible and significance interaction between the equivalent variables, respectively [224]. In each plot, the effects of two variables are varied within the experimental ranges and the other variable fixed to the zero level.

Effect of temperature and *pH* on adsorption process

The role of *pH* and temperature are considered to be the most influencing variables in adsorption process. The response surface and counter plot are developed to illustrate the combining effect of temperature and *pH* on the removal percentage of safranin-O at constant adsorbent dose of 0.55 g and initial concentration of 30 mg/L (Figure 7.6). The figure shows that, the adsorption percentage of the safranin-O dye increases with increase in temperature from 10 ℃ to 30 ℃. However, beyond this temperature percentage removal begins to decrease, which indicates that the adsorption of safranin-O onto the surface of adsorbent particles is favored at lower temperatures and is controlled by an exothermic process. This may be due to the weakening of attractive forces between the dye molecules and the surface of particles [226]. In addition, the percentage removal of safranin-O increases with increase in *pH* of the solution from 2 to 10 and after *pH* 10 the percentage removal becomes constant. This is because, at higher *pH*, OH^- concentration on the adsorbent surface increases. Thus the electrostatic force of attraction between positively dye cation and negatively charged adsorbent sites increases [227]. By using a response optimizer, the predicted % removal, i.e., 93.73% is obtained at *pH* 8.8 and temperature 32.3 ℃.

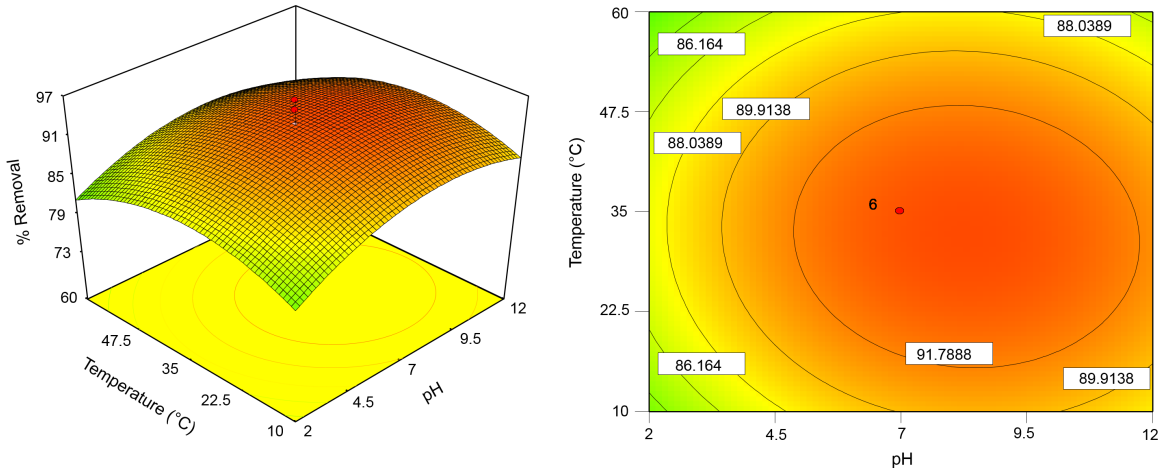

Figure 7.6: 3D response surface and 2D counter plot represents independent interaction of temperature and *pH* for the safranin-O dye adsorption

Effect of temperature and dye concentration on adsorption process

The combined effect of initial dye concentration and temperature on the dye adsorption onto activated red mud at constant *pH* 7 and adsorbent dose 0.55 g is shown in Figure 7.7. It is evident that adsorption of safranin-O increases with increase in initial dye concentration. This is because, when the safranin-O concentration increases in the solution, the active sites of the adsorbent will be surrounded by much more safranin-O molecule of it. Therefore, the percentage removal increases with increase in the initial concentration of the dye. The removal percentage increases very slightly with increase in temperature. This may be due to that, the number of binding sites increases with increase in temperature, hence enhancing the adsorption process [228]. A maximum dye removal of 94.09% is obtained at temperature 29.59 ℃ and initial dye concentration of 38.65 mg/L.

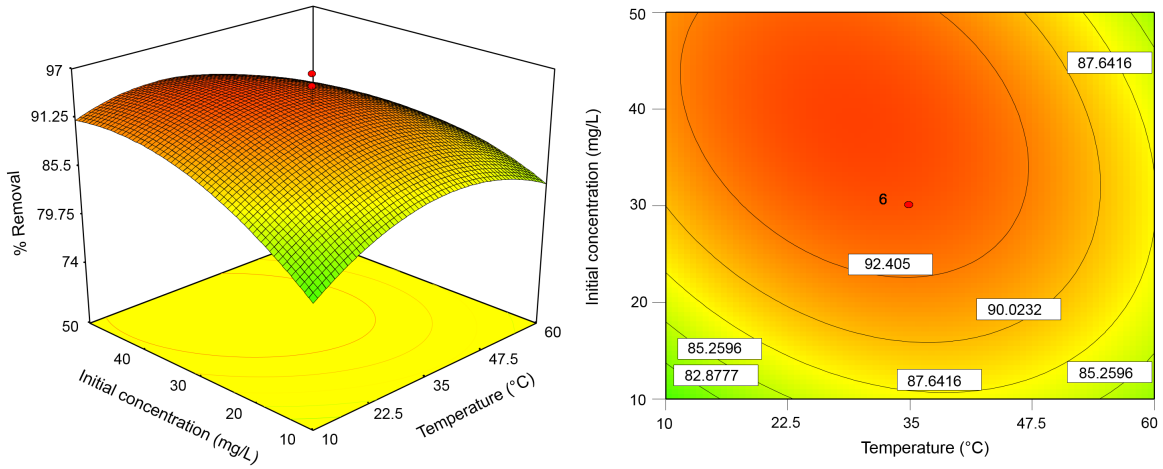

Figure 7.7: 3D response surface and 2D counter plot represents independent interaction of initial concentration and temperature for the safranin-O dye adsorption

Effect of temperature and adsorbent dose on adsorption process

The interactive effect of temperature and adsorbent dose on adsorption at constant *pH* 7 and initial dye concentration 30 mg/L is shown in Figure 7.8. It may be noted that the dye adsorption decreases with increase in temperature and increases with increase in absorbent dose within the experimental range. The reason of this observation is thought to be the fact that, an increase in adsorbent dose in the solution of constant dye concentration, increase the surface area and hence more availability of active site to safranin-O molecules caused an enhancement in dye removal. A maximum dye uptake is found to be 93.78% at temperature 31.61 ℃ and adsorbent dose of 0.66 g.

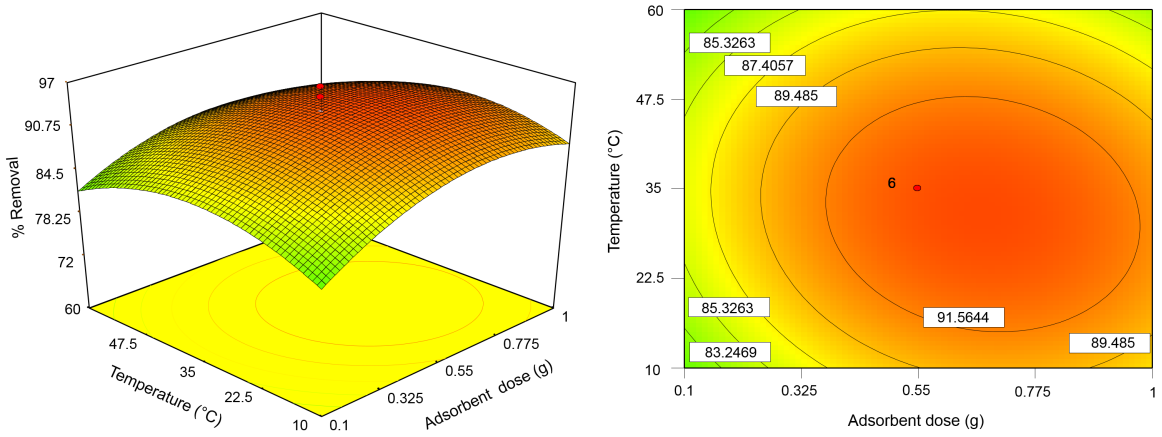

Figure 7.8: 3D response surface and 2D counter plot represents independent interaction of temperature and adsorbent dose for the safranin-O dye adsorption

Effect of *pH* and initial dye concentration on adsorption process

Figure 7.9 represents the combined effect of *pH* and initial dye concentration on removal of safranin-O dye onto activated red mud at constant adsorbent dose of 0.55 g and temperature 35 ℃. It is evident that the percentage removal of dye increases with the increase in both *pH* and the dye concentration, as in the cases discussed earlier. The maximum removal of dye is observed at higher *pH*, this may be due to the pH_{zpc} of the adsorbent. A maximum dye removal of 94.14% is determined at *pH* 8.35 and initial dye concentration of 37.03 mg/L.

Effect of *pH* and adsorbent dose on adsorption process

Figure 7.10 depicted the combined effects of the adsorbent dosage and the initial *pH* for the dye adsorption by the activated red mud at constant temperature 35 ℃ and initial concentration of 30 mg/L. The percentage removal of safranin-O increases with increase in both adsorbent dose and the solution *pH*. As already mentioned above, at higher *pH* of the solution, a great number of OH^- in the experiment solution. On the other hand, at lower *pH*, there are a considerable number of OH^- in the aqueous medium. Therefore, the surface of the adsorbent can provide more negative charges in basic medium rather than acid

medium, and since the dye is cationic, removing dye from the basic solution will be easier. In addition, the change of adsorbent dose increase the dye removal percentage even in higher *pH*. A maximum dye removal 94.01% is obtained at *pH* 8.22 and adsorbent dose of 0.68 g.

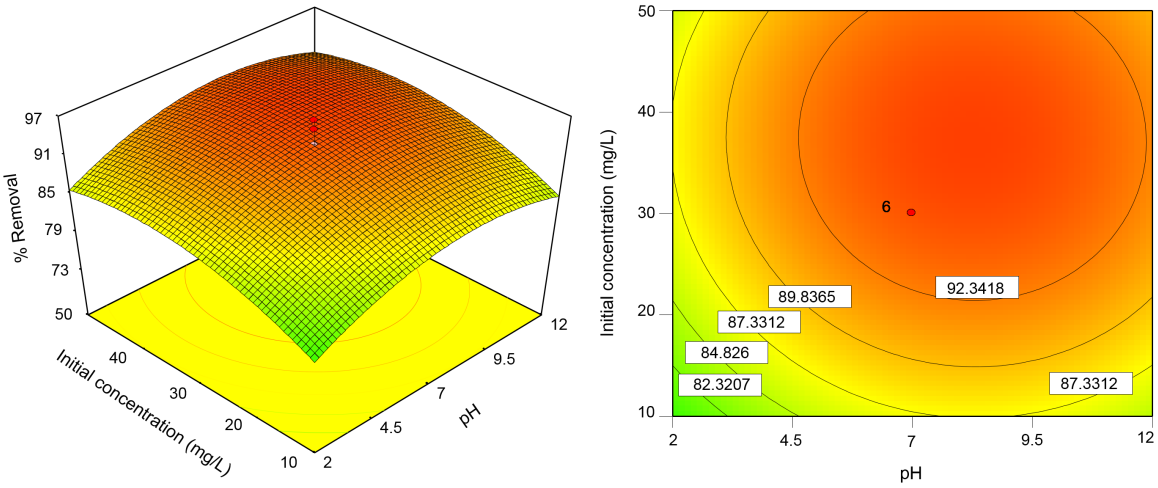

Figure 7.9: 3D response surface and 2D counter plot represents independent interaction of *pH* and initial dye concentration for the safranin-O dye adsorption

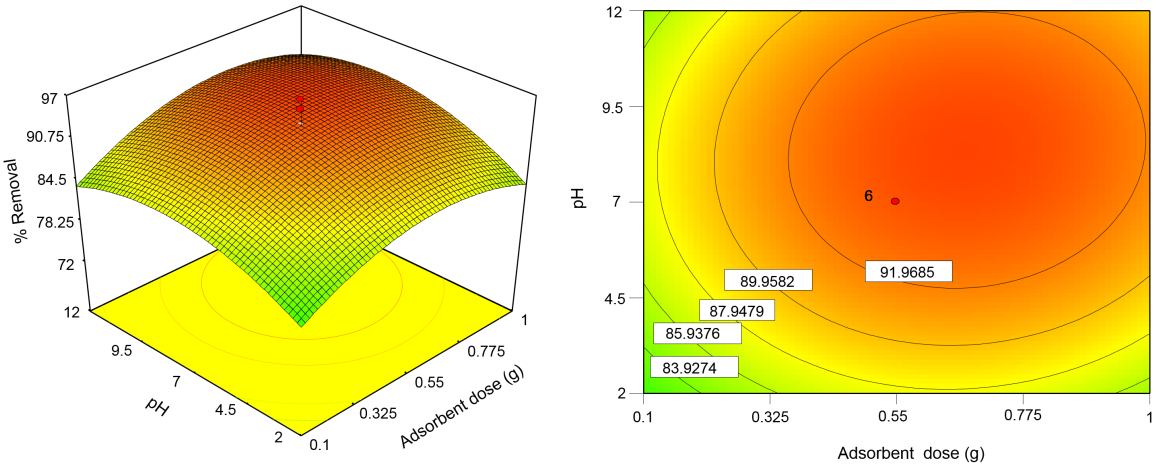

Figure 7.10: 3D response surface and 2D counter plot represents independent interaction of *pH* and adsorbent dose for the safranin-O dye adsorption

Effect of initial dye concentration and adsorbent dose on adsorption process

The combined effect of initial dye concentration and adsorbent dose at constant temperature of 35 ℃ and *pH* 7 is shown in Figure 7.11. It is clear from the figure that, both initial dye concentration and adsorbent dose shows positive effects on percentage removal of safranin-O from aqueous solution. When initial dye concentration increase, the removal of dye increases with increase in adsorbent dose. This trend may be due to that, at lower dye concentrations and lower adsorbent dose, there are not sufficient dye molecules in the solution to adsorb on lees available binding sites of the adsorbent. Thus an increase in the adsorbent dose

and dye concentration, the adsorption will be relatively higher due to presence of enough dye molecules in the solution to be adsorbed by more active binding sites provided by the adsorbent. At initial dye concentration of 36.49 mg/L and adsorbent dose of 0.60 g, a maximum dye uptake of 93.95% is reached.

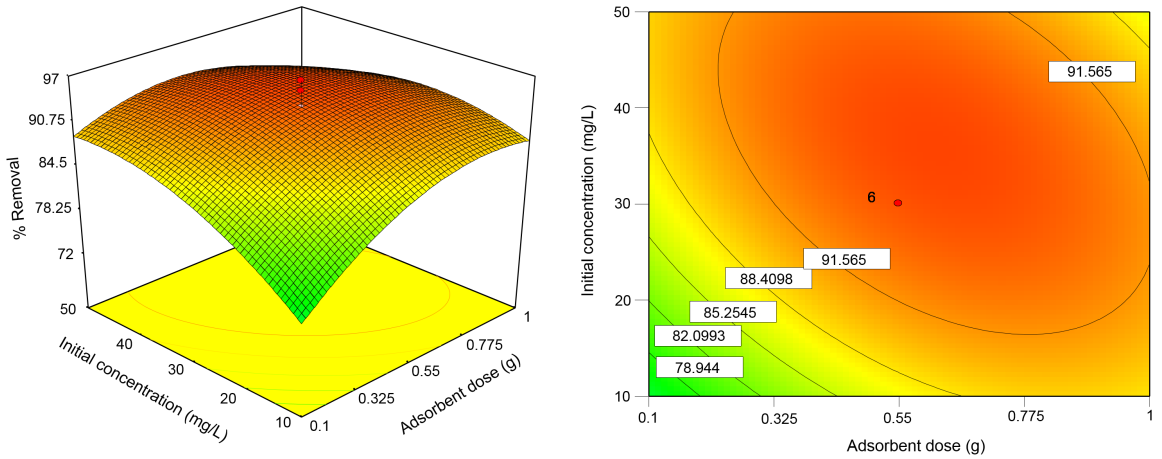

Figure 7.11: 3D response surface and 2D counter plot represents independent interaction of initial dye concentration and adsorbent dose for the safranin-O dye adsorption

7.2.6 Conformation of the optimal condition

The percentage removal and the operation conditions for maximum percentage removal of safranin-O from aqueous solution were calculated from the second-order equation obtained from the experimental data. The first-order partial differential equations are obtained from Equation 7.2 for X_i as follows:

$$\frac{\partial Y}{\partial X_1} = 2.36 - 3.39X_4 - 9.06X_1 \tag{7.3}$$

$$\frac{\partial Y}{\partial X_2} = -1.07 - 2.48X_4 - 9.48X_2 \tag{7.4}$$

$$\frac{\partial Y}{\partial X_3} = 2.20 - 8.66X_3 \tag{7.5}$$

$$\frac{\partial Y}{\partial X_4} = 2.67 - 3.39X_1 - 2.48X_2 - 3.72X_4 \tag{7.6}$$

The second-order differential equations are:

$$\frac{\partial^2 Y}{\partial X_1} = -9.06 \tag{7.7}$$

$$\frac{\partial^2 Y}{\partial X_2} = -9.48 \tag{7.8}$$

$$\frac{\partial^2 Y}{\partial X_3} = -8.66 \tag{7.9}$$

$$\frac{\partial^2 Y}{\partial X_4} = -7.32 \tag{7.10}$$

The value of X_i (X_1, X_2, X_3 and X_4) could be obtained after solving Equation 7.3 to Equation 7.6 when $\partial Y/\partial X_i$ = 0, which gives the maximum value of Y (% removal). The solution of the above Equation 7.3 to Equation 7.6 are found to be X_1 = 0.117, X_2 = - 0.212, X_3 = 0.254 and X_4 = 0.382. Then the values are converted to actual values (uncoded) of X_1 (adsorbent dose) = 0.62 g, X_2 (temperature) = 29.06 ℃, X_3 (pH) = 8.3 and X_4 (initial concentration) = 37.3 mg/L according to Table 3.2. At these optimum condition, the maximum predicted percentage removal of safranin-O dye is 94.5 ± 01% shown in Figure 7.12.

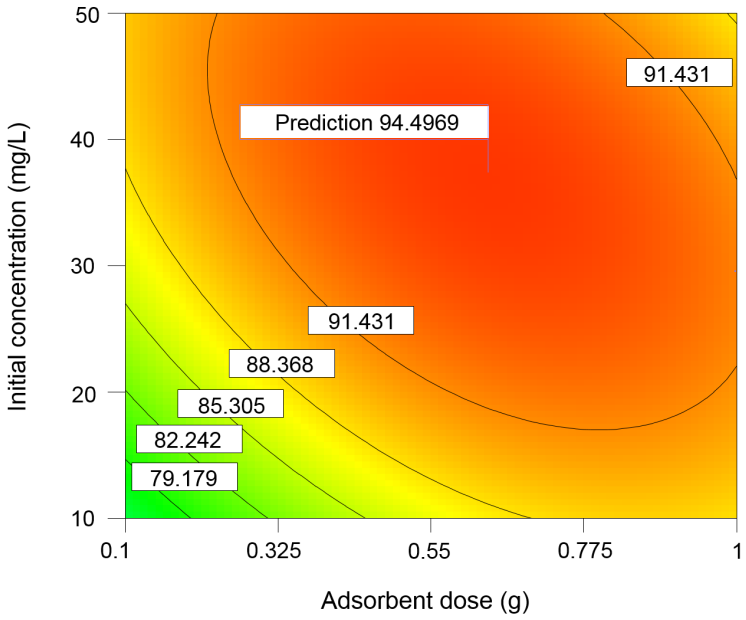

Figure 7.12: Optimum removal efficiency (contour plot obtained from RSM optimization)

7.2.7 Model verification

Five confirmation runs with a duplicate set were performed at the selected optimum conditions, in order to confirm the validity of the RSM model. The conditions are listed in Table 7.6. The dye removal conditions for the first run was done in new operation condition within the range of the levels that were not conducted. The next two confirmation experiments were taken from the Table 3.2, while the last two runs were the operation conditions for maximum percentage removal of safranin-O dye. The error percentage among the actual and calculated values ranges from 0.38% to 10.11%. Therefore, it could be concluded that the second-order polynomial regression equation is able to predict the

percentage removal of safranin-O dye from aqueous solution accurately.

Table 7.6: Results of confirmation experiments

(X_1)	(X_2)	(X_3)	(X_4)	% Removal	
				Observed	Predicted
0.55	60	2	50	77.62	77.58
1	60	12	50	77.24	75.46
0.1	10	12	10	67.51	67.47
0.6	29	8.3	37	94.02	94.49
0.6	29	8.3	37	93.89	94.49

7.2.8 Adsorption isotherm models

For the study of adsorption models, data are plotted as an adsorption capacity (q_e) as a function of equilibrium concentration (C_e) as shown in Figure 7.13. The analysis of the different models (Langmuir, Freundlich, and Temkin model) were performed by means of a nonlinear fitting procedure. The Langmuir isotherm model is best fitted with the experimental data with the high R^2 value (0.994). The maximum adsorption capacity q_m and Langmuir constant b are found to be 9.768 mg/g and 0.197 L/mg respectively as shown in Table 7.7.

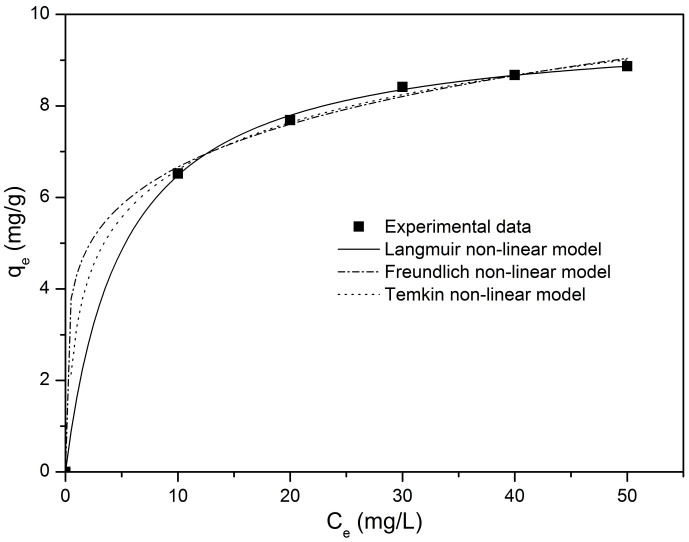

Figure 7.13: Adsorption isotherm for safranin-O onto CO_2 neutralized activated red mud at optimum condition (obtained from RSM optimization)

Table 7.7: Langmuir, Freundlich and Temkin isotherm parameters at optimum condition

Isotherm model parameters					
Langmuir isotherm		Freundlich isotherm		Temkin isotherm	
q_m	9.7680	$1/n$	0.1897	B_T	0.6693
b	0.1972	k	4.3063	K_T	8.3078
R^2	0.9996	R^2	0.9977	R^2	0.9987

7.3 Conclusions

In this study, a central composite design with the RSM was successfully applied to establish the optimum condition for the removal of safranin-O from aqueous solution by activated red mud. A quadratic polynomial equation was develop by RSM to predict the percentage removal of safranin-O and describe the relationship between response and variables. The model fitted the experimental data well, with a coefficient of determination, R^2 of 0.9549 and an $Adj - R^2$ of 0.9312. Analysis of the model variance (ANOVA) shows that there is a high coefficient between adsorbent dose with initial concentration and reaction temperature with initial concentration of safranin-O dye. The adsorbent dose of 0.62 g, temperature of 29.06 ℃, *pH* of 8.3 and initial concentration of 37.3 mg/L is found to be optimum for the maximum adsorption of safranin-O dye. The optimal response obtained from the RSM is 94.5 ±0.1 %, which is very close to the experimental value of 93.38%. The high correlation coefficient value R^2 (0.994) indicates that Langmuir isotherm is best suited model with adsorption capacity of 9.7680 mg/g. It means that 1 g of red mud remove 9.7680 mg of safranin-O from 37.3 ppm safranin-O containing wastewater. At optimum condition (*pH* = 8.3, and temperature = 29.06 ℃), 1 tons of CO_2 neutralized activated red mud can remove 9.768 kg of safranin-O from 2,61,876 liters of standard wastewater containing 37.3 ppm safranin-O. Therefore, it may be concluded that the activated red mud neutralized by CO_2 can be used as a promising adsorbent for removal of safranin-O dye from aqueous systems.

Chapter 8

Summary & Conclusions

The red mud is a by-product of the caustic leaching of bauxite ore to produce alumina by Bayer´s process. Red mud is composed of mainly the oxides and hydroxides of silicon, aluminum, iron, calcium and titanium in very fine particles form, which are responsible for its high surface reactivity. Active research for utilization of red mud has been carried out which includes, the removal of toxic heavy metals from wastewater and acid mine drainage besides the other use. In this thesis, red mud was modified and their utilizations for removal of lead, cadmium and safranin-O have been investigated. The novelty of the present work was to utilize the waste red mud after modification to solve another environmental problem of water treatment.

In this research work, the caustic red mud was successfully neutralized using acid and CO_2 gas by precipitation methods. The formation, phase, size, surface morphology, surface area, stability of the neutralized red mud and surface modified neutralized red mud was characterized by using XRD, SEM, EDX, FTIR, UV-VIS,TGA/DSC and BET analytical techniques. The modified neutralized red mud were used as an adsorbent for the adsorptive removal of the toxic metal ions Pb(II), Cd(II) and organic safranin-O dye from aqueous solution separately.

The following major conclusions are inferred from the work of this thesis.

1. The red mud was neutralized with HCl and activated by calcination at 500 ℃ for two hours to form ARM and used for the removal of Pb(II) from the aqueous solutions by batch mode. The percentage removal was found to increase with decrease in *pH* with maximum removal at *pH* 4. The most important driving force for the metal ions to the surface of the adsorbent is the concentration gradient of metal ions in solution. The pseudo-second-order kinetics describes the adsorption kinetic of the adsorption process. The experimental adsorption data were fitted to linearly transformed Langmuir isotherm with a maximum adoption capacity of 6.0273 mg/g.

2. The red mud was activated by acid dilution followed by ammonia precipitation and calcination which was used as a low-cost adsorbent (ARM) for the removal of Cd(II) ions from aqueous solution by batch mode. The maximum adsorption capacity of Cd(II) on activated red mud were found to be 12.046 and 12.548 mg/g at temperature

of 293 and 303 K respectively. Experimental data of Cd(II) adsorption were best fitted to linearly transformed Langmuir isotherm with a value of R^2 >0.99. The pseudo-second-order model describes the kinetics of Cd(II) adsorption successfully to predict the rate constant of adsorption. Thermodynamic parameters reveals the endothermic, spontaneous and feasible nature of adsorption of Cd(II) onto ARM. The mass transfer study led to compute the external mass transfer coefficient (k_f) is 0.084×10^{-3} to 0.012×10^{-3} for McKay $et\ al.$ equation and 9.9×10^{-3} to 11.5×10^{-3} for Waber-Mathews equation for temperature 293 K and 303 K respectively. The desorption efficiency of Cd(II) ions from ARM is 91.29% using 0.2 $mol/L\ HCl$.

3. Safranin-O dye removal from aqueous solutions using modified red mud as an adsorbent was investigated. The surface of the red mud was modified by the addition of sodium dodecyl sulphate as an anionic surfactant to prevent the agglomeration of a large ratio of surface area to volume which reduces the surface energy. Sodium dodecyl sulphate (SDS) was selected for the surface modification of red mud, because of its extensive use for its admicellar sorption properties as well as its high biodegradability. Kinetics data of the adsorption process were best fitted to pseudo-second-order model. The experimental data were fitted to the Langmuir adsorption isotherms model with a maximum monolayer adsorption capacity of 8.94 mg/g at 308 K. Desorption experiments were carried out by using several solvents such as water, sulphuric acid, hydrochloric acid and acetic acid and the maximum (93.2%) desorption was obtained with hydrochloric acid.

4. Response surface methodology (RSM) modeling techniques was applied to predict and optimized the removal of hazardous safranin-O dye from aqueous solution using CO_2 neutralized activated red mud as an adsorbent. Three-level, four factor central composite design (CCD) was employed to determine the relationship between experimental variables and optimum adsorption conditions for activated red mud. Analysis of variance (ANOVA) exhibit a high R^2 value of 0.9655, indicating second-order regression model which validate excellently the experimental data. The optimum operating condition for adsorption of safranin-O dye were obtained from RSM : adsorbent dose of 0.62 g, temperature of 29.06 ℃, pH of 8.3 and initial safranin-O concentration of 37.3 mg/L. In addition, the isotherm study revealed that, the adsorption data were best fitted to Langmuir model with high correlation value of 0.994 and adsorption capacity of 9.768 mg/g.

The red mud waste has no significant industrial and commercial uses, but becomes an issue and contributes to serious environmental problems. Hence, the utilization of such industrial solid waste for wastewater treatment is most desirable. The cost of this waste as an adsorbent is only associated with the transport and process expenses which are approximately

US$ 0.1/kg whereas the average price of activated carbon used for waste water treatment as an adsorbent is US$ 4.962/kg. Thus the industrial waste is more than 50 times cheaper than activated carbon. Although the adsorption capacity of red mud may be slightly lower than commercial activated carbons but it is more or similar than most of the reported adsorbent. Moreover the adsorbent is renewable material, abundantly available and therefore, low-cost adsorbent. The red mud would be an economical alternative for the commercially available activated carbon in removal of hazardous contaminants from aqueous solutions.

From the above results, it is clear that the red mud is an excellent adsorbent for the removal of inorganic and organic pollutants from water. Hence red mud can be used as a low cost adsorbent for potential application for wastewater remediation. The utilization of red mud not only benefit the environment but also enhance the socio-ecological and economic benefit to the alumina extraction industries.

Chapter 9

Scope for Further Research

Based on the findings of the present invention, the followings are the future scope of studies in the red mud.

1. Large-scale neutralization of red mud using CO_2 gas is highly needed for sustainable development of alumina industry.
2. Extraction of valuable element such as iron, titanium and silicon from red mud using cost effective environment friendly technology.
3. Enhancement of adsorption capacity of red mud through modification.
4. Mechanistic modelling to understand the adsorption mechanisms.
5. Preparation of catalyst from red mud and used for the degradation of organic pollutants.
6. Investigation of the adsorption capacities of red mud with real industrial effluents.

References

[1] Singh, A., and Kohli, J. S., 2012. "Effect of pollution on common man in india: a legal perspective". *Advances in Life Science and Technology,* **4**, pp. 35–41.

[2] Nadaroglu, H., Kalkan, E., and Demir, N., 2010. "Removal of copper from aqueous solution using red mud". *Desalination,* **251**(1), pp. 90–95.

[3] Ghorbani, A., Farahani, M., Rabbani, M., Aflaki, F., and Waqifhosain, S., 2008. "Uncertainty estimation for the determination of Ni, Pb and Al in natural water samples by SPE-ICP-OES". *Measurement Science Review,* **8**(6), pp. 151–157.

[4] Gong, J., Chen, L., Zeng, G., Long, F., Deng, J., Niu, Q., and He, X., 2012. "Shellac-coated iron oxide nanoparticles for removal of cadmium(II) ions from aqueous solution". *Journal of Environmental Sciences,* **24**(7), pp. 1165–1173.

[5] Chai, L. Y., Chen, Y. N., Shu, Y. D., Chang, H., and Li, Q. Z., 2007. "Adsorption and removal of cadmium(II) from aqueous solutions by bio-formulation". *Transactions of Nonferrous Metals Society of China,* **17**(5), pp. 1057–1062.

[6] Wang, C., Wang, B., Liu, J., Yu, L., Sun, H., and Wu, J., 2012. "Adsorption of Cd(II) from acidic aqueous solutions by tourmaline as a novel material". *Chinese Science Bulletin,* **57**(24), pp. 3218–3225.

[7] Kurniawan, T. A., Chan, G. Y., Lo, W. H., and Babel, S., 2006. "Comparisons of low-cost adsorbents for treating wastewaters laden with heavy metals". *Science of the Total Environment,* **366**(2), pp. 409–426.

[8] Newson, T., Dyer, T., Adam, C., and Sharp, S., 2006. "Effect of structure on the geotechnical properties of bauxite residue". *Journal of Geotechnical and Geoenvironmental Engineering,* **132**(2), pp. 143–151.

[9] Mohan, D., and Pittman, C. U., 2007. "Arsenic removal from water/wastewater using adsorbents–a critical review". *Journal of Hazardous Materials,* **142**(1), pp. 1–53.

[10] Peck, M. J., 2015. *The world aluminum industry in a changing energy era*. Routledge.

[11] Wagh, A. S., and Desai, P., 1987. "Bauxite Tailings: Red Mud". In *The Jamaican Bauxite Institute and the University of West Indies*. Kingston.

[12] Piga, L., Pochetti, F., and Stoppa, L., 1993. "Recovering metals from red mud generated during alumina production". *Journal of Metals,* **45**(11), pp. 54–59.

[13] Prasad, P., Kachhawaha, J., Gupta, R., Mankhand, T., and Sharma, J., 1985. "Processing and applications of red muds". In Key Engineering Materials, Vol. 8, Trans Tech Publication, pp. 31–52.

[14] Tor, A., Danaoglu, N., Arslan, G., and Cengeloglu, Y., 2009. "Removal of fluoride from water by using granular red mud: batch and column studies". *Journal of Hazardous Materials,* **164**(1), pp. 271–278.

[15] Costa, R. C., Moura, F. C., Oliveira, P. E., Magalhães, F., Ardisson, J. D., and Lago, R. M., 2010. "Controlled reduction of red mud waste to produce active systems for environmental applications: heterogeneous fenton reaction and reduction of Cr(VI)". *Chemosphere,* **78**(9), pp. 1116–1120.

[16] Genç-Fuhrman, H., Tjell, J. C., and McConchie, D., 2004. "Adsorption of arsenic from water using activated neutralized red mud". *Environmental science & technology,* **38**(8), pp. 2428–2434.

[17] Zhu, C., Luan, Z., Wang, Y., and Shan, X., 2007. "Removal of cadmium from aqueous solutions by adsorption on granular red mud (GRM)". *Separation and Purification Technology,* **57**(1), pp. 161–169.

[18] Apak, R., Tütem, E., Hügül, M., and Hizal, J., 1998. "Heavy metal cation retention by unconventional sorbents (red muds and fly ashes)". *Water Research,* **32**(2), pp. 430–440.

[19] Palmer, S. J., Nothling, M., Bakon, K. H., and Frost, R. L., 2010. "Thermally activated seawater neutralised red mud used for the removal of arsenate, vanadate and molybdate from aqueous solutions". *Journal of Colloid and Interface Science,* **342**(1), pp. 147–154.

[20] Yue, Q., Zhao, Y., Li, Q., Li, W., Gao, B., Han, S., Qi, Y., and Yu, H., 2010. "Research on the characteristics of red mud granular adsorbents (RMGA) for phosphate removal". *Journal of Hazardous Materials,* **176**(1), pp. 741–748.

[21] Zhao, Y., Wang, J., Luan, Z., Peng, X., Liang, Z., and Shi, L., 2009. "Removal of phosphate from aqueous solution by red mud using a factorial design". *Journal of Hazardous Materials,* **165**(1), pp. 1193–1199.

[22] Smiljanić, S., Smičiklas, I., Perić-Grujić, A., Lončar, B., and Mitrić, M., 2010. "Rinsed and thermally treated red mud sorbents for aqueous Ni^{2+} ions". *Chemical Engineering Journal,* **162**(1), pp. 75–83.

[23] Namasivayam, C., and Arasi, D., 1997. "Removal of congo red from wastewater by adsorption onto waste red mud". *Chemosphere,* **34**(2), pp. 401–417.

[24] Collazo, A., Cristóbal, M., Nóvoa, X., Pena, G., and Perez, M., 2005. "Electrochemical impedance spectroscopy as a tool for studying steel corrosion inhibition in simulated concrete environments–red mud used as rebar corrosion inhibitor". *Journal of ASTM International,* **3**(2), pp. 1–10.

[25] Davy, S. H., 2007. "State of Environment : Bauxite Mining & Alumina". *Envis Newsletter,* **7**, pp. 1–8.

[26] Samal, S., Ray, A. K., and Bandopadhyay, A., 2013. "Proposal for resources, utilization and processes of red mud in india–a review". *International Journal of Mineral Processing,* **118**, pp. 43–55.

[27] Paramguru, R., Rath, P., and Misra, V., 2004. "Trends in red mud utilization–a review". *Mineral Processing and Extractive Metallurgy Review,* **26**(1), pp. 1–29.

[28] Liu, Y., Naidu, R., and Ming, H., 2011. "Red mud as an amendment for pollutants in solid and liquid phases". *Geoderma,* **163**(1), pp. 1–12.

[29] Wang, S., Ang, H., and Tade, M., 2008. "Novel applications of red mud as coagulant, adsorbent and catalyst for environmentally benign processes". *Chemosphere,* **72**(11), pp. 1621–1635.

[30] Mahadevan, H., Chandwani, H., and Prasad, P., 1996. "An appraisal of the methods for red mud disposal under indian conditions". In In Proceedings of National Seminar on Bauxites and Alumina (BAUXAL-96), Allied Publishers New Delhi, India, pp. 337–347.

[31] Prasad, P., Sharma, J., Vishwanathan, V., Nandi, A., and Singh, M., 1996. "Production of bricks/stabilised blocks from red mud". In In Proceedings of National Seminar on Bauxites and Alumina (BAUXAL-96), pp. 387–396.

[32] Rai, S., Wasewar, K., Mukhopadhyay, J., Yoo, C. K., and Uslu, H., 2012. "Neutralization and utilization of red mud for its better waste management". *Archives of Environmental Science,* **6**, pp. 5410–5430.

[33] Chaddha, M. J., 2009. Asia pacific partnership of clean development & climate on industry perspectives-an overview. Tech. rep., Jawaharlal Nehru Aluminum Research Development and Design Centre.

[34] Kiraly, A., Mudrunka, J., and Lyckova, B., 2016. "Disposal of gastro waste in the czech republic related to valid legislation". *Inżynieria Mineralna,* **17**.

[35] Enick, R. M., Beckman, E. J., Shi, C., Xu, J., and Chordia, L., 2001. "Remediation of metal-bearing aqueous waste streams via direct carbonation". *Energy & Fuels,* **15**(2), pp. 256–262.

[36] Brunori, C., Cremisini, C., Massanisso, P., Pinto, V., and Torricelli, L., 2005. "Reuse of a treated red mud bauxite waste: studies on environmental compatibility". *Journal of Hazardous Materials,* **117**(1), pp. 55–63.

[37] Glenister, D., and Thornber, M., 1985. "Alkalinity of red mud and its application for the management of acid wastes". *Chemica,* **85**, pp. 100–113.

[38] Szirmai, E., Babusek, S., Balogh, G., Nedves, A., Horvath, G., Lebenyi, Z., and Pinter, J., 1991. Method for the multistage, waste-free processing of red mud to recover basic materials of chemical industry. US Patent 5,053,144.

[39] Khaitan, S., Dzombak, D. A., and Lowry, G. V., 2009. "Mechanisms of neutralization of bauxite residue by carbon dioxide". *Journal of Environmental Engineering,* **135**(6), pp. 433–438.

[40] Shi, C., Xu, J., Beckman, E., and Enick, R., 2000. "Carbon dioxide sequestration via ph reduction of red mud using liquid CO_2". *ACS Division of Fuel Chem,* **45**(4), pp. 703–705.

[41] Sahu, R. C., Patel, R. K., and Ray, B. C., 2010. "Neutralization of red mud using CO_2 sequestration cycle". *Journal of Hazardous Materials,* **179**(1), pp. 28–34.

[42] McConchie, D., Clark, M., and Hanahan, C., 2000. "The use of seawater neutralized bauxite refinery residues in the management of acid sulphate soils, sulphidic mine tailings and acid mine drainage". In 3rd Queensland Environmental Conference: Sustainable Solutions or Industry and Government, pp. 201–208.

[43] Virotec, 2003. "Dealing with red mud-Byproduct of the Bayer process for refining aluminium". *Materials World,* **11**(6), pp. 22–24.

[44] Agrawal, A., Sahu, K., and Pandey, B., 2004. "Solid waste management in non-ferrous industries in india". *Resources, Cosenvation and Recycling,* **42**(2), pp. 99–120.

[45] Agarwal, S. K., 2009. *Heavy metal pollution*, Vol. 4. APH publishing.

[46] Martins, R. J., Pardo, R., and Boaventura, R. A., 2004. "Cadmium(II) and zinc(II) adsorption by the aquatic moss fontinalis antipyretica: effect of temperature, pH and water hardness". *Water Research,* **38**(3), pp. 693–699.

[47] Sarı, A., and Tuzen, M., 2008. "Biosorption of cadmium(II) from aqueous solution by red algae (Ceramium virgatum): equilibrium, kinetic and thermodynamic studies". *Journal of Hazardous Materials,* **157**(2), pp. 448–454.

[48] Becker, P., 2014. *Sustainability science: managing risk and resilience for sustainable development*. Newnes.

[49] Hani, A., and Pazira, E., 2011. "Heavy metals assessment and identification of their sources in agricultural soils of Southern Tehran, Iran". *Environmental Monitoring and Assessment,* **176**(1-4), pp. 677–691.

[50] Aroguz, A. Z., Gulen, J., and Evers, R., 2008. "Adsorption of methylene blue from aqueous solution on pyrolyzed petrified sediment". *Bioresource Technology,* **99**(6), pp. 1503–1508.

[51] Shore, J., 1996. "Advances in direct dyes". *Indian Journal of Fibre and Textile Research,* **21**, pp. 1–29.

[52] Christensen, E. R., and Delwiche, J. T., 1982. "Removal of heavy metals from electroplating rinsewaters by precipitation, flocculation and ultrafiltration". *Water Research,* **16**(5), pp. 729–737.

[53] Wu, J., Lu, J., Chen, T., He, Z., Su, Y., Jin, X., and Yao, X., 2010. "In situ biotreatment of acidic mine drainage using straw as sole substrate". *Environmental Earth Sciences,* **60**(2), pp. 421–429.

[54] Bhattacharya, A. K., and Venkobachar, C., 1984. "Removal of cadmium(II) by low cost adsorbents". *Journal of Environmental Engineering,* **110**(1), pp. 110–122.

[55] Casas, I., Miralles, N., Sastre, A., and Aguilar, M., 1986. "Extraction of cadmium(II) by organophosphorus compounds". *Polyhedron,* **5**(12), pp. 2039–2045.

[56] Stenström, S., 1987. "Extraction of cadmium from phosphoric acid solutions with amines. Part III. a thermodynamic extraction model". *Hydrometallurgy,* **18**(1), pp. 1–20.

[57] Mazid, M., 1984. "Mechanisms of transport through reverse osmosis membranes". *Separation Science and Technology,* **19**(6-7), pp. 357–373.

[58] Marder, L., Sulzbach, G. O., Bernardes, A. M., and Ferreira, J. Z., 2003. "Removal of cadmium and cyanide from aqueous solutions through electrodialysis". *Journal of the Brazilian Chemical Society,* **14**(4), pp. 610–615.

[59] Tripathy, S. S., Sarangi, K., and Das, R. P., 2002. "Extraction of cadmium(II) by supported liquid membrane using tops-99 as mobile carrier". *Separation Science and Technology,* **37**(12), pp. 2897–2911.

[60] Đukić, A. B., Kumrić, K. R., Vukelić, N. S., Dimitrijević, M. S., Baščarević, Z. D., Kurko, S. V., and Matović, L. L., 2015. "Simultaneous removal of Pb^{2+}, Cu^{2+}, Zn^{2+} and Cd^{2+} from highly acidic solutions using mechanochemically synthesized montmorillonite–kaolinite/TiO_2 composite". *Applied Clay Science,* **103**, pp. 20–27.

[61] Kumrić, K. R., Đukić, A. B., Trtić-Petrović, T. M., Vukelić, N. S., Stojanović, Z., Grbović Novaković, J. D., and Matović, L. L., 2013. "Simultaneous removal of divalent heavy metals from aqueous solutions using raw and mechanochemically treated interstratified montmorillonite/kaolinite clay". *Industrial & Engineering Chemistry Research,* **52**(23), pp. 7930–7939.

[62] Nenadovic, S., Nenadovic, M., Kovacevic, R., Matovic, L., Matovic, B., Jovanovic, Z., and Novakovic, J. G., 2009. "Influence of diatomite microstructure on its adsorption capacity for Pb(II)". *Science of Sintering,* **41**(3), pp. 309–17.

[63] Wang, X., Guo, Y., Yang, L., Han, M., Zhao, J., and Cheng, X., 2012. "Nanomaterials as sorbents to remove heavy metal ions in wastewater treatment". *Journal of Environmental & Analytical Toxicology,* **2**(7), pp. 1–7.

[64] Panday, K., Prasad, G., and Singh, V., 1985. "Copper(II) removal from aqueous solutions by fly ash". *Water Research,* **19**(7), pp. 869–873.

[65] Oubagaranadin, J. U. K., and Murthy, Z., 2009. "Adsorption of divalent lead on a montmorillonite- illite type of clay". *Industrial & Engineering Chemistry Research,* **48**(23), pp. 10627–10636.

[66] Wang, X., Zheng, Y., and Wang, A., 2009. "Fast removal of copper ions from aqueous solution by chitosan-g-poly (acrylic acid)/attapulgite composites". *Journal of Hazardous Materials,* **168**(2), pp. 970–977.

[67] Kikuchi, Y., Qian, Q., Machida, M., and Tatsumoto, H., 2006. "Effect of ZnO loading to activated carbon on Pb(II) adsorption from aqueous solution". *Carbon,* **44**(2), pp. 195–202.

[68] Shirzad-Siboni, M., Jafari, S. J., Giahi, O., Kim, I., Lee, S. M., and Yang, J. K., 2014. "Removal of acid blue 113 and reactive black 5 dye from aqueous solutions by activated red mud". *Journal of Industrial and Engineering Chemistry,* **20**(4), pp. 1432–1437.

[69] Zhang, L., Zhang, H., Guo, W., and Tian, Y., 2014. "Removal of malachite green and crystal violet cationic dyes from aqueous solution using activated sintering process red mud". *Applied Clay Science,* **93**, pp. 85–93.

[70] Tor, A., and Cengeloglu, Y., 2006. "Removal of congo red from aqueous solution by adsorption onto acid activated red mud". *Journal of Hazardous Materials,* **138**(2), pp. 409–415.

[71] Wang, S., Boyjoo, Y., Choueib, A., and Zhu, Z., 2005. "Removal of dyes from aqueous solution using fly ash and red mud". *Water research,* **39**(1), pp. 129–138.

[72] Wang, Q., Luan, Z., Wei, N., Li, J., and Liu, C., 2009. "The color removal of dye wastewater by magnesium chloride/red mud (MRM) from aqueous solution". *Journal of Hazardous Materials,* **170**(2), pp. 690–698.

[73] Khan, T. A., Chaudhry, S. A., and Ali, I., 2015. "Equilibrium uptake, isotherm and kinetic studies of Cd(II) adsorption onto iron oxide activated red mud from aqueous solution". *Journal of Molecular Liquids,* **202**, pp. 165–175.

[74] Grudic, V. V., Peric, D., Blagojevic, N. Z., Vukasinovic-Pesic, V. L., Brasanac, S., and Mugosa, B., 2013. "Pb(II) and Cu(II) sorption from aqueous solutions using activated red mud–evaluation of kinetic, equilibrium and thermodynamic models". *Polish Journal of Environmental Studies,* **22**(2), pp. 377–385.

[75] Kalkan, E., Nadaroglu, H., Dikbas, N., Tasgin, E., and Celebi, N., 2013. "Bacteria-modified red mud for adsorption of cadmium ions from aqueous solutions". *Polish Journal of Environmental Studies,* **22**(2), pp. 105–117.

[76] Ju, S. H., Lu, S. D., Peng, J. H., Zhang, L. B., Srinivasakannan, C., Guo, S. H., and Wei, L., 2012. "Removal of cadmium from aqueous solutions using red mud granulated with cement". *Transactions of Nonferrous Metals Society of China,* **22**(12), pp. 3140–3146.

[77] Ghorbani, A., Nazarfakhari, M., Pourasad, Y., and Abbasi, S. M., 2013. "Removal of Pb ion from water samples using red mud (bauxite ore processing waste)". In E3S Web of Conferences, Vol. 1, EDP Sciences, pp. 41019–41021.

[78] Gupta, V. K., Gupta, M., and Sharma, S., 2001. "Process development for the removal of lead and chromium from aqueous solutions using red mud–an aluminium industry waste". *Water research,* **35**(5), pp. 1125–1134.

[79] Vaclavikova, M., Misaelides, P., Gallios, G., Jakabsky, S., and Hredzak, S., 2005. "Removal of cadmium, zinc, copper and lead by red mud, an iron oxides containing hydrometallurgical waste". *Studies in Surface Science and Catalysis,* **155**, pp. 517–525.

[80] Lopez, E., Soto, B., Arias, M., Nunez, A., Rubinos, D., and Barral, M., 1998. "Adsorbent properties of red mud and its use for wastewater treatment". *Water Research,* **32**(4), pp. 1314–1322.

[81] Gupta, V. K., and Sharma, S., 2002. "Removal of cadmium and zinc from aqueous solutions using red mud". *Environmental Science & Technology,* **36**(16), pp. 3612–3617.

[82] Han, S. W., Kim, D. K., Hwang, I. G., Bae, J. H., et al., 2002. "Development of pellet-type adsorbents for removal of heavy metal ions from aqueous solutions using red mud". *Journal of Industrial and Engineering Chemistry,* **8**(2), pp. 120–125.

[83] Santona, L., Castaldi, P., and Melis, P., 2006. "Evaluation of the interaction mechanisms between red muds and heavy metals". *Journal of Hazardous Materials,* **136**(2), pp. 324–329.

[84] Kong, C. Y., 2011. "Adsorption characteristics of activated red mud for lead removal". *Asian Journal of Chemistry,* **23**(5), pp. 1963–1965.

[85] Box, G. E. P., and Draper, N. R., 1987. *Empirical model-building and response surfaces*, Vol. 424. John Wiley & Sons, New York.

[86] Baş, D., and Boyacı, İ. H., 2007. "Modeling and optimization I: Usability of response surface methodology". *Journal of Food Engineering,* **78**(3), pp. 836–845.

[87] Geyikçi, F., Kılıç, E., Çoruh, S., and Elevli, S., 2012. "Modelling of lead adsorption from industrial sludge leachate on red mud by using RSM and ANN". *Chemical Engineering Journal,* **183**, pp. 53–59.

[88] Gupta, V., Suhas, Ali, I., and Saini, V., 2004. "Removal of rhodamine B, fast green, and methylene blue from wastewater using red mud, an aluminum industry waste". *Industrial & Engineering chemistry Research,* **43**(7), pp. 1740–1747.

[89] de Souza, K. C., Antunes, M. L. P., Couperthwaite, S. J., da Conceição, F. T., de Barros, T. R., and Frost, R., 2013. "Adsorption of reactive dye on seawater-neutralised bauxite refinery residue". *Journal of Colloid and Interface Science,* **396**, pp. 210–214.

[90] Balarak, D., Yousef, M., and Sadeghi, S., 2015. "Adsorptive removal of acid blue 15 dye (AB15) from aqueous solutions by red mud: characteristics, isotherm and kinetic studies". *Scientific Journal of Environmental Sciences,* **4**(5), pp. 102–112.

[91] Namasivayam, C., Yamuna, R., and Arasi, D., 2001. "Removal of acid violet from wastewater by adsorption on waste red mud". *Environmental Geology,* **41**(3-4), pp. 269–273.

[92] Pratt, K. C., and Christoverson, V., 1982. "Hydrogenation of a model hydrogen-donor system using activated red mud catalyst". *Fuel,* **61**(5), pp. 460–462.

[93] Zhu, X., Li, W., Tang, S., Zeng, M., Bai, P., and Chen, L., 2017. "Selective recovery of vanadium and scandium by ion exchange with D201 and solvent extraction using P507 from hydrochloric acid leaching solution of red mud". *Chemosphere,* **175**, pp. 365 – 372.

[94] Genç-Fuhrman, H., Tjell, J. C., and McConchie, D., 2004. "Adsorption of arsenic from water using activated neutralized red mud". *Environmental Science & Technology,* **38**(8), pp. 2428–2434.

[95] Mansour, M., Ossman, M., and Farag, H., 2011. "Removal of Cd(II) ion from waste water by adsorption onto polyaniline coated on sawdust". *Desalination,* **272**(1), pp. 301–305.

[96] El-Latif, M. M. A., Ibrahim, A. M., Showman, M. S., and Hamide, R. R. A., 2013. "Alumina/iron oxide nano composite for cadmium ions removal from aqueous solutions". *International Journal of Nonferous Metallurgy,* **2**(2), pp. 47–62.

[97] Gupta, V., Gupta, B., Rastogi, A., Agarwal, S., and Nayak, A., 2011. "Pesticides removal from waste water by activated carbon prepared from waste rubber tire". *Water Research,* **45**(13), pp. 4047–4055.

[98] Boyd, G., Adamson, A., and Myers Jr, L., 1947. "The exchange adsorption of ions from aqueous solutions by organic zeolites II. kinetics1". *Journal of the American Chemical Society,* **69**(11), pp. 2836–2848.

[99] Mohan, D., and Singh, K. P., 2002. "Single-and multi-component adsorption of cadmium and zinc using activated carbon derived from bagasse–an agricultural waste". *Water Research,* **36**(9), pp. 2304–2318.

[100] McKay, G., Allen, S. J., McConvey, I. F., and Otterburn, M. S., 1981. "Transport processes in the sorption of colored ions by peat particles". *Journal of Colloid and Interface Science,* **80**(2), pp. 323–339.

[101] Mathew, A., and Waber, W., 1976. "Physical, chemical wasterwater treatment". *AIChE symposium series,* **166**(73), pp. 91–98.

[102] Islam, M., and Patel, R., 2007. "Evaluation of removal efficiency of fluoride from aqueous solution using quick lime". *Journal of Hazardous Materials,* **143**(1), pp. 303–310.

[103] Crini, G., 2008. "Kinetic and equilibrium studies on the removal of cationic dyes from aqueous solution by adsorption onto a cyclodextrin polymer". *Dyes and Pigments,* **77**(2), pp. 415–426.

[104] Tempkin, M. J., and Pyzhev, V., 1940. "Recent modification to Langmuir isotherms". *Acta Physicochimica U.R.S.S,* **12**, pp. 217–222.

[105] Kausar, A., Bhatti, H. N., and MacKinnon, G., 2013. "Equilibrium, kinetic and thermodynamic studies on the removal of U(VI) by low cost agricultural waste". *Colloids and Surfaces B: Biointerfaces,* **111**, pp. 124–133.

[106] Zhang, Z., and Zhang, Y., 1998. "Method of calculating the thermodynamic parameters from some isothermal absorption models". *Acta of Northwest Sci-Tech University of Agriculture and Forestry,* **26**(2), pp. 94–98.

[107] Amini, M., Younesi, H., Bahramifar, N., Lorestani, A. A. Z., Ghorbani, F., Daneshi, A., and Sharifzadeh, M., 2008. "Application of response surface methodology for optimization of lead biosorption in an aqueous solution by aspergillus niger". *Journal of Hazardous Materials,* **154**(1), pp. 694–702.

[108] Yurtsever, M., and Şengil, İ. A., 2009. "Biosorption of Pb(II) ions by modified quebracho tannin resin". *Journal of Hazardous Materials,* **163**(1), pp. 58–64.

[109] Kazi, T. G., Jalbani, N., Kazi, N., Jamali, M. K., Arain, M. B., Afridi, H. I., Kandhro, A., and Pirzado, Z., 2008. "Evaluation of toxic metals in blood and urine samples of chronic renal failure patients, before and after dialysis". *Renal Failure,* **30**(7), pp. 737–745.

[110] Afridi, H. I., Kazi, T. G., Kazi, G. H., Jamali, M. K., and Shar, G. Q., 2006. "Essential trace and toxic element distribution in the scalp hair of pakistani myocardial infarction patients and controls". *Biological Trace Element Research,* **113**(1), pp. 19–34.

[111] Teoh, Y. P., Khan, M. A., and Choong, T. S., 2013. "Kinetic and isotherm studies for lead adsorption from aqueous phase on carbon coated monolith". *Chemical Engineering Journal,* **217**, pp. 248–255.

[112] WHO, 2011. *Guidelines for drinking-water quality*. Geneva: world health organization.

[113] Li, K., and Wang, X., 2009. "Adsorptive removal of Pb(II) by activated carbon prepared from spartina alterniflora: equilibrium, kinetics and thermodynamics". *Bioresource Technology,* **100**(11), pp. 2810–2815.

[114] Toft, P., 1987. "Guidelines for canadian drinking water quality". In Second National Conference on Drinking Water, Edmonton (Canada), Pergamon Press.

[115] Office of water, U. S. E. P. A., 2011. Drinking water standards and health advisories.

[116] Ünlü, N., and Ersoz, M., 2006. "Adsorption characteristics of heavy metal ions onto a low cost biopolymeric sorbent from aqueous solutions". *Journal of Hazardous Materials,* **136**(2), pp. 272–280.

[117] Panday, K., Prasad, G., and Singh, V., 1985. "Copper(II) removal from aqueous solutions by fly ash". *Water Research,* **19**(7), pp. 869–873.

[118] Ajmal, M., Rao, R. A. K., Anwar, S., Ahmad, J., and Ahmad, R., 2003. "Adsorption studies on rice husk: removal and recovery of Cd(II) from wastewater". *Bioresource Technology,* **86**(2), pp. 147–149.

[119] Al-Asheh, S., and Duvnjak, Z., 1998. "Binary metal sorption by pine bark: study of equilibria and mechanisms". *Separation Science and Technology,* **33**(9), pp. 1303–1329.

[120] Bulut, Y., 2007. "Removal of heavy metals from aqueous solution by sawdust adsorption". *Journal of Environmental Sciences,* **19**(2), pp. 160–166.

[121] Bertocchi, A. F., Ghiani, M., Peretti, R., and Zucca, A., 2006. "Red mud and fly ash for remediation of mine sites contaminated with As, Cd, Cu, Pb and Zn". *Journal of Hazardous Materials,* **134**(1), pp. 112–119.

[122] Cengeloglu, Y., Tor, A., Ersoz, M., and Arslan, G., 2006. "Removal of nitrate from aqueous solution by using red mud". *Separation and Purification Technology,* **51**(3), pp. 374–378.

[123] Tor, A., Cengeloglu, Y., and Ersoz, M., 2009. "Increasing the phenol adsorption capacity of neutralized red mud by application of acid activation procedure". *Desalination,* **242**(1), pp. 19–28.

[124] Al-Asheh, S., Banat, F., and Mohai, F., 1999. "Sorption of copper and nickel by spent animal bones". *Chemosphere,* **39**(12), pp. 2087–2096.

[125] Momčilović, M., Purenović, M., Bojić, A., Zarubica, A., and Ranđelović, M., 2011. "Removal of lead(II) ions from aqueous solutions by adsorption onto pine cone activated carbon". *Desalination,* **276**(1), pp. 53–59.

[126] Rao, M. M., Ramesh, A., Rao, G. P. C., and Seshaiah, K., 2006. "Removal of copper and cadmium from the aqueous solutions by activated carbon derived from Ceiba pentandra hulls". *Journal of Hazardous Materials,* **129**(1), pp. 123–129.

[127] Pulford, I., Hargreaves, J., Ďurišová, J., Kramulova, B., Girard, C., Balakrishnan, M., Batra, V., and Rico, J., 2012. "Carbonised red mud–a new water treatment product made from a waste material". *Journal of Environmental Management,* **100**, pp. 59–64.

[128] Power, G., Gräfe, M., and Klauber, C., 2011. "Bauxite residue issues: I. current management, disposal and storage practices". *Hydrometallurgy,* **108**(1), pp. 33–45.

[129] Atasoy, A., 2005. "An investigation on characterization and thermal analysis of the Aughinish red mud". *Journal of Thermal Analysis and Calorimetry,* **81**(2), pp. 357–361.

[130] Atasoy, A., 2007. "The comparison of the bayer process wastes on the base of chemical and physical properties". *Journal of Thermal Analysis and Calorimetry,* **90**(1), pp. 153–158.

[131] Alp, A., and Goral, M., 2003. "The influence of soda additive on the thermal properties of red mud". *Journal of Thermal Analysis and Calorimetry,* **73**(1), pp. 201–207.

[132] Liu, Y., Lin, C., and Wu, Y., 2007. "Characterization of red mud derived from a combined bayer process and bauxite calcination method". *Journal of Hazardous Materials,* **146**(1), pp. 255–261.

[133] Kim, J. S., Han, S. W., Hwang, I. G., Bae, J. H., and Shuzo, T., 2002. "A study on removal of Pb^{2+} ion using pellet-type red mud adsorbents". *Environmental Engineering Research,* **7**(1), pp. 33–37.

[134] Orešcanin, V., Nad, K., Valkovic, V., Mikulic, N., and Meštrovic, O., 2001. "Red mud and waste base: raw materials for coagulant production". *Journal of Trace and Microprobe Techniques,* **19**(3), pp. 419–428.

[135] Orescanin, V., Tibljas, D., and Valkovic, V., 2002. "A study of coagulant production from red mud and its use for heavy metals removal". *Journal of Trace and Microprobe Techniques,* **20**(2), pp. 233–245.

[136] Orescanin, V., Nad, K., Mikelic, L., Mikulic, N., and Lulic, S., 2006. "Utilization of bauxite slag for the purification of industrial wastewaters". *Process Safety and Environmental Protection,* **84**(4), pp. 265–269.

[137] Lee, J. R., Hwang, I. G., and Bae, J. H., 2009. "Leaching of iron and aluminum from red mud and preparation of coagulants". *Clean Technology,* **15**(1), pp. 38–41.

[138] Luo, H. L., Huang, S. S., Luo, L., Wu, G. Y., and Liu, Y., 2012. "Modified granulation of red mud by weak gelling and its application to stabilization of Pb". *Journal of Hazardous Materials,* **227**, pp. 265–273.

[139] Lee, H. K., Lee, H. Y., and Jeon, J. M., 2007. "Codeposition of micro-and nano-sized sic particles in the nickel matrix composite coatings obtained by electroplating". *Surface and Coatings Technology,* **201**(8), pp. 4711–4717.

[140] Elouear, Z., Bouzid, J., Boujelben, N., Feki, M., Jamoussi, F., and Montiel, A., 2008. "Heavy metal removal from aqueous solutions by activated phosphate rock". *Journal of Hazardous Materials,* **156**(1), pp. 412–420.

[141] Ahalya, N., Ramachandra, T., and Kanamadi, R., 2003. "Biosorption of heavy metals". *Research Journal of Chemistry and Environment,* **7**(4), pp. 71–79.

[142] Smiljanić, S., Smičiklas, I., Perić-Grujić, A., Šljivić, M., Đukić, B., and Lončar, B., 2011. "Study of factors affecting Ni^{2+} immobilization efficiency by temperature activated red mud". *Chemical Engineering Journal,* **168**(2), pp. 610–619.

[143] Maleki, A., Mahvi, A. H., Zazouli, M. A., Izanloo, H., and Barati, A. H., 2011. "Aqueous cadmium removal by adsorption on barley hull and barley hull ash". *Asian Journal of Chemistry,* **23**(3), p. 1373.

[144] Yan, N., and Masliyah, J. H., 1996. "Effect of *pH* on adsorption and desorption of clay particles at oil–water interface". *Journal of Colloid and Interface Science,* **181**(1), pp. 20–27.

[145] Zheng, L., Dang, Z., Zhu, C., Yi, X., Zhang, H., and Liu, C., 2010. "Removal of cadmium(II) from aqueous solution by corn stalk graft copolymers". *Bioresource Technology,* **101**(15), pp. 5820–5826.

[146] O'Connell, D. W., Birkinshaw, C., and O'Dwyer, T. F., 2008. "Heavy metal adsorbents prepared from the modification of cellulose: A review". *Bioresource Technology,* **99**(15), pp. 6709–6724.

[147] Grayson, M., and Othumer, K., 1978. Encyclopedia of Chemical Technology.

[148] Forstner, V., and Wittman, G. T. W., 1981. *Metal pollution in the aquatic environment*. Springer-Verlag, Heidelberg, Germany.

[149] Salim, R., Al-Subu, M., and Sahrhage, E., 1992. "Uptake of cadmium from water by beech leaves". *Journal of Environmental Science & Health Part A,* **27**(3), pp. 603–627.

[150] Cheung, C. W., Porter, J. F., and McKay, G., 2000. "Elovich equation and modified second-order equation for sorption of cadmium ions onto bone char". *Journal of Chemical Technology and Biotechnology,* **75**(11), pp. 963–970.

[151] An, L. H., Wang, J. B., Fu, Q., Wang, C. Y., Zhang, L., Li, Z. C., Zhen, B. H., and Shang, J. J., 2011. "Impacts of environmental cadmium pollution on reproduction system: A review of recent researches". *Journal of Environment and Health,* **28**(1), pp. 89–92.

[152] Mcdowell, L. R., 1992. "Mineral in animals and human nutrition [M]". Academic Press Inc, New York, p. 359−364.

[153] Miretzky, P., Muñoz, C., and Carrillo-Chavez, A., 2010. "Cd(II) removal from aqueous solution by eleocharis acicularis biomass, equilibrium and kinetic studies". *Bioresource Technology,* **101**(8), pp. 2637–2642.

[154] Kumar, M., Puri, A., et al., 2012. "A review of permissible limits of drinking water". *Indian Journal of Occupational and Environmental Medicine,* **16**(1), pp. 40–44.

[155] Xu, Y., Yang, L., and Yang, J., 2010. "Removal of cadmium(II) from aqueous solutions by two kinds of manganese coagulants". *International Journal of Engineering, Science and Technology,* **2**(7), pp. 1–8.

[156] Doyurum, S., and Celik, A., 2006. "Pb(II) and Cd(II) removal from aqueous solutions by olive cake". *Journal of Hazardous Materials,* **138**(1), pp. 22–28.

[157] Escudero, C., Gabaldón, C., Marzal, P., and Villaescusa, I., 2008. "Effect of EDTA on divalent metal adsorption onto grape stalk and exhausted coffee wastes". *Journal of Hazardous Materials,* **152**(2), pp. 476–485.

[158] Garg, U., Kaur, M., Jawa, G., Sud, D., and Garg, V., 2008. "Removal of cadmium(II) from aqueous solutions by adsorption on agricultural waste biomass". *Journal of Hazardous Materials,* **154**(1), pp. 1149–1157.

[159] Mohan, D., Pittman, C. U., Bricka, M., Smith, F., Yancey, B., Mohammad, J., Steele, P. H., Alexandre-Franco, M. F., Gomez-Serrano, V., and Gong, H., 2007. "Sorption of arsenic, cadmium, and lead by chars produced from fast pyrolysis of wood and bark during bio-oil production". *Journal of Colloid and Interface Science,* **310**(1), pp. 57–73.

[160] Anwar, J., Shafique, U., Zaman, W. U., Salman, M., Dar, A., and Anwar, S., 2010. "Removal of Pb(II) and Cd(II) from water by adsorption on peels of banana". *Bioresource Technology,* **101**(6), pp. 1752–1755.

[161] Bedoui, K., Bekri-Abbes, I., and Srasra, E., 2008. "Removal of cadmium(II) from aqueous solution using pure smectite and lewatite S 100: the effect of time and metal concentration". *Desalination,* **223**(1), pp. 269–273.

[162] Kula, I., Uğurlu, M., Karaoğlu, H., and Celik, A., 2008. "Adsorption of Cd(II) ions from aqueous solutions using activated carbon prepared from olive stone by $ZnCl_2$ activation". *Bioresource Technology,* **99**(3), pp. 492–501.

[163] Kumar, P. S., Ramakrishnan, K., Kirupha, S. D., and Sivanesan, S., 2010. "Thermodynamic and kinetic studies of cadmium adsorption from aqueous solution onto rice husk". *Brazilian Journal of Chemical Engineering,* **27**(2), pp. 347–355.

[164] Rathinam, A., Maharshi, B., Janardhanan, S. K., Jonnalagadda, R. R., and Nair, B. U., 2010. "Biosorption of cadmium metal ion from simulated wastewaters using hypnea valentiae biomass: A kinetic and thermodynamic study". *Bioresource Technology,* **101**(5), pp. 1466–1470.

[165] Singh, K., Singh, A., and Hasan, S., 2006. "Low cost bio-sorbent 'wheat bran' for the removal of cadmium from wastewater: kinetic and equilibrium studies". *Bioresource Technology,* **97**(8), pp. 994–1001.

[166] Kalkan, E., 2006. "Utilization of red mud as a stabilization material for the preparation of clay liners". *Engineering Geology,* **87**(3), pp. 220–229.

[167] Ma, Y., Lin, C., Jiang, Y., Lu, W., Si, C., and Liu, Y., 2009. "Competitive removal of water-borne copper, zinc and cadmium by a $CaCO_3$-dominated red mud". *Journal of Hhazardous Materials,* **172**(2), pp. 1288–1296.

[168] Saifuddin, M., Kumaran, P., et al., 2005. "Removal of heavy metal from industrial wastewater using chitosan coated oil palm shell charcoal". *Electronic Journal of Biotechnology,* **8**(1), pp. 43–53.

[169] Wang, C., Liu, J., Zhang, Z., Wang, B., and Sun, H., 2012. "Adsorption of Cd(II), Ni(II), and Zn(II) by tourmaline at acidic conditions: Kinetics, thermodynamics, and mechanisms". *Industrial & Engineering Chemistry Research,* **51**(11), pp. 4397–4406.

[170] Unuabonah, E., Adebowale, K., Olu-Owolabi, B., Yang, L., and Kong, L., 2008. "Adsorption of Pb(II) and Cd(II) from aqueous solutions onto sodium tetraborate-modified kaolinite clay: equilibrium and thermodynamic studies". *Hydrometallurgy,* **93**(1), pp. 1–9.

[171] Wang, F. Y., Wang, H., and Ma, J. W., 2010. "Adsorption of cadmium(II) ions from aqueous solution by a new low-cost adsorbent–bamboo charcoal". *Journal of Hazardous Materials,* **177**(1), pp. 300–306.

[172] Azouaou, N., Sadaoui, Z., Djaafri, A., and Mokaddem, H., 2010. "Adsorption of cadmium from aqueous solution onto untreated coffee grounds: Equilibrium, kinetics and thermodynamics". *Journal of Hazardous Materials,* **184**(1), pp. 126–134.

[173] Ding, Y., Jing, D., Gong, H., Zhou, L., and Yang, X., 2012. "Biosorption of aquatic cadmium(II) by unmodified rice straw". *Bioresource Technology,* **114**, pp. 20–25.

[174] Arvand, M., and Pakseresht, M. A., 2013. "Cadmium adsorption on modified chitosan-coated bentonite: batch experimental studies". *Journal of Chemical Technology and Biotechnology,* **88**(4), pp. 572–578.

[175] Hossain, A., and Aditya, G., 2013. "Cadmium biosorption potential of shell dust of the fresh water invasive snail physa acuta". *Journal of Environmental Chemical Engineering,* **1**(3), pp. 574–580.

[176] Wang, L., and Wang, A., 2008. "Adsorption properties of congo red from aqueous solution onto surfactant-modified montmorillonite". *Journal of Hazardous Materials,* **160**(1), pp. 173–180.

[177] Boamah, P. O., Huang, Y., Hua, M., Zhang, Q., Liu, Y., Onumah, J., Wang, W., and Song, Y., 2015. "Removal of cadmium from aqueous solution using low molecular weight chitosan derivative". *Carbohydrate polymers,* **122**, pp. 255–264.

[178] Wong, C.-W., Barford, J. P., Chen, G., and McKay, G., 2014. "Kinetics and equilibrium studies for the removal of cadmium ions by ion exchange resin". *Journal of Environmental Chemical Engineering,* **2**(1), pp. 698–707.

[179] Tu, M., Pan, X., and Saddler, J. N., 2009. "Adsorption of cellulase on cellulolytic enzyme lignin from lodgepole pine". *Journal of Agricultural and Food Chemistry,* **57**(17), pp. 7771–7778.

[180] Kumar, P. S., Gayathri, R., Senthamarai, C., Priyadharshini, M., Fernando, P. S. A., Srinath, R., and Kumar, V. V., 2012. "Kinetics, mechanism, isotherm and thermodynamic analysis of adsorption of cadmium ions by surface-modified Strychnos potatorum seeds". *Korean Journal of Chemical Engineering,* **29**(12), pp. 1752–1760.

[181] Yaacoubi, H., Zidani, O., Mouflih, M., Gourai, M., and Sebti, S., 2014. "Removal of cadmium from water using natural phosphate as adsorbent". *Procedia Engineering,* **83**, pp. 386–393.

[182] Zheng, W., Li, X.-m., Wang, F., Yang, Q., Deng, P., and Zeng, G.-m., 2008. "Adsorption removal of cadmium and copper from aqueous solution by areca–a food waste". *Journal of Hazardous Materials,* **157**(2), pp. 490–495.

[183] Ulmanu, M., Marañón, E., Fernández, Y., Castrillón, L., Anger, I., and Dumitriu, D., 2003. "Removal of copper and cadmium ions from diluted aqueous solutions by low cost and waste material adsorbents". *Water, Air, and Soil Pollution,* **142**(1-4), pp. 357–373.

[184] Sharma, N., Kaur, K., and Kaur, S., 2009. "Kinetic and equilibrium studies on the removal of Cd^{2+} ions from water using polyacrylamide grafted rice (Oryza sativa) husk and (Tectona grandis) saw dust". *Journal of Hazardous Materials,* **163**(2), pp. 1338–1344.

[185] Phuengprasop, T., Sittiwong, J., and Unob, F., 2011. "Removal of heavy metal ions by iron oxide coated sewage sludge". *Journal of Hazardous Materials,* **186**(1), pp. 502–507.

[186] Brown, P., Jefcoat, I. A., Parrish, D., Gill, S., and Graham, E., 2000. "Evaluation of the adsorptive capacity of peanut hull pellets for heavy metals in solution". *Advances in Environmental Research,* **4**(1), pp. 19–29.

[187] Gupta, V. K., Jain, C., Ali, I., Sharma, M., and Saini, V., 2003. "Removal of cadmium and nickel from wastewater using bagasse fly ash–a sugar industry waste". *Water Research,* **37**(16), pp. 4038–4044.

[188] Jiang, M. Q., Jin, X. Y., Lu, X. Q., and Chen, Z. L., 2010. "Adsorption of Pb(II), Cd(II), Ni(II) and Cu(II) onto natural kaolinite clay". *Desalination,* **252**(1), pp. 33–39.

[189] Kumar, U., and Bandyopadhyay, M., 2006. "Sorption of cadmium from aqueous solution using pretreated rice husk". *Bioresource Technology,* **97**(1), pp. 104–109.

[190] Duan, J., and Su, B., 2014. "Removal characteristics of Cd(II) from acidic aqueous solution by modified steel-making slag". *Chemical Engineering Journal,* **246**, pp. 160–167.

[191] Sari, A., and Tuzen, M., 2014. "Cd(II) adsorption from aqueous solution by raw and modified kaolinite". *Applied Clay Science,* **88**, pp. 63–72.

[192] Garg, V., Kumar, R., and Gupta, R., 2004. "Removal of malachite green dye from aqueous solution by adsorption using agro-industry waste: a case study of Prosopis cineraria". *Dyes and Pigments,* **62**(1), pp. 1–10.

[193] Royer, B., Cardoso, N. F., Lima, E. C., Macedo, T. R., and Airoldi, C., 2010. "A useful organofunctionalized layered silicate for textile dye removal". *Journal of Hazardous Materials,* **181**(1-3), pp. 366–374.

[194] Al-Degs, Y. S., El-Barghouthi, M. I., El-Sheikh, A. H., and Walker, G. M., 2008. "Effect of solution pH, ionic strength, and temperature on adsorption behavior of reactive dyes on activated carbon". *Dyes and Pigments,* **77**(1), pp. 16–23.

[195] Crini, G., 2006. "Non-conventional low-cost adsorbents for dye removal: a review". *Bioresource Technology,* **97**(9), pp. 1061–1085.

[196] de Lima, R. O. A., Bazo, A. P., Salvadori, D. M. F., Rech, C. M., de Palma Oliveira, D., and de Aragão Umbuzeiro, G., 2007. "Mutagenic and carcinogenic potential of a textile azo dye processing plant effluent that impacts a drinking water source". *Mutation Research/Genetic Toxicology and Environmental Mutagenesis,* **626**(1), pp. 53–60.

[197] Rosenkranz, H. S., Cunningham, S. L., Mermelstein, R., and Cunningham, A. R., 2007. "The challenge of testing chemicals for potential carcinogenicity using multiple short-term assays: an analysis of a proposed test battery for hair dyes". *Mutation Research/Genetic Toxicology and Environmental Mutagenesis,* **633**(1), pp. 55–66.

[198] Koch, M., Yediler, A., Lienert, D., Insel, G., and Kettrup, A., 2002. "Ozonation of hydrolyzed azo dye reactive yellow 84 (CI)". *Chemosphere,* **46**(1), pp. 109–113.

[199] Malik, P., and Saha, S., 2003. "Oxidation of direct dyes with hydrogen peroxide using ferrous ion as catalyst". *Separation and Purification Technology,* **31**(3), pp. 241–250.

[200] Nataraj, S., Hosamani, K., and Aminabhavi, T., 2009. "Nanofiltration and reverse osmosis thin film composite membrane module for the removal of dye and salts from the simulated mixtures". *Desalination,* **249**(1), pp. 12–17.

[201] Panswad, T., and Wongchaisuwan, S., 1986. "Mechanisms of dye wastewater colour removal by magnesium carbonate-hydrated basic". *Water Science and Technology,* **18**(3), pp. 139–144.

[202] Purkait, M., DasGupta, S., and De, S., 2004. "Removal of dye from wastewater using micellar-enhanced ultrafiltration and recovery of surfactant". *Separation and purification Technology,* **37**(1), pp. 81–92.

[203] Seshadri, S., Bishop, P. L., and Agha, A. M., 1994. "Anaerobic/aerobic treatment of selected azo dyes in wastewater". *Waste Management,* **14**(2), pp. 127–137.

[204] Thinakaran, N., Baskaralingam, P., Pulikesi, M., Panneerselvam, P., and Sivanesan, S., 2008. "Removal of acid violet 17 from aqueous solutions by adsorption onto activated carbon prepared from sunflower seed hull". *Journal of Hazardous Materials,* **151**(2), pp. 316–322.

[205] Wu, F. C., and Tseng, R. L., 2008. "High adsorption capacity $NaOH$-activated carbon for dye removal from aqueous solution". *Journal of Hazardous Materials,* **152**(3), pp. 1256–1267.

[206] Asgher, M., and Bhatti, H. N., 2012. "Evaluation of thermodynamics and effect of chemical treatments on sorption potential of citrus waste biomass for removal of anionic dyes from aqueous solutions". *Ecological Engineering,* **38**(1), pp. 79–85.

[207] Bhatti, H. N., Akhtar, N., and Saleem, N., 2012. "Adsorptive removal of methylene blue by low-cost citrus sinensis bagasse: equilibrium, kinetic and thermodynamic characterization". *Arabian Journal for Science and Engineering,* **37**(1), pp. 9–18.

[208] El Haddad, M., Slimani, R., Mamouni, R., Laamari, M. R., Rafqah, S., and Lazar, S., 2013. "Evaluation of potential capability of calcined bones on the biosorption removal efficiency of safranin as cationic dye from aqueous solutions". *Journal of the Taiwan Institute of Chemical Engineers,* **44**(1), pp. 13–18.

[209] Haq, I. U., Bhatti, H. N., and Asgher, M., 2011. "Removal of solar red BA textile dye from aqueous solution by low cost barley husk: equilibrium, kinetic and thermodynamic study". *The Canadian Journal of Chemical Engineering,* **89**(3), pp. 593–600.

[210] Malekbala, M. R., Hosseini, S., Yazdi, S. K., Soltani, S. M., and Malekbala, M. R., 2012. "The study of the potential capability of sugar beet pulp on the removal efficiency of two cationic dyes". *Chemical Engineering Research and Design,* **90**(5), pp. 704–712.

[211] Moawed, E. A., and Abulkibash, A. B., 2012. "Selective separation of light green and Safranin-O from aqueous solution using Salvadora persica (Miswak) powder as a new biosorbent". *Journal of Saudi Chemical Society,* **20**, pp. S178–S185.

[212] Safa, Y., and Bhatti, H. N., 2011. "Kinetic and thermodynamic modeling for the removal of Direct Red-31 and Direct Orange-26 dyes from aqueous solutions by rice husk". *Desalination,* **272**(1), pp. 313–322.

[213] El Haddad, M., Regti, A., Slimani, R., and Lazar, S., 2014. "Assessment of the biosorption kinetic and thermodynamic for the removal of safranin dye from aqueous solutions using calcined mussel shells". *Journal of Industrial and Engineering Chemistry,* **20**(2), pp. 717–724.

[214] Mohammed, M., Ibrahim, A., and Shitu, A., 2014. "Batch removal of hazardous Safranin-O in wastewater using pineapple peels as an agricultural waste based adsorbent". *International Journal of Environmental Monitoring and Analysis,* **2**(3), pp. 128–133.

[215] Chowdhury, S., Mishra, R., Kushwaha, P., and Saha, P., 2012. "Removal of safranin from aqueous solutions by $NaOH$-treated rice husk: thermodynamics, kinetics and isosteric heat of adsorption". *Asia-Pacific Journal of Chemical Engineering,* **7**(2), pp. 236–249.

[216] Chowdhury, S., Misra, R., Kushwaha, P., and Das, P., 2011. "Optimum sorption isotherm by linear and nonlinear methods for safranin onto alkali-treated rice husk". *Bioremediation Journal,* **15**(2), pp. 77–89.

[217] Sahu, R. C., Patel, R., and Ray, B. C., 2010. "Utilization of activated CO_2-neutralized red mud for removal of arsenate from aqueous solutions". *Journal of Hazardous Materials,* **179**(1), pp. 1007–1013.

[218] Birol, F., Cozzi, L., and Gül, T., 2013. "Redrawing the energy-climate map". *World Energy Outlook Special Report 2013: IEA, Paris*.

[219] Preethi, S., Sivasamy, A., Sivanesan, S., Ramamurthi, V., and Swaminathan, G., 2006. "Removal of safranin basic dye from aqueous solutions by adsorption onto corncob activated carbon". *Industrial & Engineering Chemistry Research,* **45**(22), pp. 7627–7632.

[220] Ma, W., Song, X., Pan, Y., Cheng, Z., Xin, G., Wang, B., and Wang, X., 2012. "Adsorption behavior of crystal violet onto opal and reuse feasibility of opal-dye sludge for binding heavy metals from aqueous solutions". *Chemical Engineering Journal,* **193**, pp. 381–390.

[221] Ravikumar, K., Pakshirajan, K., Swaminathan, T., and Balu, K., 2005. "Optimization of batch process parameters using response surface methodology for dye removal by a novel adsorbent". *Chemical Engineering Journal,* **105**(3), pp. 131–138.

[222] Das, B., Mondal, N. K., Roy, P., and Chattoraj, S., 2013. "Application of response surface methodology for hexavalent chromium adsorption onto alluvial soil of indian origin". *International Journal of Environmental Pollution and Solutions,* **2**, pp. 72–87.

[223] Su, S. N., Nie, H. L., Zhu, L. M., and Chen, T. X., 2009. "Optimization of adsorption conditions of papain on dye affinity membrane using response surface methodology". *Bioresource Technology,* **100**(8), pp. 2336–2340.

[224] Fan, J., Yi, C., Lan, X., and Yang, B., 2013. "Optimization of synthetic strategy of 4′4″(5″)-Di-tert-butyldibenzo-18-crown-6 using Response Surface Methodology". *Organic Process Research & Development,* **17**(3), pp. 368–374.

[225] Evans, M., 2003. *Optimisation of manufacturing processes: a response surface approach*, Vol. 791. Maney Publication.

[226] Özcan, A., Öncü, E. M., and Özcan, A. S., 2006. "Adsorption of Acid Blue 193 from aqueous solutions onto DEDMA-sepiolite". *Journal of Hazardous Materials,* **129**(1), pp. 244–252.

[227] Deniz, F., 2013. "Adsorption properties of low-cost biomaterial derived from Prunus Amygdalus L. for dye removal from water". *The Scientific World Journal,* **2013**, pp. 1–8.

[228] Han, R., Zhang, J., Han, P., Wang, Y., Zhao, Z., and Tang, M., 2009. "Study of equilibrium, kinetic and thermodynamic parameters about methylene blue adsorption onto natural zeolite". *Chemical Engineering Journal,* **145**(3), pp. 496–504.

Dissemination

Internationally indexed journals

1. **Manoj Kumar Sahu**, Sandip Mandal, Saswati S. Dash, Pranati Badhai, Raj Kishore Patel, Removal of Pb(II) from aqueous solution by acid activated red mud, *Journal of Environmental Chemical Engineering*, 1 (2013) 1315-1324. doi:10.1016/j.jece.2013.09.027

2. **Manoj Kumar Sahu** and Raj Kishore Patel, Removal of safranin-O dye from aqueous solution using modified red mud: kinetics and equilibrium studies, *RSC Advances*, 6, (2016) 25472-25472. doi:10.1039/C6RA90024K

3. **Manoj Kumar Sahu**, Uttam Kumar Sahu and Raj Kishore Patel, Adsorption of safranin-O dye on CO_2 neutralized activated red mud waste: process modelling, analysis and optimization using statistical design, *RSC Advances*, 5, (2015) 42294-42304. doi:10.1039/C5RA03777H

4. **Manoj Kumar Sahu**, Sandip Mandal, Lallan Singh Yadav, Saswati Soumya Dash and Raj Kishore Patel, Equilibrium and kinetic studies of Cd(II) ion adsorption from aqueous solution by activated red mud, *Desalination and Water Treatment*, 1, (2015) 1-15. doi:10.1080/19443994.2015.1062428

5. **Manoj Kumar Sahu** and Raj Kishore Patel, Novel visible-light-driven cobalt loaded neutralized red mud (Co/NRM) composite with photocatalytic activity toward methylene blue dye degradation, *Journal of Industrial and Engineering Chemistry*, 40 (2016) 72-82. doi:10.1016/j.jiec.2016.06.008

6. Sandip Mandal, Swagatika Tripathy, Tapswani Padhi, **Manoj Kumar Sahu**, Raj Kishore Patel, Removal efficiency of fluoride by novel Mg-Cr-Cl layered double hydroxide by batch process from water, *Journal of Environmental Sciences*, 25 (2013) 993-1000. doi:10.1016/S1001-0742(12)60146-6

7. Sandip Mandal, Siba Sankar Mahapatra, **Manoj Kumar Sahu**, Raj Kishore Patel, Artificial neural network modelling of As(III) removal from water by novel hybride material, *Process Safety and Environmental Protection*, 93 (2015) 249-264. doi:10.1016/j.psep.2014.02.016

8. Sandip Mandal, **Manoj Kumar Sahu**, Anil Kumar Giri, Raj Kishore Patel, Adsorption studies of chromium (VI) removal from water by lanthanum diethanolamine hybrid material, *Environmental Technology*, 35 (2014) 817-832. doi:10.1080/09593330.2013.852627

9. Sandip Mandal, **Manoj Kumar Sahu**, Raj Kishore Patel, Adsorption studies of As(III) removal from water by zirconium polyacrylamide hybrid material (ZrPACM-43), *Water Resources and Industry*, 4 (2013) 51-67. doi:10.1016/j.wri.2013.09.003

10. Basanti Ekka, Lipeeka Rout, **Manoj Kumar Sahu**, Aniket Kumar, Raj Kishore Patel, , Priyabrat Dash, Removal efficiency of Pb(II) from aqueous solution by 1-alkyl-3-methylimidazolium bromide ionic liquid mediated mesoporous silica, *Journal of Environmental Chemical Engineering*, 3 (2015) 1356-1364. doi:10.1016/j.jece.2014.12.004

11. Saswati Soumya Dash, **Manoj Kumar Sahu**, Eleena Sahu and Raj Kishore Patel, Fluoride removal from aqueous solutions using cerium loaded mesoporous zirconium Phosphate, *New Journal of Chemistry*, 39, (2015) 7300-7308. doi:10.1039/C5NJ01030F

12. Uttam Kumar Sahu, **Manoj Kumar Sahu** and Raj Kishore Patel, Removal of As(V) from aqueous solution by Ce-Fe bimetal mixed oxide, *Journal of Environmental Chemical Engineering*, 4, (2016) 2892-2899. doi:10.1016/j.jece.2016.05.041

13. Uttam Kumar Sahu, **Manoj Kumar Sahu**, Siba Sankar Mahapatra and Raj Kishore Patel, Removal of As(III) from Aqueous Solution Using Fe_3O_4 Nanoparticles: Process Modeling and Optimization Using Statistical Design, *Water Air Soil Pollution*, 45, (2017) 228-243. doi:10.1007/s11270-016-3224-1

14. Basanti Ekka, **Manoj Kumar Sahu**, Raj Kishore Patel and Priyabrat Dash, Titania coated silica nanocomposite prepared via encapsulation method for the degradation of Safranin-O dye from aqueous solution: Optimization using statistical design, *Water Resources and Industry*, doi:10.1016/j.wri.2016.08.001

Conference Presentations

1. **Manoj Kumar Sahu** and Raj Kishore Patel, Synthesis of red mud supported nanoscale zero-valent iron (RM-nZVI) and their efficient removal of Hg(II) from aqueous solution: characterization, reactivity and mechanism, **International conference on role of microscopy and allied techniques in the development of multifunctional and nanomaterial's (ICMAMN-2016)**, 25^{th}-27^{th} November 2016, Fakir Mohan University, Balasore, Odisha, India.

2. **Manoj Kumar Sahu** and Raj Kishore Patel, Solar light-induced degradation of methylene blue dye with Cobalt loaded neutralised red mud (Co/NRM): A study of mechanism and operational parameters, **19 CRSI National Symposium in Chemistry (CRSI NSC-19)**, 14^{th} -16^{th} July 2016, University of North Bengal, Darjeeling, West Bengal. India.

3. **Manoj Kumar Sahu** and Raj Kishore Patel, Solar light-induced degradation of methylene blue dye with Cobalt loaded neutralized red mud (Co/NRM): A study of mechanism and operational parameters, **Research Scholar Week – 2016**, 12^{th} -14^{th} March 2016, NIT, Rourkela, Odisha, India.

4. **Manoj Kumar Sahu** and Raj Kishore Patel, Extraction of magnetic iron oxide from red mud, **International Conference on Frontiers in Materials Science and Technology (ICFMST-2015)**, 10^{th} -12^{th} December 2015, NIST, Berhampur, Odisha, India.

5. **Manoj Kumar Sahu** and Raj Kishore Patel, Adsorption of Cd(II) on activated red mud: Neutralized by CO_2, **National Seminar on "Recent Trends in Chemical Sciences (RETICS-2013)**, 16^{th} -17^{th} March 2013, Sambalpur University, Sambalpur, Odisha. India.

6. **Manoj Kumar Sahu** and Raj Kishore Patel, Neutralization, Characterization and Extraction of fine Iron from Red Mud, **National Seminar on "Chemistry in Technology" of Orissa Chemical Society (OCS)**, 8^{th}-9^{th} December 2012, Ravenshaw University, Cuttack, Odisha, India.

Book chapters

1. **Manoj Kumar Sahu** and Raj Kishore Patel
   Methods for Utilization of Red Mud and Its Management
   Chapter: 19
   Environmental Materials and Waste: Resource Recovery and Pollution Prevention
   Publisher: Elsevier Academic Press, 2016
   Editors: M.N.V. Prasad & Kaimin Shih
   ISBN: 978-0-12-803837-6
   doi:10.1016/B978-0-12-803837-6.00019-6

Article under preparation

1. **Manoj Kumar Sahu** and Raj Kishore Patel, Synthesis of red mud supported nanoscale zero-valent iron (RMnZVI) and their efficient removal of Hg(II) from aqueous solution: characterization, reactivity and mechanism, *Journal of Hazardous Materials*.